Fall 2019

Investigation of Electrostatic Interactions Towards Controlling Silylation-Based Kinetic Resolutions and Exploring the Effect of the Polymer Backbone on Silylation-Based Kinetic Resolutions Employing a Polymer-Supported Triphenylsilyl Chloride

Tian Zhang

INVESTIGATION OF ELECTROSTATIC INTERACTIONS TOWARDS CONTROLLING SILYLATION-BASED KINETIC RESOLUTIONS AND EXPLORING THE EFFECT OF THE POLYMER BACKBONE ON SILYLATION-BASED KINETIC RESOLUTIONS EMPLOYING A POLYMER-SUPPORTED TRIPHENYLSILYL CHLORIDE

by

Tian Zhang

Bachelor of Science
Wuhan University, 2014

Submitted in Partial Fulfillment of the Requirements

For the Degree of Doctor of Philosophy in

Chemistry

College of Arts and Sciences

University of South Carolina

2019

Accepted by:

Sheryl L. Wiskur, Major Professor

Linda Shimizu, Committee Member

Aaron Vannucci, Committee Member

Campbell McInnes, Committee Member

Cheryl L. Addy, Vice Provost and Dean of the Graduate School

DEDICATION

This is dedicated to my beloved mother Juan Xie and father Liangming Zhang.

ACKNOWLEDGEMENTS

My deepest gratitude goes first and foremost to my advisor Dr. Sheryl Wiskur for her constant guidance and support. I always remembered the morning I talked to her for the first in an interview on picking a research group. I was impressed by her consideration, patience and love in research, so I made my decision even though I still had two more interviews to go. What impressed me most is her being consistently kind and patient for the whole time in the past five years. She teaches me not only to look down to your work, but also to treasure your family. Smiles on her children show that she is a wonderful mom too. I will balance my work and family in the future as I have already known the secrets of happy life. I would also like to thank the rest of my committee member: Dr. Linda Shimizu, Dr. Aaron Vannucci, and Dr. Campbell McInnes, for their insightful comments and encouragement of my plan, proposal and dissertation.

My sincere thanks also go to the former and current members in Wiskur group. Special thanks to Brandon Redden, thank you for being such a reliable pal both in and outside the lab, I really appreciate the time working and having fun with you. To Shelby Dickerson and Grace Hollenbeck, you two are the most reliable friends to ask for. No matter what problems I had, I can always count on you two. To Dr. Li Wang, you were my mentor in graduate school, our discussion in chemistry will be remembered. To Mia, Julia, Naomi and those in the Wiskur group, I wish you all success. I am a lucky person to be a graduate student in this group because I do enjoy my life in this group a lot.

I would like to show the sincerest thanks to my parent Juan Xie and Liangming Zhang, I would not achieve anything without your supports and love. I wouldn't forget my beloved girlfriend Yiming Shi, you are such a charming animal, source of happiness. It is such a blessing to have you in my life.

ABSTRACT

This dissertation focuses on studies of silylation-based kinetic resolution methodology developed by the Wiskur group, which is a powerful method for the separation of a single enantiomer from a mixture of racemic secondary alcohols. Chapter 1 introduces the background of our silylation-based kinetic resolution.

Chapter 2 involves mechanistic studies of electrostatic interactions in controlling enantioselectivities of our silylation-based kinetic resolution. Electrostatic interactions between a silylated isothiourea intermediate and an ester π system is determined via linear free energy relationship study. To be specific, how variations in sterics and electronics affect the selectivity of a silylation-based kinetic resolution.

Chapter 3 is the following research of chapter 2 on the electrostatic interaction in controlling the enantioselectivities. Similar research approaches such as linear free energy relationship study is applied. Computation data on the proposed intermediate and transition state in silylation-based kinetic resolution our will be discussed.

Chapter 4 introduce an optimization of polystyrene-supported triphenylsilyl chlorides that were developed in our group in obtaining enantioenriched secondary alcohols via a chromatography-free isolation. Second generation's polystyrene-supported triphenylsilyl chloride is proposed by incorporating polar methyl methacrylate to the adjacent position of active site, promoting a more polar microenvironment. Effect of variations in polarity and percentage of incorporating monomer will be discussed.

TABLE OF CONTENTS

LIST OF TABLES

LIST OF FIGURES

LIST OF SCHEMES

CHAPTER 1

BACKGROUND AND INTRODUCTION OF ASYMMETRIC SILYLATION

1.1 Chirality

Chirality is an important property of natural substances that influences their biological activities. A compound is chiral if it is non-superimposable onto its mirror image, producing a pair of enantiomers with opposite stereochemistry (Figure 1.1).[1-2] A ubiquitous example to explain chirality is our hands. Our left hand is the mirror image to our right hand, and since they are not superimposable on each other suggests our hands are chiral. Chiral molecules usually contain at least one carbon atom with four nonidentical substituents, which is labeled a chiral center. Any molecule that contains a chiral center will be chiral except for a meso compound. Since one chiral center can produce enantiomers, it is necessary to label the orientation of the chiral center. A convenient way to define the configuration of a chiral center is through the designation of *R*/*S*.[3] An enantiomer can also be named by the direction in which it rotates the plane of polarized light. If it rotates the light clockwise (as seen by a viewer towards whom the light is traveling), that enantiomer is labeled (+). Its mirror-image is labeled (−).

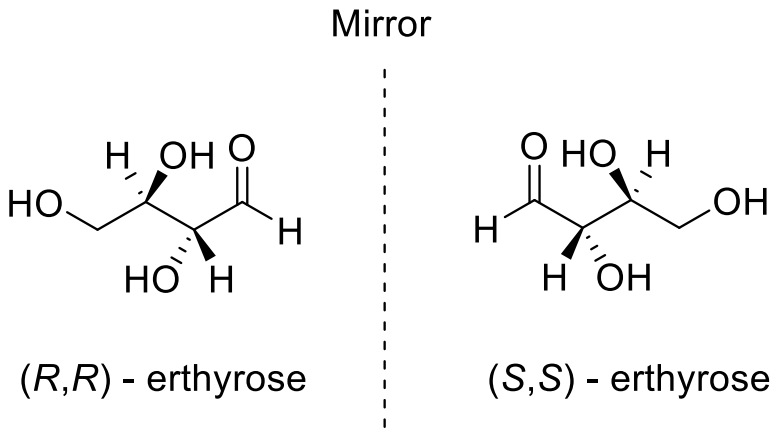

Figure 1.1 Example of a Pair of Enantiomers

Enantiomers, pairs of chiral compounds, rotate the direction of plane polarized light to equal, but opposite angles and share identical chemical and physical properties in a nonchiral environment.[4] Interest in chiral compounds increased in the 1950s, when numerous medical disasters occurred. The reason for the occurrence of medical disasters were mostly related to the different physiological effects of pairs of enantiomers in chiral environments. One enantiomer could be beneficial to health, while the other enantiomer could have serious negative side effects. One of the most far-reaching cases is thalidomide (Figure 1.2), which was used to treat cancers (multiple myeloma), leprosy and morning sickness in pregnant women. Thalidomide was an over-the-counter drug first sold in West Germany in 1957.[5] Between 5,000 and 7,000 infants were born with malformation of the limbs resulting from the consumption of thalidomide by their mothers and only 40% of these children survived. Studies showed that thalidomide was first sold as a racemic mixture (50:50 mixture of two enantiomers) of (*R*)-thalidomide which had sedative effects and (*S*)-thalidomide, which led to malformation of the limbs to the infants that were passed from their mothers (Figure 1.2).[6]

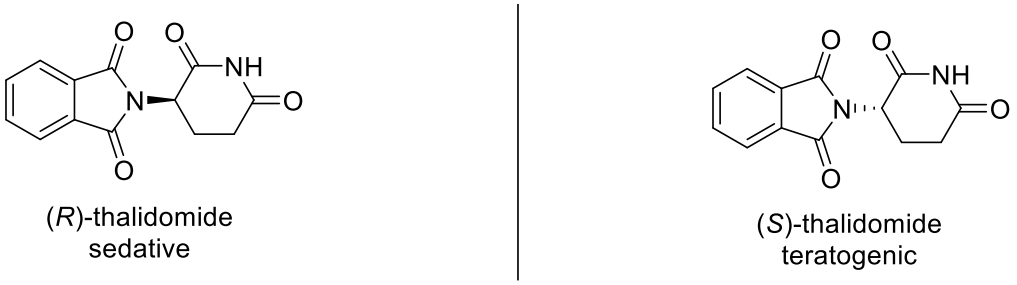

Figure 1.2 Enantiomers of Thialidomide and their Physiological Effects

$$\%\ \text{ee} = \frac{|R - S|}{|R + S|} \times 100\%$$

Equation 1.1

Since any new chiral drug must be enantiopure based on FDA's regulations if it is sold as a single enantiomer, increased attention was paid to develop access to enantiopure compounds. As a matter of fact, "chiral pool" (enantiopure compounds directly from nature) was the main source of enantiomerically pure compounds by 1980s.[10] These natural compounds obtained from nature have some advantageous properties: their *ee* is normally close to 100% and many of them are inexpensive. Even though most of the pharmaceutical target compounds are not found in the "chiral pool", it was discovered that some of the pharmaceutical target compounds are structurally similar to some of the natural compounds. This discovery provides an alternative for obtaining chiral compounds through synthetic transformations from an enantiomerically pure starting compound.[11] Preparations of α-amino acids, hydroxyacids, carbohydrates and terpenes greatly benefited from this strategy. The drug oseltamivir, more commonly known as Tamiflu, a World Health Organization's List of Essential Medicines, is one of the most effective antiviral medicines to treat influenza A and influenza B. Oseltamivir can be commercially synthesized through several

chemical reactions starting with shikimic acid (Scheme 1.1), which is a natural compound isolated from Chinese star anise.[12] The basic core structure of oseltamivir is the same as the shikimic acid starting material, and the desired stereochemistry of the target product was easily achieved by several steps via inversion of stereochemistry. In this way, target product with certain requirement of stereochemistry could be obtained handily using a natural starting material.

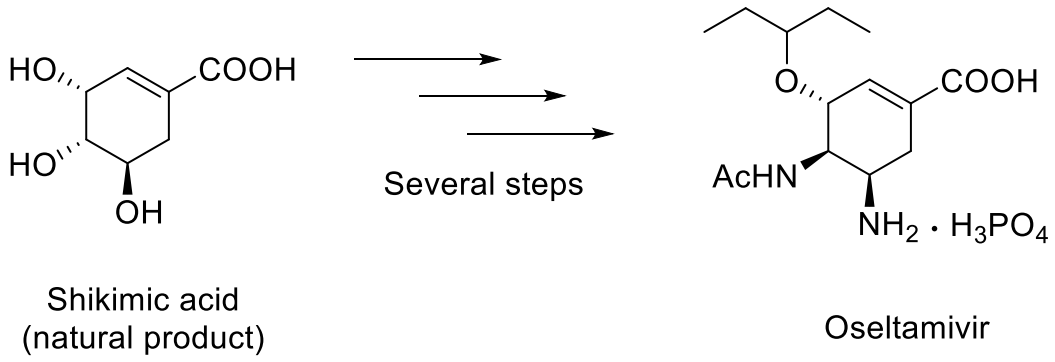

Scheme 1.1 Preparation of Oseltamivir from Shikimic Acid

1.2 Asymmetric Catalysis

Asymmetric catalysis is a type of catalysis in which a chiral catalyst directs the yield of an enantiomerically enriched product from an achiral compound.[13] One of the most influential asymmetric catalysis is the selective reduction of a ketone using chiral BINAP-Ru(II) catalyst which was developed by Ryoji Noyori, who shared the Nobel Prize with William S. Knowles for the study of chirality catalyzed hydrogenations in 2001 (Figure 1.3). With the help of this catalyst, acetophenone and its derivatives are selectively reduced to chiral alcohols with an *ee* up to 99% while the catalyst loading in this reaction is as low

as 0.001%, leading to remarkable efficient asymmetric catalysis (Scheme 1.2).[14-16] Loading of catalyst is important parameter for the industrious application.

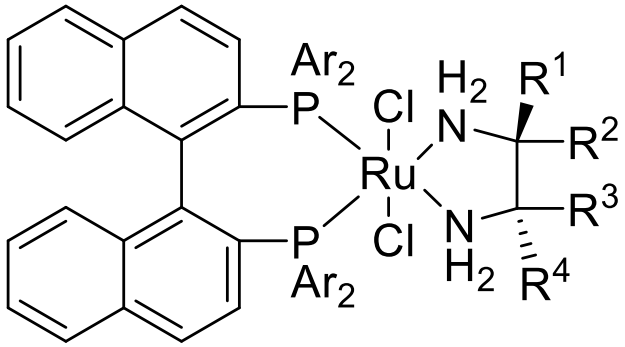

(S)-BINAP/(S)-diamine-Ru^{II} catalyst

Figure 1.3 Noyori's BINAP-Ru(II) Catalyst

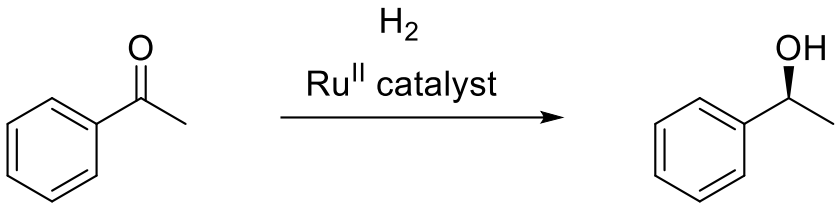

Scheme 1.2 Asymmetric Hydrogenation of Ketone using BINAP-Ru(II) Catalyst

Chiral products can be generated with high *ee* and decent yields through asymmetric catalysis when the chiral catalysts and achiral starting materials are perfectly matched. However, not every asymmetric catalyst has such an amazing performance as Noyori's BINAP-Ru(II) catalyst on ketones. In most cases, products with only a moderate *ee* (50 – 80%) are generated when an optimized catalyst is utilized in another system. Whenever the performance of an asymmetric catalyst is not ideal, the main disadvantage of asymmetric catalysis occurs, which is the independence of *ee* on conversion. The *ee* of

the product does not change over the course of a reaction, which means that the *ee* cannot be adjusted by pushing the reaction to higher yield. An increase in selectivity of asymmetric catalysis can only be achieved by strengthening the interaction between the chiral catalyst and the prochiral starting material, which is done by adjusting the structure of the chiral catalyst. Redesigning a chiral catalyst takes time and energy and may not work. Due to this drawback of asymmetric catalysis, it is important for us to have alternative approaches to obtain enantiomerically enriched products.

1.3 Classical Resolution

An alternative approach to produce enantiomerically enriched products is resolution, a sorting process of enantiomers by chemical or physical means.[17] Classical resolution was one of the earliest forms of resolution and is still applied today.[18-19] A classical resolution involves the use of an achiral resolving agent that covalently or non-covalently associates to the substrate being resolved, resulting in a pair of diastereomers. The generated diastereomers can then be isolated from each other through crystallization of one of the diastereomers. The separation of 1-phenylethylamine enantiomers using tartaric acid demonstrates this principle.[20] To be more specific, (*S*)-1-phenylethylamine and (*R*)-1-phenylethylamine are separated using (*R*,*R*)-tartaric acid as the resolving agent (Scheme 1.3). The carboxylic acids of tartaric acid protonates both enantiomers of 1-phenylethylamine, forming two diastereomeric salts. The two salts formed are now diastereomers and are therefore no longer enantiomers. The (*S*)-1-phenylethylammonium-(*R*,*R*)-tartrate salt crystallizes faster than the (*R*)-1-phenylethylammonium-(*R*,*R*)-tartrate salt under controlled conditions, making the (*S*)-1-phenylethylammonium-(*R*,*R*)-tartrate

salt the only compound to be crystalized. Afterwards, corresponding enantiomers of 1-phenylethylamine can be recovered after an easy basic work up to deprotonate the amine. The main advantage of a classic resolution is its relatively cheaper cost, making it a popular technique widely used in industry.[21] The main limitation of classic resolution is the stoichiometric amount of chiral resolving agent used and only a 50% theoretical yield can be achieved.

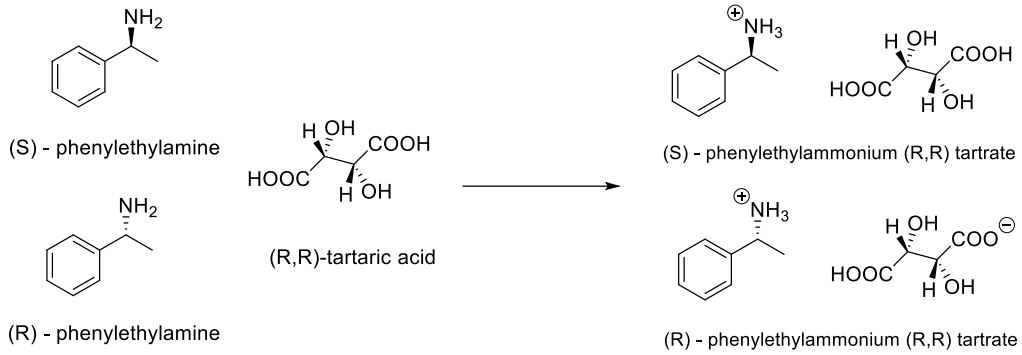

Scheme 1.3 Classical Resolution of Phenylethylamine using Tartaric Acid

1.4 Kinetic Resolution

Later, an updated method of resolution called a kinetic resolution emerged and became a popular approach to isolate chiral products.[22] This also involves a sorting process of enantiomerically enriched compounds, but this time depends on the difference in reaction rates between starting materials and chiral catalysts. Specifically, one enantiomer of the racemic starting material reacts faster with the chiral catalyst while the other enantiomer reacts slower with the chiral catalyst (Scheme 1.4). In the end, the remaining starting material becomes highly enriched with increasing conversion to product. Ideally, the slower enantiomer doesn't react at all, thereby converting all of the faster enantiomer

to the product while the slower enantiomer remains as unreacted starting material. Since the newly formed product is now a completely different compound than the recovered starting material it has different physical properties and can be separated through common separation procedures like chromatography, extractions or distillation ultimately separating the enantiomers.

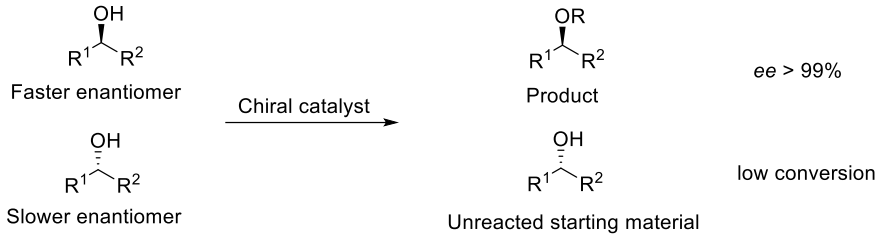

Scheme 1.4 General Strategy of Kinetic Resolution

The selectivity factor, *s*, is a way to describe this difference in reaction rates. The selectivity factor equals the reaction rate of the faster enantiomer divided by the reaction rate of the slower enantiomer (Equation 1.1). This means that for a reaction with a selectivity factor of 10, one enantiomer reacts 10 times faster than the other enantiomer. The higher the selectivity factor, the more selective a kinetic resolution is. A selectivity factor of 10 suggests a decent performance of a kinetic resolution, which means the unreacted substrate can be recovered in high *ee* (>99%) with a conversion of 70%. In terms of energy, the selectivity factor also tells the difference in energy between the diastereomeric transition states of the enantiomers (Equation 1.2).

$$s = k_{rel} = k_{fast}/k_{slow} = e^{\Delta\Delta G^{\ddagger}/RT}$$

Equation 1.2

It was previously mentioned that one disadvantage of asymmetric catalysis is that the *ee* never changes throughout the reaction. In a kinetic resolution the *ee* is constantly changing, which is the main advantage of a kinetic resolution and makes it a complementary technique to asymmetric catalysis. As the kinetic resolution goes on, the *ee* of the slow enantiomer increases as more and more of the fast enantiomer converts. When all of the fast reacting enantiomer has converted to product, the slow reacting enantiomer will be enantiomerically pure. The amount of starting material you have remaining in the end depends on how selective the reaction is, or in other words how much material needed to be converted to product to have only one enantiomer left. This process demonstrates how the *ee* of the starting material and the product changes over time and the relationship between *ee* and conversion. This relationship is described in Equation 1.3.[22]

$$\text{conv} = \frac{ee_{sm}}{ee_{sm} + ee_{pr}}$$

Equation 1.3

Since the *ee* of the product and starting material are constantly changing over the course of the reaction, the best way to evaluate a kinetic resolution is through its selectivity factor which should be a constant. Selectivity factors for a kinetic resolution can be calculated from the conversion and the *ee* of the starting material (Equation 1.4) or the conversion and the *ee* of the product (Equation 1.5). With the selectivity factor in hand, one could determine the extent of conversion needed to obtain the recovered starting material enantiomerically pure.

$$s = \frac{\ln[(1-c)(1-ee_{sm})]}{\ln[(1-c)(1+ee_{sm})]}$$

Equation 1.4

$$s = \frac{\ln[1-c(1+ee_{pr})]}{\ln[1-c(1+ee_{pr})]}$$

Equation 1.5

Kinetic resolutions can be catalyzed by enzymes[23] and chiral organocatalysts.[24]. Among all the potential chiral catalysts, enzymes are usually the most effective and efficient catalysts for the kinetic resolution of a wide variety of different functional groups. For example, nitrilase, a commercially available enzyme, is utilized to activate an enantioselective hydrolysis of a racemic nitrile compound (Scheme 1.5), affording 95% of the *S* enantioenriched product.[25] To be specific, only one enantiomer is obtained because three-dimensional structure of enzyme is very specific, catalyzing starting material with certain three-dimensional structure.

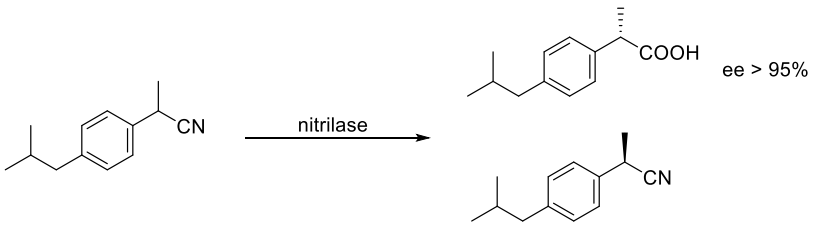

Scheme 1.5 Kinetic Resolution Catalyzed by Nitrilase

As for the kinetic resolutions using organometallic catalysts, the Sharpless epoxidation of allylic alcohols was a major contribution due to the high selectivity of this

reaction. With the aid of a tartrate titanium complex, the alkene on the *S* enantiomer reacts over a hundred times faster to form an epoxide while the alkene on the *R* enantiomer remains unreacted (Scheme 1.6).[26] The selectivity factor for this kinetic resolution is as high as 104 for the best substrate of allylic alcohol, and good selectivity factors were also obtained on derivatives of it. Inspired by Sharpless's research, many research groups started exploring other means to obtain enantiopure alcohols and amines.[27]

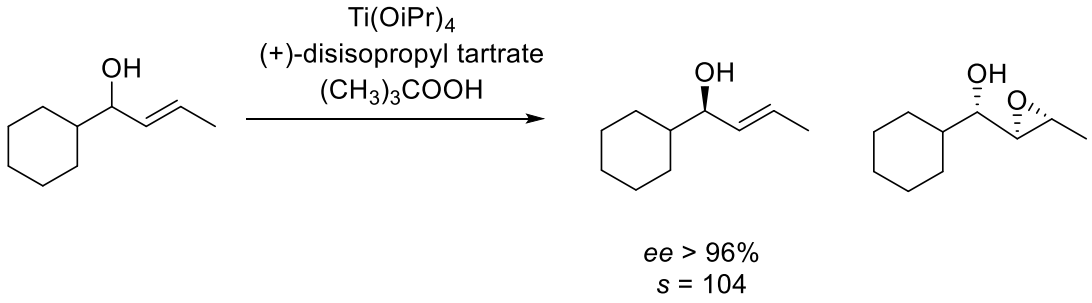

Scheme 1.6 Sharpless Epoxidation of Allylic Alcohol

1.5 Kinetic resolutions of secondary alcohol

Many effective and efficient approaches to resolve secondary alcohols have been developed in the past 20 years. Among these approaches, the most well-known methods are through acylation[28-35] and silylation[36-41]. The main strategy to perform enantioselective acylation on secondary alcohols is based on chiral nucleophilic catalysts (Scheme 1.7). The chiral catalyst normally activates the acyl compound such as an anhydride to form a complex, which is then selectively attacked by the one enantiomer of the secondary alcohol over the other enantiomer because of the favorable orientation to the complex.

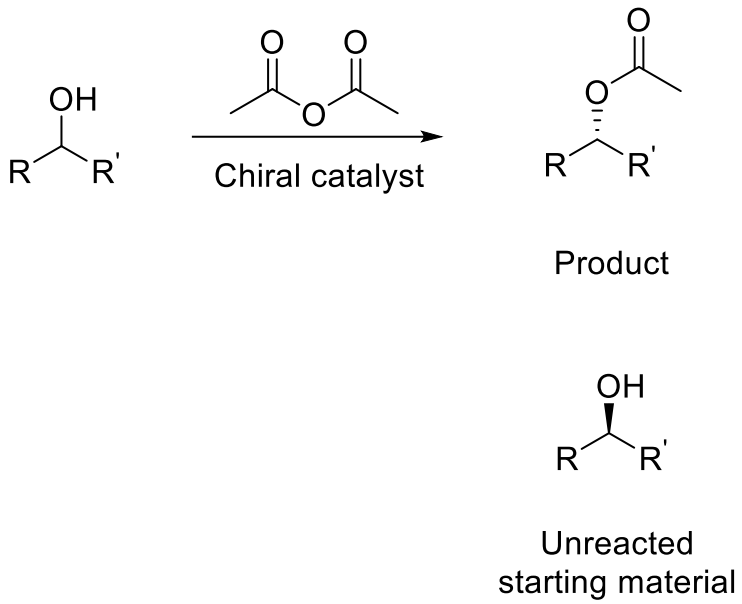

Scheme 1.7 General Strategy of Enantioselective Acylation

In 1996, the first effective enantioselective formation of a carbonate using secondary alcohols was reported by Vedejs.[28] DMAP derivative **1.1** with a chiral center was synthesized from commercially available materials and employed as an acyl transfer complex on a naphthyl secondary alcohol (Scheme 1.8). As the kinetic resolution began, the magnesium bromide served as a Lewis acid to activate the carbonyl group of 4-dimethylaminopyridine derivative **1.1**. The activated **1.1** was then easily attacked by the faster reacting enantiomer of the naphthyl secondary alcohol. The kinetic resolution showed high selectivity on aromatic derivatives of these secondary alcohols, with a selectivity factor as high as 48 obtained. Vedejs's work demonstrated the potential of chiral 4-dimethylaminopyridine derivatives as nucleophilic catalysts to obtain high selectivity factors.

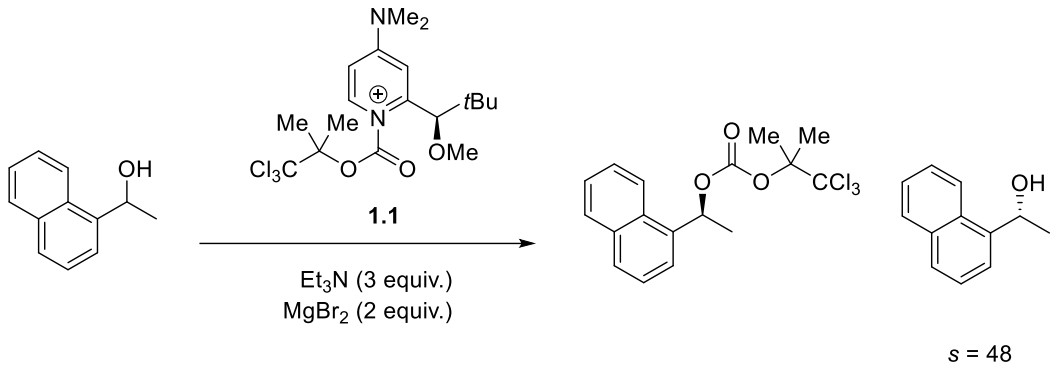

Scheme 1.8 Enantioselective Acylation Reported by Vedejs

Another highlighted application of DMAP based catalysts is in the kinetic resolutions of various substrates with the planar chiral DMAP ferrocene catalysts developed by Fu.[42] A planar-chiral π-complex of heterocycles with Fe serve as effective nucleophilic catalysts (**1.2**) for the acylation of secondary alcohols, especially secondary aryl alcohols, generating selectivity factors over 50 (Scheme 1.9). This three-dimensional chiral catalyst proved to be very efficient for various types of secondary alcohols.[43-44] Other than the versatility of the ferrocene catalyst, its main selling point is the efficiency. Unlike the stoichiometric DMAP based catalyst **1.1** developed by Vedejs, catalyst loading was as low as 2 mol % when **1.2** was applied.

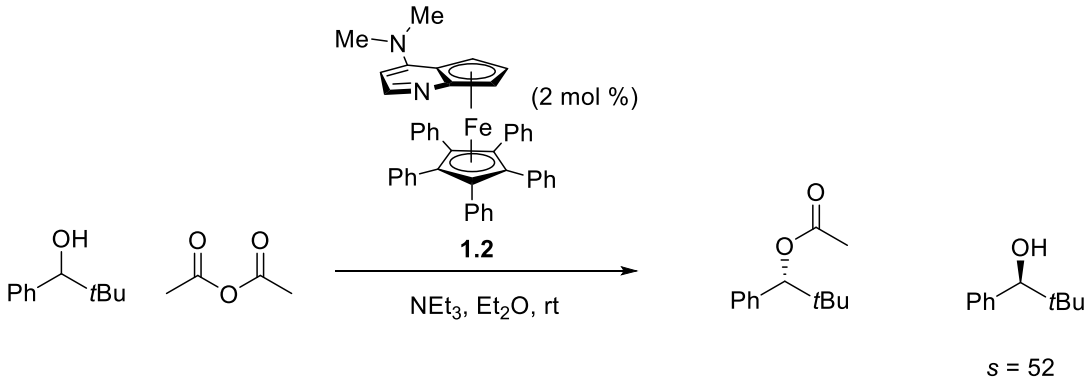

Scheme 1.9 Kinetic Resolution using Fu's Planar Chiral DMAP Catalyst

Numerous nucleophilic catalysts had been developed and employed to resolve secondary alcohols, including diamine-based catalysts by Oriyama,[45] PPY derivative catalysts by Fuji,[46] peptide catalysts by Miller,[47] and isothiourea based catalysts by Birman.[48] The isothiourea based catalysts developed by Birman are remarkable enantioselective acyl transfer catalysts. Two of the isothiourea catalysts, (-)-tetramisole (**1.3**) and (-)-benzotetramisole (**1.4**) (Figure 1.4), have been applied in our silylation-based kinetic resolutions which will be discussed in the following chapter of this dissertation. With the use of isothiourea based catalysts in acylation-based kinetic resolutions, incredible selectivities (up to 300) were obtained for the enantioselective acylation of various alcohols employing an anhydride (Scheme 1.10). Latter studies suggested an involvement of a certain intermolecular electrostatic interaction between the acylated catalyst intermediate and the substrate molecule.[32-33] The proposed intermolecular electrostatic interaction plays an essential role in drawing in the substrate to perform the reaction. Since the catalyst is chiral, one enantiomer of alcohol preferentially binds to the acylated catalyst over the other enantiomer, leading to the control of enantioselectivity.

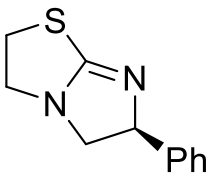

1.3

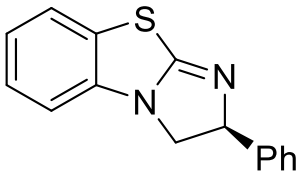

1.4

Figure 1.4 Levamisole (1.3) and (-)-Benzotetramisole (1.4)

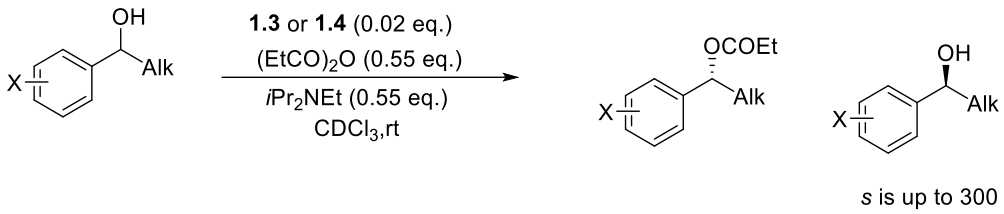

Scheme 1.10 Birman's Kinetic Resolution of Secondary Alcohols

Silylation is a common strategy to protect alcohols and the silyl ether formed in the protection is stable and easy to be deprotected. Since it is easy to put on and take off, researchers starting looking at employing silyl groups kinetic resolutions and asymmetric silylations. A novel silylation-based kinetic resolution was reported by Ishikawa in 2001.[36] Chiral guanidine **1.5** was ultilized as the catalyst to afford a selective silylation of secondary alcohols (Scheme 1.11). It used stoichiometric amount of catalyst and took 6 days to reach a moderate conversion. Although the selectivity factor was low (*s* = 2.2), it initiated a unique approach towards the kinetic resolution of secondary alcohols. Many other enantioselective silylations have been developed in light of Ishikawa's work, supporting silylation as an alternative approach to resolve secondary alcohols.

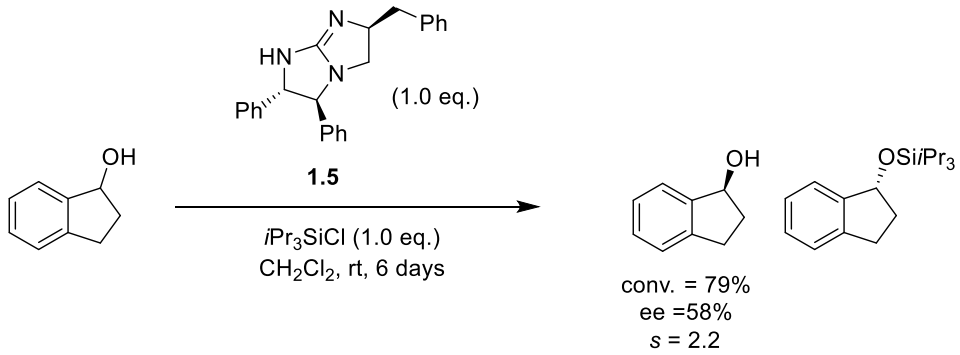

Scheme 1.11 First Silylation-Based Kinetic Resolution by Ishikawa

As we know from undergraduate chemistry, the silylation of an alcohol is a common method to protect alcohols. The resulting silyl ether has a high tolerance to many highly reactive reagents, such as Grignard reagents, and the deprotection of silyl ethers is easily achieved in one step.[49] A general silylation-based kinetic resolution involves the selective protection of one enantiomer, which is controlled by the chiral catalyst, followed by the isolation of enantioenriched silyl ether from enantioenriched unreacted starting material (Scheme 1.12). Enantioenriched silyl ethers can be easily restored to alcohols after desilylation.

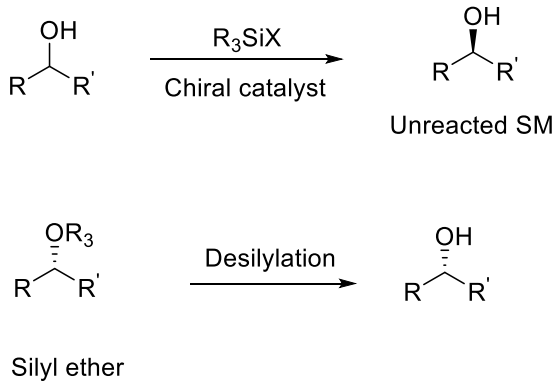

Scheme 1.12 General Strategy of Silylation

A few successful silylation-based resolutions have been developed in the recent years including Oestreich[37, 50-53], Hoveyda[38, 54-55] Tan,[56-58] List,[59] Song,[60] Nakata[61] and Wiskur.[39-41] In 2005, a remarkable kinetic resolution of secondary alcohols using silicon-stereogenic silane **1.6** as the chiral reagent was reported by Oestreich. He introduced a unique enantioselective silylation via a diastereoselective rhodium-catalyzed dehydrogenative Si-O coupling (Scheme 1.13).[37] An *N*-heterocyclic carbene ligand (1,3-bis(2,6-diisopropylphenyl)imidazol-2-ylidene) was used with a rhodium catalyst to form a reactive complex. The resulting complex was employed in the kinetic resolution of donor-

functionalized alcohols. The kinetic resolution is incredibly selective. Selectivity factors above 50 were obtained on most alcohols and one alcohol had a selectivity factor of about 900. Since the initial work, Oestreich has found conditions that eliminate need for the pyridyl group adjacent to alcohol and has found that copper also works as a catalyst.[50-53]

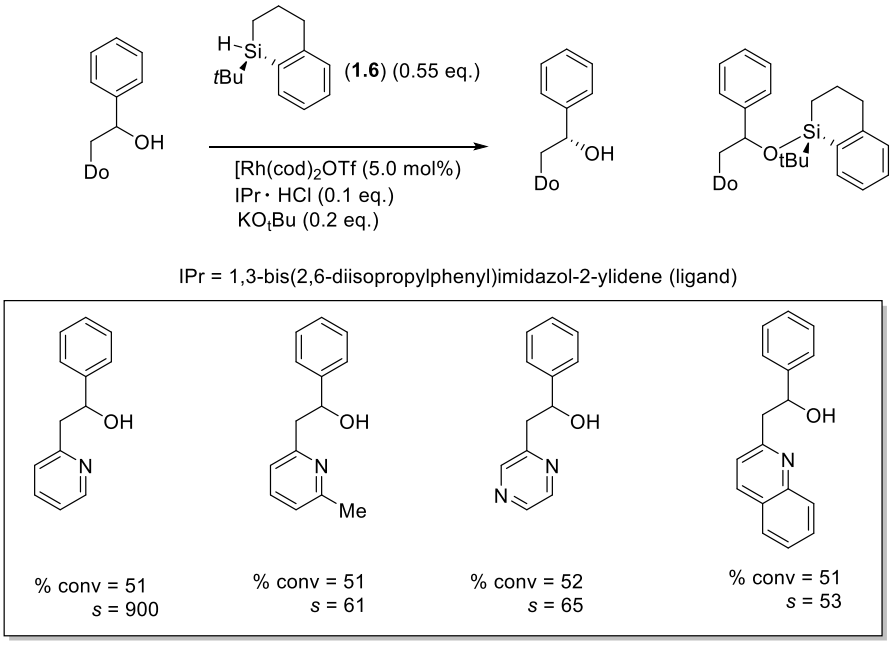

Scheme 1.13 Ostreich's Silylation-Based Kinetic Resolution using Silicon-Stereogenic Silanes

Other silylation-based kinetic resolutions were also developed that employed nucleophilic catalysts. Hoveyda and Snapper developed a chiral imidazole-based catalyst **1.7** which could be used to resolve *syn*-1-2 diols (Scheme 1.14).[54] The interesting part of this kinetic resolution is the duo function of the catalyst **1.7**, which serves as a Lewis base and a hydrogen bonding site at the same time. During the reaction, secondary amines interact with the alcohol through hydrogen bonding to locate the catalyst while the imidazole moiety activates the silyl chloride nearby. Chirality of the catalyst is controlled

by the chiral centers adjacent to the amines. Due to this special design of catalyst, one hydroxyl group of the diol was more likely to silylate while the other hydroxyl group remained unreacted (yield difference = 98:2). Other than the significant site selectivity of hydroxyl silylation, the *ee* of the silyl ether and unreacted starting material are very high (ee_{PR} of the best diol is above 98%). Beside the kinetic resolution of diol, Hoveyda and Snapper also reported the enantioselective silylation of triols and the mechanistic study of the kinetic resolution of diols and triols.[38,55]

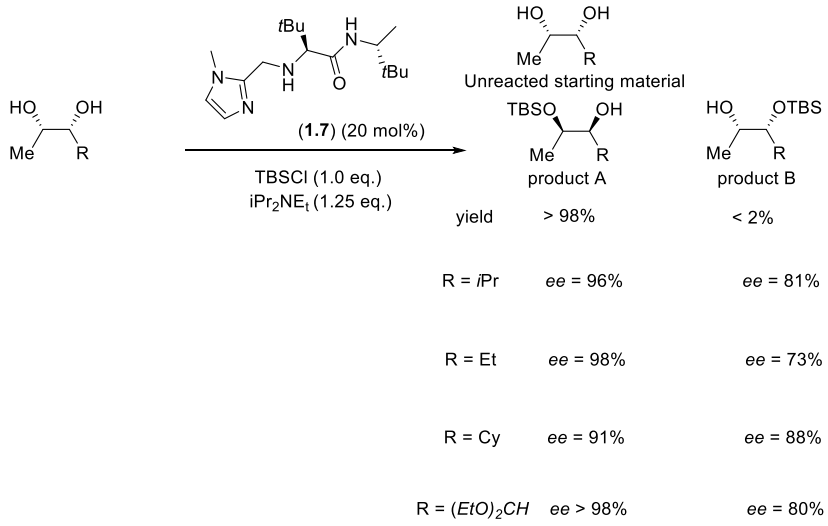

Scheme 1.14 Silylation-Based Kinetic Resolution of *syn*-1,2-Diol by Hoveyda and Snapper

During the same period to Hoveyda and Snapper's report on kinetic resolution of diols, Tan proposed an alternative approach to desymmetrize diols. Tan developed an electrophilic-transfer catalyst that could be used to resolve diols. The most interesting part is the design of the catalyst.[56] The methoxy on the catalyst can undergoe reversible covalent bonding to a hydroxyl group. Therefore, when introduced to a diol, the chiral catalyst binds to one hydroxyl group while the imidazole-based end catalyzes the asymmetric

silylation of the other hydroxyl group for the enantioselective silylation of diols (Scheme 1.15). Enantioselectivity of the product was controlled by the chiral center on the catalyst. Once the kinetic resolution is completed, methanol is added to the reaction to break the reversible covalent bond and free the product. Afterwards, Tan also reported the desymmetrization of nonsymmetric diols and triols.[57-58]

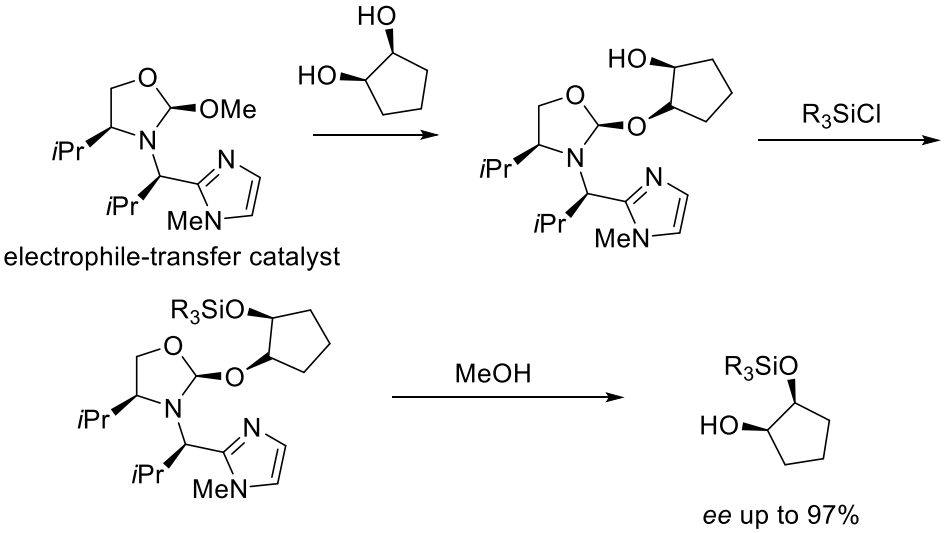

Scheme 1.15 Catalytic Procedure for Silylation using Tan's Catalyst

In 2011, the Wiskur's group reported a successful silylation-based kinetic resolution of cyclic secondary alcohols that employed isothiourea catalysts[32-33] originally developed by Birman (Scheme 1.16).[39] Selective silylation of cyclic secondary alcohols using (-)-tetramisole **1.3** as the chiral catalyst and triphenylsilyl chloride **1.8** as the silyl source was accomplished. Further substrate expansions were explored after the success of the cyclic secondary alcohols. The silylation-based kinetic resolution was applied to α-hydroxy lactones and lactams with the (-)-benzotetramisole **1.4** chiral catalyst performing

better with these substrates (Scheme 1.17).[40] The optimized methodology resolved the α-hydroxy lactones and lactams with high selectivity, ranging up to 100.

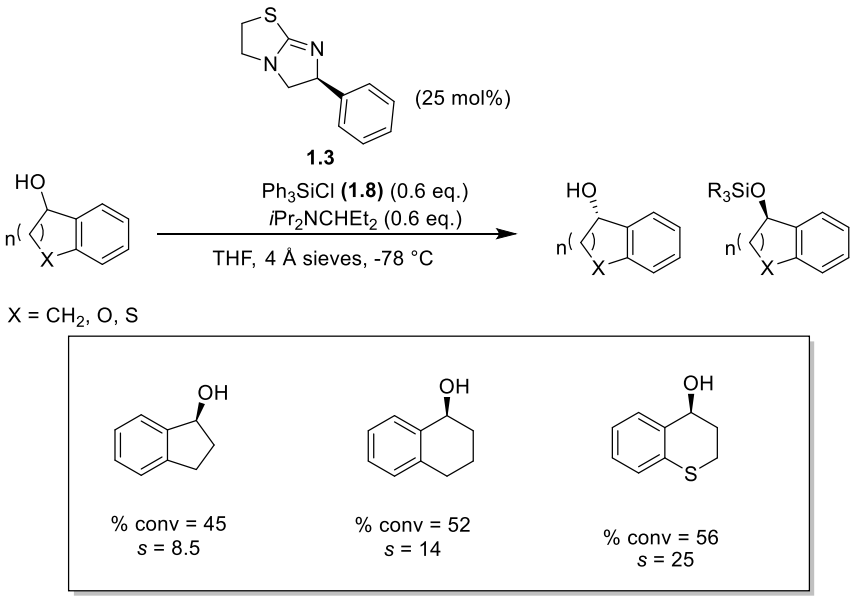

Scheme 1.16 Wiskur's Silylation-Based Kinetic Resolution of Cyclic Secondary Alcohols

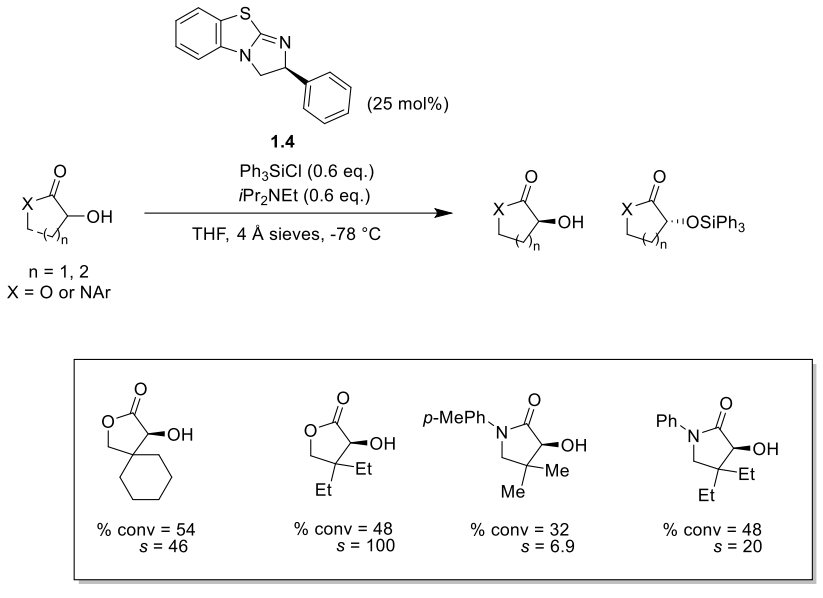

Scheme 1.17 Wiskur's Silylation-Based Kinetic Resolution of *α*-Hydroxy Lactones and Lactams

After we finished the last substrate expansion on *trans*-2-aryl cyclohexanol (Scheme 1.18), the mechanistic studies on the methodology were performed simultaneously. In 2014, a linear free-energy relationship study was applied to explore the substituent effect of different *p*-substituted triarylsilyl chlorides in the system, proposing a pentavalent S_N2-like transition state with the catalyst as the leaving group and the alcohol as the incoming nucleophile.[62] The insight of how the chirality is transmitted from the chiral catalyst to the product through the triphenylsilyl chloride was also discovered and reported.[63]

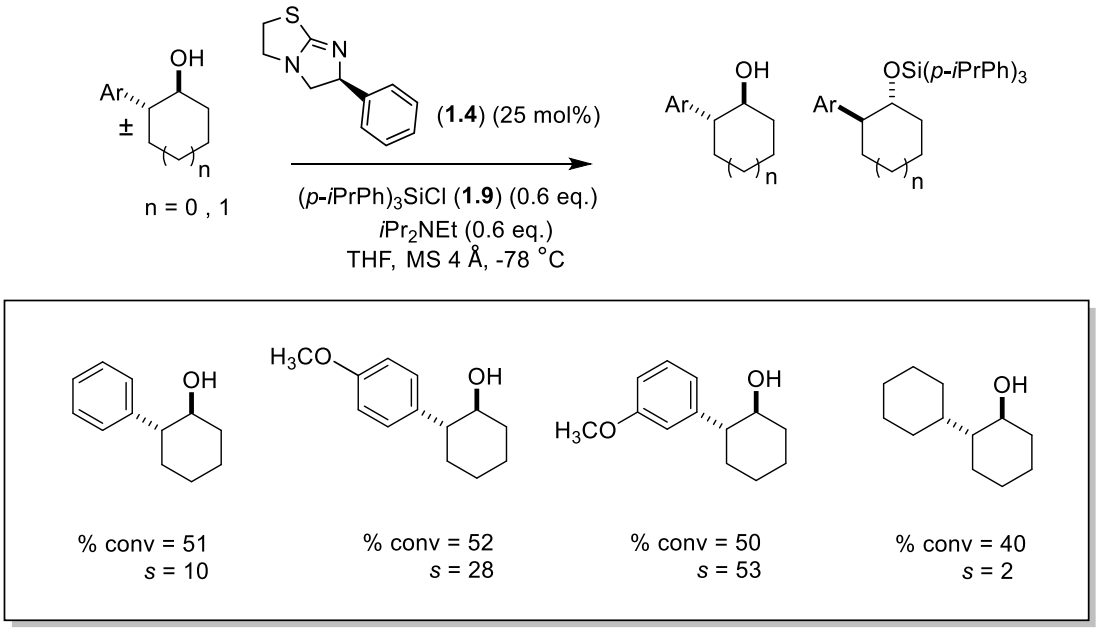

Scheme 1.18 Wiskur's Silylation-Based Kinetic Resolution of *trans* 2-Arylcyclohexanols

The next focus on the mechanistic study of our silylation-based kinetic resolution is exploring the interactions that control the selectivity. In general, asymmetric catalysis selectivity is obtained with the employment of chiral catalysts. To be specific, the origin of

enantioselectivity is the attractive, noncovalent interactions between a chiral catalyst and a substrate.[64] These noncovalent interactions involve hydrogen bonding, ion pairing, π-π stacking and cation-π interactions. Specifically, this dissertation will focus on a potential cation- π interaction as a controlling factor in silylation-based kinetic resolutions.

A cation–π interaction is a covalent attractive force between an electron rich π-system and a proximal cation. Since cation-π interactions were discovered in the 1980s, it has become a mainstay of catalyst design since it is comparable in strength to a hydrogen bond. In a kinetic resolution where selectivity is controlled by a cation-π interaction, many times the catalyst is cationic and the substrate that is being resolved has a π system adjacent to the reactive functional group. Since the catalyst is chiral, one enantiomer of the substrate forms a lower energy cation-pi complex than the other. This difference in association energies leads to the complexed enantiomer undergoing the reaction faster than the unfavorable enantiomer.

Cation-π interactions have been hypothesized to play an important role in controlling the selectivity of kinetic resolutions catalyzed by isothiourea catalysts.[32-33] As we discussed early in this chapter, Birman's acylation-based kinetic resolution employes isothiourea catalysts to control the enantioselectivity. Based on the experimental data, Birman discovered that π-containing functionality on the acyl acceptor is the key factor in deciding enantioselectivity.[32-34] Figure 1.5 shows the transition state of acylation using one of the isothiourea catalysts. Isothiourea catalyst is nucleophilic and became cationic after acylation of the catalyst, resulting in attraction of the incoming alcohol via cation-π interaction. Ultimately the enantioselectivity was controlled. Birman also conducted a computational study to provide further evidence for this hypothesis, ultimately

corroborating the significance of a cation-π interaction.[65] As our silylation-based kinetic resolutions also utilize isothiourea catalysts to obtain selectivity, it is natural to hypothesize that a cation-π interaction is involved in our kinetic resolution. Therefore, the 2nd and 3rd chapter will focus on the exploration of the cation-π interaction within our kinetic resolution.

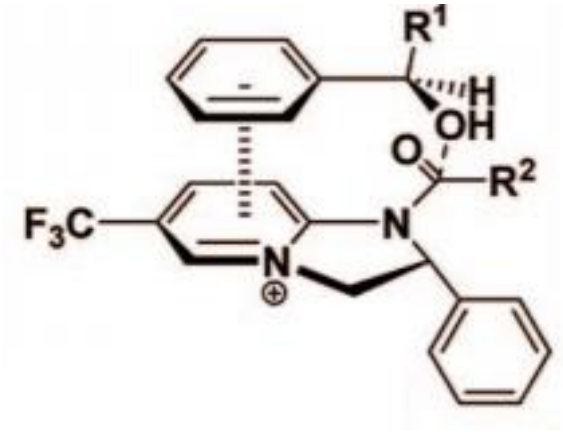

Figure 1.5 TS of Birman's Acylation

1.6 Conclusions

The silylation-based kinetic resolution developed by the Wiskur group had shown great promise in resolving secondary alcohols and providing decent selectivities to resolve a variety of substrates. In recent years, the Wiskur group has focused on the mechanistic studies of these kinetic resolutions. Understanding the mechanism would enlighten the way to further substrate expansion as well as the development of kinetic resolutions using the isothiourea based catalysts or the catalysts with similar structures.

In chapter two, a mechanistic study on the interaction between the isothiourea based catalyst and the alcohol are discussed.[66] To be more specific, how the interactions between (-)-benzotetramisole (**1.4**) and a variety of alkyl 2-hydroxycyclohexanecarboxylates

control enantioselective silylation to achieve selectivity. In chapter 3, another mechanistic study employing a kinetic resolution is introduced. This mechanistic study eliminates the effect of the non-related functional groups and solely focuses on the potential cation-π interactions between the phenyl ring of 2-phenylcyclohexanol and the cationic (-)-benzotetramisole intermediate. The study employs linear free energy relationship studies[67] and computational studies in an effort to understand how selectivity is achieved.[68] The final chapter is an optimization of our previously developed polystyrene-supported triphenylsilyl chloride for the chromatography free separation of enantiomers. The previous work provided facile separation, but selectivity was lost by incorporating the silyl chloride into a polymer. By incorporating a polar monomer into the polymer backbone we were able to obtain better selectivity factors.

1.7 References

1. Wade, L. G.; Simek, J. W., *Organic chemistry*. Ninth edition. ed.; Pearson: Glenview, IL, 2017.

2. Eliel, E. L.; Wilen, S. H.; Mander, L. N., *Stereochemistry of organic compounds*. Wiley: New York, 1994.

3. Cahn, R.; Ingold, C., Specification of configuration about quadricovalent asymmetric atoms. *J. Am. Chem. Soc.* **1951**, 612-622.

4. IUPAC, Compendium of Chemical Terminology, 2nd ed. (the "Gold Book") (1997). Online corrected version: (2006–) "racemate". doi:10.1351/goldbook.R05025

5. Hofland P. "Reversal of Fortune: How a Vilified Drug Became a Life-saving Agent in the "War" Against Cancer". Onco'Zine.

6. Fabro, S.; Smith, R. L.; Williams, R., Toxicity and teratogenicity of optical isomers of thalidomide. *Nature* **1967**, 215 (5098), 296

7. Shah, R. R.; Midgley, J. M.; Branch, S. K., Stereochemical origin of some clinically significant drug safety concerns: Lessons for future drug development. *Adverse. Drug. React .T.* **1998,** *17* (2-3), 145-190.

8. Administration F.a.D. Development of new stereoisomeric drugs. 2005 Jul 6; www.fda.gov/Drugs/GuidanceComplianceRegulatorylnformation/Guidances/ucm122883 .htm.

9. Breuer, M.; Ditrich, K.; Habicher, T.; Hauer, B.; Kesseler, M.; Sturmer, R.; Zelinski, T., Industrial methods for the production of optically active intermediates. *Angew. Chem. Int. Ed.* **2004,** *43* (7), 788-824.

10. Blaser, H. U. The chiral pool as a source of enantioselective catalysts and auxiliaries. *Chem. Rev.* **1992**, 92, 935-952.

11. Carey, J. S.; Laffan, D.; Thomson, C.; Williams, M. T. Analysis of the reactions used for the preparation of drug candidate molecules. *Org. Biomol. Chem.* **2006**, 4, 2337-2347.

12. Nie, L.-D.; Shi, X.-X.; Ko, K. H.; Lu, W.-D., A short and practical synthesis of oseltamivir phosphate (Tamiflu) from (−)-shikimic acid. *J. Org. Chem.* **2009**, 74 (10), 3970-3973.

13. Noyori, R. Asymmetric catalysis: science and opportunities (Nobel lecture). *Angew. Chem. Int. Ed.* **2002**, 41 (12), 2008-2022.

14. Noyori, R.; Ohkuma, T.; Kitamura, M.; Takaya, H.; Sayo, N.; Kumobayashi, H.; Akutagawa, S., Asymmetric Hydrogenation of Beta-Keto Carboxylic Esters - a Practical, Purely Chemical Access to Beta-Hydroxy Esters in High Enantiomeric Purity. *J. Am. Chem. Soc.* **1987,** *109* (19), 5856-5858.

15. Noyori, R.; Ohta, M.; Hsiao, Y.; Kitamura, M.; Ohta, T.; Takaya, H., Asymmetric-Synthesis of Isoquinoline Alkaloids by Homogeneous Catalysis. *J. Am. Chem. Soc.* **1986,** *108* (22), 7117-7119.

16. Mashima, K.; Kusano, K. H.; Sato, N.; Matsumura, Y.; Nozaki, K.; Kumobayashi, H.; Sayo, N.; Hori, Y.; Ishizaki, T.; Akutagawa, S.; Takaya, H., Cationic Binap-Ru(Ii) Halide-Complexes - Highly Efficient Catalysts for Stereoselective Asymmetric Hydrogenation of Alpha-Functionalized and Beta-Functionalized Ketones. *J. Org. Chem.* **1994,** *59* (11), 3064-3076.

17. Keith, J. M.; Larrow, J. F.; Jacobsen, E. N., Practical considerations in kinetic resolution reactions. *Adv. Synth. Catal.* **2001,** *343* (1), 5-26.

18. J. Jacques, A. Collet, S. H. Wilen, *Enantiomers, Racemates,and Resolutions*, Krieger, Malabar, FL, **1991**.

19. Secor, R. M. Resolution of Optical Isomers by Crystallization Procedures. *Chem. Rev.* **1963**, 63, 297-309

20. Ault, A, Org. Synth., Coll. Vol. V, 932 (1973).

21. Ulrich, J.; Jone, M. J. Industrial Crystallization: Developments in Research and Technology. *Chem. Eng. Res. Des.* **2004**, 82, 1567-1570.

22. Fiaud, J. C.; Kagan, H. B., *In Topics in Stereochemistry, L., E.; Wilen, S. H.,* . John Wiley and Sons, Inc.: New York, 1988; Vol. 18.

23. Sheldon R. A. Chirotechnology: Designing Economic Chiral Syntheses, *J. Chem. Tech. Biotechnol.* **1996**, 67, 1-14.

24. Hoveyda, A. H.; Didiuk, M. T., Metal-catalyzed kinetic resolution processes. *Curr. Org. Chem.* **1998,** *2* (5), 489-526.

25. Sheldon, R. A., Consider the environmental quotient. *CHEMTECH*, **1994**, 38-47.

26. Katsuki T., Sharpless K. B., *J. Am. Chem. Soc.***1980**, 102(18), 5974-5976.

27. Patel, R. N., Biocatalytic synthesis of chiral alcohols and amino acids for development of pharmaceuticals. *Biomolecules.* **2013,** *3* (4), 741-77.

28. Vedejs, E.; Chen, X. H., Kinetic resolution of secondary alcohols. Enantioselective acylation mediated by a chiral (dimethylamino)pyridine derivative. *J. Am. Chem. Soc.* **1996**, 118 (7), 1809-1810.

29. Vedejs, E.; Daugulis, O.; Diver, S. T., Enantioselective acylations catalyzed by chiral phosphines. *J. Org. Chem.* **1996,** *61* (2), 430-431.

30. Vedejs, E.; MacKay, J. A., Kinetic resolution of allylic alcohols using a chiral phosphine catalyst. *Org. Lett.* **2001,** *3* (4), 535-536.

31. Vedejs, E.; Daugulis, O., A highly enantioselective phosphabicyclooctane catalyst for the kinetic resolution of benzylic alcohols. *J. Am. Chem. Soc.* **2003,** *125* (14), 4166-4173.

32. Birman, V. B.; Li, X. M., Benzotetramisole: A remarkably enantioselective acyl transfer catalyst. *Org. Lett.* **2006,** *8* (7), 1351-1354.

33. Birman, V. B.; Li, X. M., Homobenzotetramisole: An effective catalyst for kinetic resolution of aryl-cycloalkanols. *Org. Lett.* **2008,** *10* (6), 1115-1118.

34. Li, X.; Liu, P.; Houk, K.; Birman, V. B., Origin of enantioselectivity in CF3− PIP-catalyzed kinetic resolution of secondary benzylic alcohols. *J. Am. Chem. Soc.* **2008,** *130* (42), 13836-13837.

35. Li, X. M.; Jiang, H.; Uffman, E. W.; Guo, L.; Zhang, Y. H.; Yang, X.; Birman, V. B., Kinetic Resolution of Secondary Alcohols Using Amidine-Based Catalysts. *J. Org Chem.* **2012,** *77* (4), 1722-1737.

36. Isobe, T.; Fukuda, K.; Araki, Y.; Ishikawa, T., Modified guanidines as chiral superbases: the first example of asymmetric silylation of secondary alcohols. *Chem. Commun.* **2001,** (03), 243-244.

37. Rendler, S.; Auer, G.; Oestreich, M., Kinetic resolution of chiral secondary alcohols by dehydrogenative coupling with recyclable silicon-stereogenic silanes. *Angew. Chem. Int. Ed.* **2005,** *44* (46), 7620-7624.

38. Manville, N.; Alite, H.; Haeffner, F.; Hoveyda, A. H.; Snapper, M. L., Enantioselective silyl protection of alcohols promoted by a combination of chiral and achiral Lewis basic catalysts. *Nat. Chem.* **2013,** *5* (9), 768-774.

39. Sheppard, C. I.; Taylor, J. L.; Wiskur, S. L., Silylation-Based Kinetic Resolution of Monofunctional Secondary Alcohols. *Org. Lett.* **2011,** *13* (15), 3794-3797.

40. Clark, R. W.; Deaton, T. M.; Zhang, Y.; Moore, M. I.; Wiskur, S. L., Silylation-Based Kinetic Resolution of alpha-Hydroxy Lactones and Lactams. *Org. Lett.* **2013,** *15* (24), 6132-6135.

41. Wang, L.; Akhani, R. K.; Wiskur, S. L., Diastereoselective and Enantioselective Silylation of 2-Arylcyclohexanols. *Org. Lett.* **2015,** *17* (10), 2408-2411.

42. Ruble, J. C.; Latham, H. A.; Fu, G. C., Effective kinetic resolution of secondary alcohols with a planar-chiral analogue of 4-(dimethylamino)pyridine. Use of the Fe(C(5)Ph(5)) group in asymmetric catalysis. *J. Am. Chem. Soc.* **1997,** *119* (6), 1492-1493.

43. Tao, B.; Ruble, J. C.; Hoic, D. A.; Fu, G. C., Nonenzymatic kinetic resolution of propargylic alcohols by a planar-chiral DMAP derivative: Crystallographic characterization of the acylated catalyst (vol 121, pg 5091, 1999). *J. Am. Chem. Soc.* **1999,** *121* (44), 10452-10452.

44. Bellemin-Laponnaz, S.; Tweddell, J.; Ruble, J. C.; Breitling, F. M.; Fu, G. C., The kinetic resolution of allylic alcohols by a non-enzymatic acylation catalyst; application to natural product synthesis. *Chem. Commun.* **2000,** (12), 1009-1010.

45. Sano, T.; Imai, K.; Ohashi, K.; Oriyama, T. Catalytic Asymmeteric Acylation of Racemic Secondary Alcohols with Benzoyl Chloride in the Presence of a Chiral Diamine. *Chem. Lett.* **1999**, 28, 265-266.

46. Kawababa, T.; Nagato, M.; Takasu, K.; Fuji, K. Nonenzymatic Kinetic Resolution of Racemic Alcohols through an "Induced Fit" Process. *J. Am. Chem. Soc.* **1997**, 119, 3169-3170.

47. Copeland, G. T.; Jarvo, E. R.; Miller, S. J. Minimal Acylase-Like Peptides. Conformational Control of Absolute Stereospecificity. *J. Org. Chem.* **1998**, 63, 6784-6785.

48. Li, X.; Jiang, H.; Uffman, E. W.; Guo, L.; Zhang, Y.; Yang, X.; Birman, V. B. Kinetic Resolution of Secondary Alcohols Using Amidine-Based Catalysts. *J org. Chem.* **2012**, 77, 1722-1737.

49. Wuts, P. G. M.; Greene, T. W., Protective Groups in Organic Synthesis. Third ed.; Wiley-Interscience: New York, 1999.

50. Weickgenannt, A.; Mohr, J.; Oestreich, M., Catalytic enantioselective dehydrogenative Si-O coupling of oxime ether-functionalized alcohols. *Tetrahedron.* **2012,** *68* (17), 3468-3479.

51. Steves, A.; Oestreich, M., Facile preparation of CF3-substituted carbinols with an azine donor and subsequent kinetic resolution through stereoselective Si-O coupling. *Org. Biomol. Chem.* **2009,** *7* (21), 4464-4469.

52. Rendler, S.; Plefka, O.; Karatas, B.; Auer, G.; Frohlich, R.; Muck-Lichtenfeld, C.; Grimme, S.; Oestreich, M., Stereoselective Alcohol Silylation by Dehydrogenative Si-O Coupling: Scope, Limitations, and Mechanism of the Cu-H-Catalyzed Non-Enzymatic Kinetic Resolution with Silicon-Stereogenic Silanes. *Chem-Eur. J.* **2008,** *14* (36), 11512-11528.

53. Karatas, B.; Rendler, S.; Frohlich, R.; Oestreich, M., Kinetic resolution of donor-functionalised tertiary alcohols by Cu-H-catalysed stereoselective silylation using a strained silicon-stereogenic silane. *Org. Biomol. Chem.* **2008,** *6* (8), 1435-1440.

54. Zhao, Y.; Mitra, A. W.; Hoveyda, A. H.; Snapper, M. L. Kinetic Resolution of 1,2-Diols through Highly Site- and Enantioselecitve Catalytic Silylation. *Angew. Chem. Int. Ed.* **2007**, 46, 8471-8474.

55. You, Z.; Hoveyda, A. H.; Snapper, M. L., Catalytic Enantioselective Silylation of Acyclic and Cyclic Triols: Application to Total Syntheses of Cleroindicins D, F, and C. *Angew. Chem. Int. Ed.* **2009,** *48* (3), 547-550.

56. Sun, X.; Worthy, A. D.; Tan, K. L., Scaffolding catalysts: highly enantioselective desymmetrization reactions. *Angew. Chem. Int. Ed.* **2011**, 50 (35), 8167-8171.

57. Worthy, A.D.; Sun, X., Tan, K. L. Site-Selective Catalysis: Toward a Regiodivergent Resolution of 1,2-Diols. *J. Am. Chem. Soc.* **2012**, 134, 7321-7324.

58. Giustra, Z. X.; Tan, K. L., The efficient desymmetrization of glycerol using scaffolding catalysis. *Chem. Commun.* **2013,** *49* (39), 4370-4372.

59. Hyodo, K.; Gandhi, S.; van Gemmeren, M.; List, B., Brønsted acid catalyzed asymmetric silylation of alcohols. *Synlett* 2015, 26 (08), 1093-1095.

60. Park, S. Y.; Lee, J.-W.; Song, C. E., Parts-per-million level loading organocatalysed enantioselective silylation of alcohols. *Nat. Commun.* **2015**, 6, 7512.

61. Yoshimatsu, S.; Yamada, A.; Nakata, K., Silylative Kinetic Resolution of Racemic 1-Indanol Derivatives Catalyzed by Chiral Guanidine. *J. Org Chem.* **2017**, 83 (1), 452-458.

62. Akhani, R. K.; Moore, M. I.; Pribyl, J. G.; Wiskur, S. L., Linear Free-Energy Relationship and Rate Study on a Silylation-Based Kinetic Resolution: Mechanistic Insights. *J. Org. Chem.* **2014,** *79* (6), 2384-2396.

63. Wang, L.; Zhang, T.; Redden, B. K.; Sheppard, C. I.; Clark, R. W.; Smith, M. D.; Wiskur, S. L., Understanding Internal Chirality Induction of Triarylsilyl Ethers Formed from Enantiopure Alcohols. *J. Org. Chem.* **2016,** *81* (18), 8187-8193.

64. Kennedy, C. R.; Lin, S.; Jacobsen, E. N., The Cation–Pi Interaction in Small-Molecule Catalysis. *Angew. Chem. Int. Ed.* **2016**, 55, 12596-12624.

65. Liu, P.; Yang, X.; Birman, V. B.; Houk, K., Origin of enantioselectivity in benzotetramisole-catalyzed dynamic kinetic resolution of azlactones. *Org. Lett.* **2012,** *14* (13), 3288-3291.

66. Zhang, T.; Redden, B, K.; Wiskur, S. L., Investigation of electrostatic interactions towards controlling silylation-based kinetic resolutions. *Eur. J. Org. Chem.* DOI: 10.1002/ejoc.201900754

67. Anslyn, E. V.; Dougherty, D. A., *Modern physical organic chemistry*. University science books: 2006.

68. Computational Chemistry, David Young, Wiley-Interscience, 2001. Appendix A. A.1.6 pg 330, Spartan

CHAPTER 2

INVESTIGATION OF ELECTROSTATIC INTERACTIONS TOWARDS CONTROLLING SILYLATION-BASED KINETIC RESOLUTIONS

2.1 Introduction

In chapter 1, the silylation-based kinetic resolution of secondary alcohols developed by the Wiskur group was introduced. The methodology aiming to isolate enantioenriched secondary alcohols was successfully applied to the substrate classes of monofunctional secondary alcohols[1], 2-aryl cyclohexanols[2], and α-hydroxy lactones and lactams[3] with selectivity factors up to 100 (Scheme 2.1).

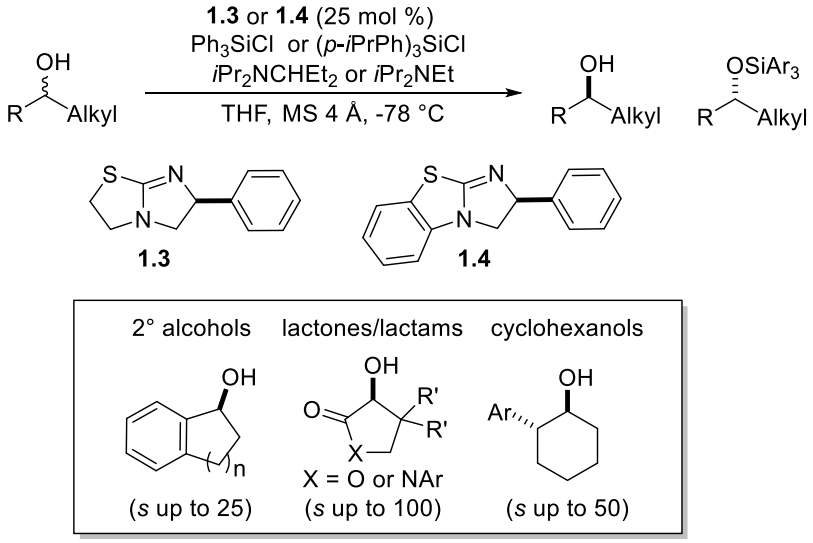

Scheme 2.1 Silylation-Based Kinetic Resolutions from the Wiskur Group

Having proved the effectiveness and efficiency of our kinetic resolution system, our next objective was to unveil the mechanism of our silylation-based kinetic resolution, which is crucial to the optimization of our methodology. This information could lead to the discovery of applicable substrate classes and could help in the design of novel catalysts for asymmetric reactions. The Wiskur group has put forth effort in a series of mechanistic studies on these kinetic resolutions, including a linear-free energy relationship study to investigate the electronic and steric effects of the substituents on the triphenylsilyl chloride (Scheme 2.2), and a study of chiral transmission from point chirality to helical chirality of a triphenylsilyl group (Scheme 2.3).[4-5] The results of these studies helped to elucidate the underlying mechanism for the above-mentioned kinetic resolution, as well as, how enantioselectivity is obtained. In these kinetic resolutions the employment of isothiourea catalysts tetramisole (**1.3**) and benzotetramisole (**1.4**) is important to the success of the kinetic resolution. The electrostatic interactions between the isothiourea catalysts and secondary alcohols are the key to the enantioselectivity. As isothiourea catalysts tend to undergo nucleophilic attack in a reaction and covert to cation complexes, cation-π interactions are commonly proposed as an interaction that aids in controlling selectivity. As discussed in chapter 1, a cation-pi interaction is a noncovalent interaction between the face of an electron-rich π system (e.g. benzene, ethylene, acetylene) and an adjacent cation. One could imagine an interaction betweencationic isothiourea catalysts and substrates with π systems to aid in orienting substrates to obtain selective reactions. This chapter will focus on understanding the electrostatic interactions (potentially cation-π interaction) between isothiourea catalysts and secondary alcohols.

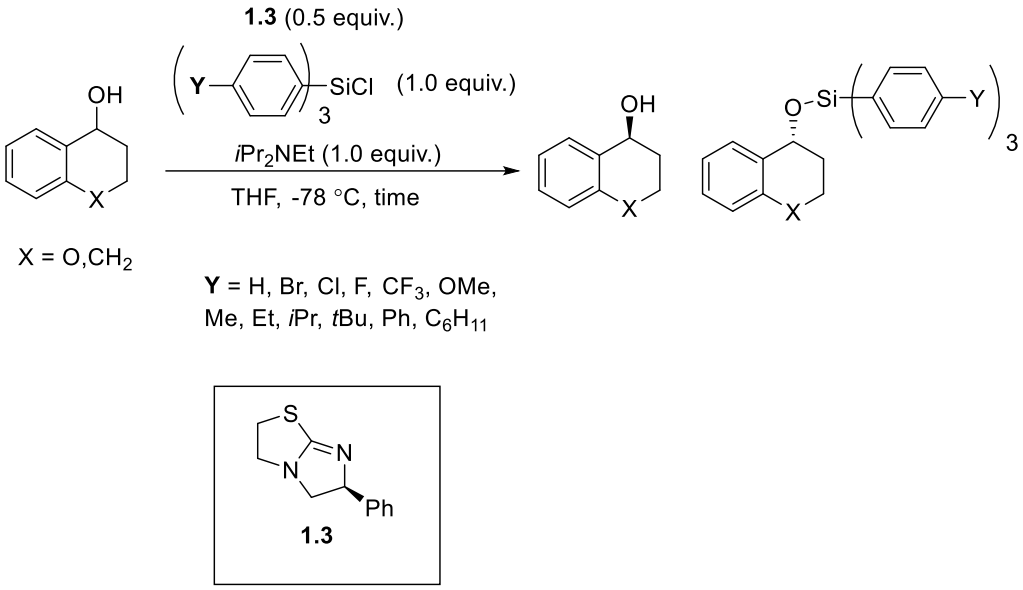

Scheme 2.2 Kinetic Resolution Using Different para-Substituted Triphenylsilyl Chlorides

In the previous study,[4] a mechanistic cycle was proposed, that simply suggested a formation of a cationic intermediate (**2.1**) between (-)-tetramisole (**1.3**) and triphenylsilyl chloride when the silyl chloride is nucleophilicly attacked by (-)-tetramisole (**1.3**). The newly formed cationic intermediate (**2.1**) would in turn be attacked by the secondary alcohol to form the final silyl ether product (Scheme 2.3). The trick to achieve the enantioselectivity is through the cation-π intermolecular interaction between the π system of secondary alcohol and cationic intermediate (**2.1**). Since the cationic intermediate (**2.1**) is chiral, the binding of one alcohol enantiomer to the cationic intermediate would be lower in energy versus the other enantiomer. The stronger intermolecular interaction between one of the secondary alcohol enantiomers and the cationic intermediate (**2.1**) would lead to one enantiomer reacting preferentially over the other, eventually leading to a kinetic resolution or a separation of enantiomers.

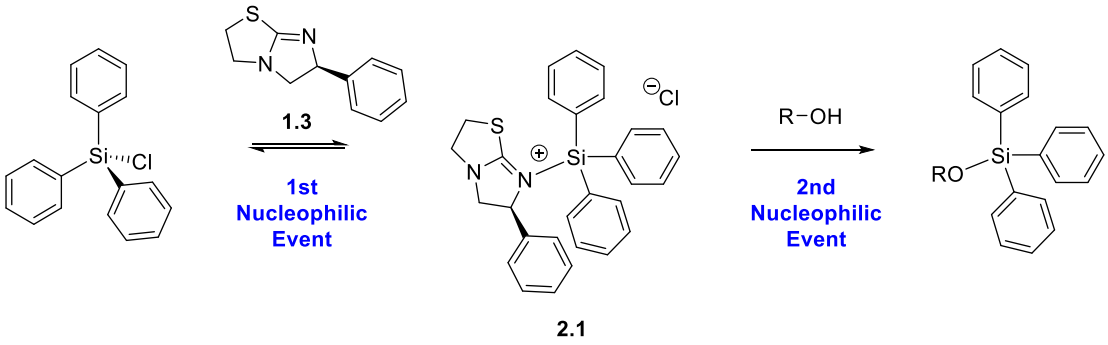

Scheme 2.3 Proposed Mechanism of Silylation-Based Kinetic Resolution

Since kinetic resolutions have emerged as a powerful approach to isolate enantiopure compounds, a great number of studies have been done to explore the intermolecular interactions controlling the selectivities. Intermolecular interactions such as hydrogen bonding, π-π stacking, and ionic forces have been shown to play a large role in controlling the selectivity and reactivity of organocatalyzed reactions, in many cases working cooperatively to obtain a favorable outcome.[6-8] Electrostatic interactions such as π-π interactions and cation-π interactions[9-11] have been shown to aid in controlling the selectivity of asymmetric reactions through an electrostatic interaction between a substrate and a catalyst.[12-16] A good example to show how these electrostatic interactions work is the asymmetric addition of chiral boronate complexes to quinolinium reported by Aggarwal (Scheme 2.4).[17] Under the aid of Troc-Cl, quinolinic amide **2.2** was treated with chiral boronate complex **2.3**, and an enantioselective addition proceeded to prepare 1,4-dihydroquinoline **2.4** with an enantiomeric excess over 99%. Such great enantioselectivity was obtained through an important transition state **2.5**. During the transition state **2.5**, a cation−π interaction was generated between the cationic complex formed by the treatment Troc-Cl on quinolinic amide **2.2** and chiral boronate complex **2.3**. The cation−π interaction

helps orientate the chiral boronate complex to approach only one reaction face of the quinolinic amide **2.2**.

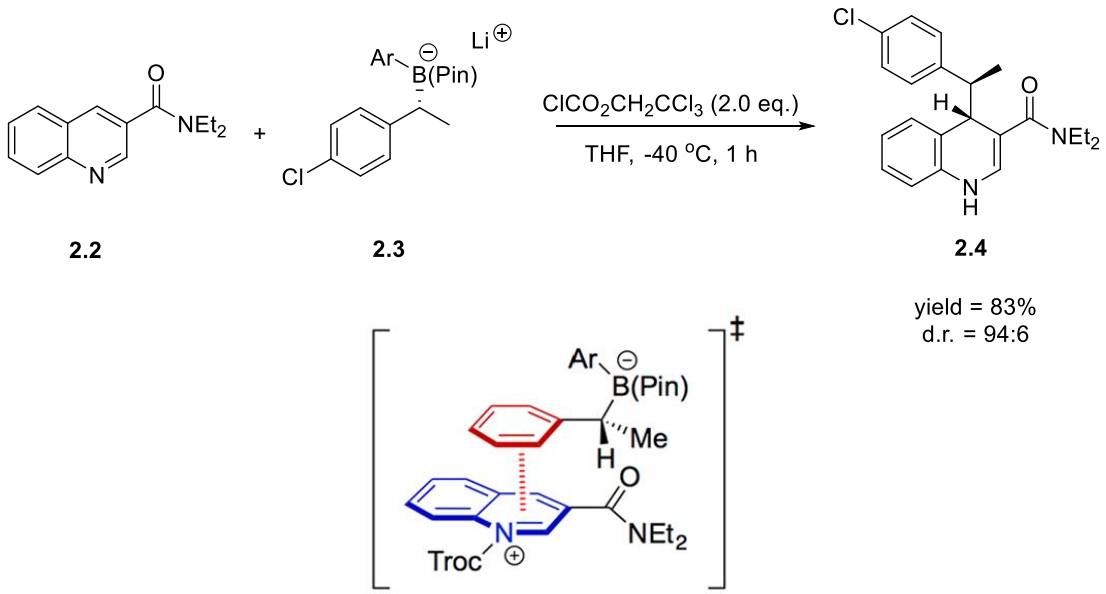

2.2 **2.3** **2.4**

yield = 83%
d.r. = 94:6

2.5

Scheme 2.4 Addition of a Chiral Boronate Complex to Quinolinic Amide

A cation-π interaction is an electrostatic interaction that is applied in the design of asymmetric reactions where the substrates contain aromatic groups as the π donors. However, there are also a number of asymmetric reactions where enantioselectivity was achieved by a cation-π interaction with a non-aromatic π system. Takahashi reported an efficient stereoselective intramolecular cyclization from *N*-acyliminium **2.6** to *N*,*N*-acetal **2.7** via an intramolecular addition of an *N*-sulfonylamino group (Scheme 2.5).[18] A diastereoselectivity over 99% was obtained through the intermediate iminium ion **2.8**. The intramolecular cation−π interaction between the iminium and the sulfonyl group selectively controls cyclization to occur on one face over the other. Inspired by the significant role cation-π interactions play in asymmetric reactions, we have theorized that these type of

electrostatic interactions are also controlling the selectivity of our silylation-based kinetic resolutions, given that our substrates need to have a π system within the structure to obtain any selectivity.[2] We presume the existence of a cation-π interaction between cationic catalyst intermediate **2.1** and the π systems on our secondary alcohols.

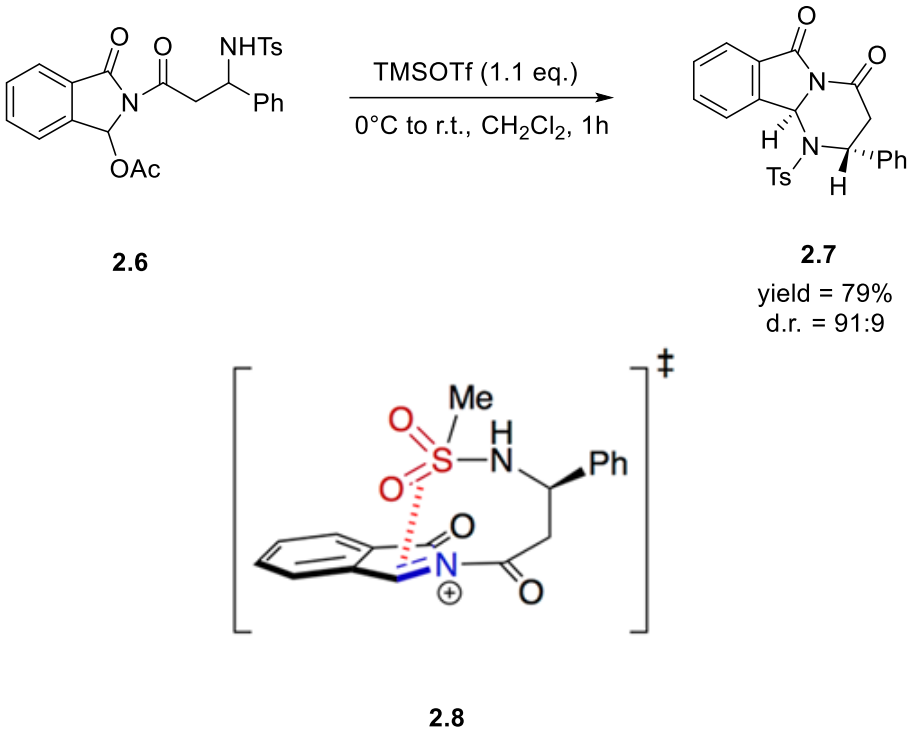

2.6

2.7
yield = 79%
d.r. = 91:9

2.8

Scheme 2.5 Intramolecular Addition of an *N*-Sulfonylamino Group to an *N*-Acyliminium Ion

We wanted to explore this potential electrostatic interaction between cationic catalysts and alcohols by employing substrates that vary in sterics and electronics to alter the strength of the asymmetric controlling interaction as the substrate changes. Ultimately, we can explore what type of linear free energy relationship exists to understand the nature of the interaction. Therefore, an appropriate substrate class is needed for the investigation. Not only does the chosen substrate class have to perform well in our

silylation-based kinetic resolution, but it also needs to possess a structure that could be easily derivatized. In our previous study, we concluded that a successful substrate class consists of a relatively planar π system on one side of the secondary alcohol and sterics on the other side of the alcohol (Figure 2.1).[2] Notice that substrates that lack a pi system in Figure 2.1 lack any selectivity in the kinetic resolution. In most cases, a cyclohexyl ring is a decent source of steric effects. Therefore, our models were designed based on cyclohexanol with the addition of a π system at the beta position. This led us to choose *trans*-alkyl-2-hydroxycyclohexanecarboxlateas, an ideal model for our silylation-based kinetic resolution. Since the preparation of an ester is easily achieved through the reaction between a carboxylic acid and an alcohol, various esters could be synthesized by utilizing different alcohols that varied in sterics and electronics. This will allow us to explore linear free energy relationship studies to explore the correlation of selectivity with both the size of the ester substituent and the electronics of the aryl group on the ester, potentially indicating how sterics and electronics affect the strength of this interaction.

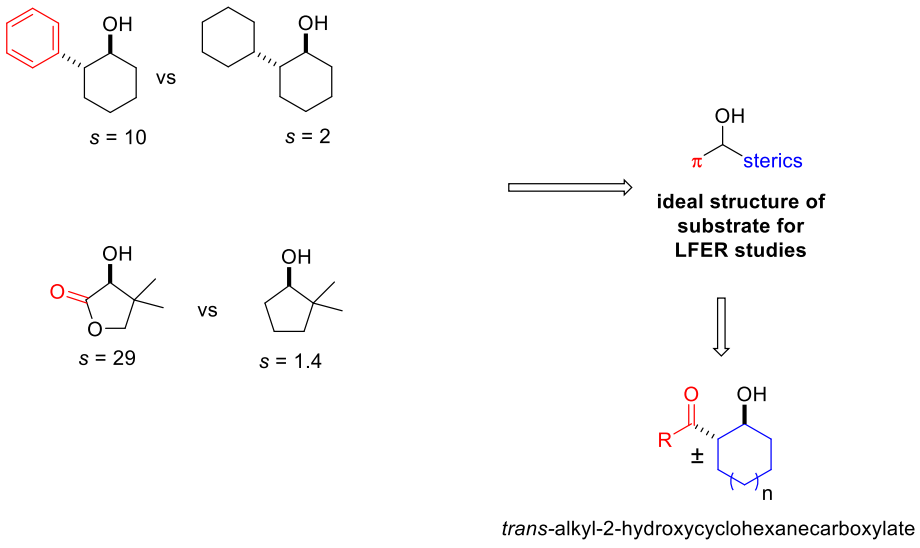

Figure 2.1 Ideal Substrate Class of Silylation-Based Kinetic Resolution

2.2 Synthesis of *trans*-alkyl-2-hydroxycyclohexanecarboxylates

trans-Alkyl-2-hydroxycyclohexanecarboxylates (**2.12**) are not commercially available and were prepared from a three-step synthesis based on existing literature (Scheme 2.6).[19-21] The synthesis started with commercially available cyclohexanone (**2.9**). One-pot synthesis of 2-oxocyclohexane-1-carboxylic acid (**2.10**) was the most challenging step and it was optimized based on the equipment of our lab. This step began with a preparation of lithium diisopropylamide simply by dropwise addition of *n*-BuLi to diisopropylamine. Then **2.9** was added dropwise to the newly formed lithium diisopropylamide, forming the enolate of **2.9.** Deprotonation of the α-carbon was normally achieved in less than an hour. The last step to synthesize **2.10** involved pumping CO_2 into the reaction. Since we did not have a tank of CO_2 in our lab, we just simply generated the CO_2 by letting dry ice sublimate in a Schlenk round-bottom flask at room temperature. The CO_2 coming from the round-bottom flask was passed through a drying tube before it reached the reaction flask. Fresh CO_2 was constantly flowing into the reaction. Compound **2.10** could be synthesized in a large scale but must be stored in the freezer to prevent decomposition. With **2.10** in hand, the rest of the steps were simple. We tried many different methods to form the ester **2.11** and found that the easiest method was the DCC coupling of **2.10** with respective alcohols (Table 2.2 substrates from entry 2-8 synthesized in this approach). The last step to synthesizing *trans*-alkyl-2-hydroxycyclohexanecarboxylates (**2.12**) was the reduction of ketone. Milder reducing reagents than $NaBH_4$ needed to be used since we observed a reduction of the ester when $NaBH_4$ was used for the reduction. We found sodium cyanoborohydride to be a perfect

reducing agent for the reduction of **2.11**, which provided a full reduction of the ketone and no reduction of ester**.**

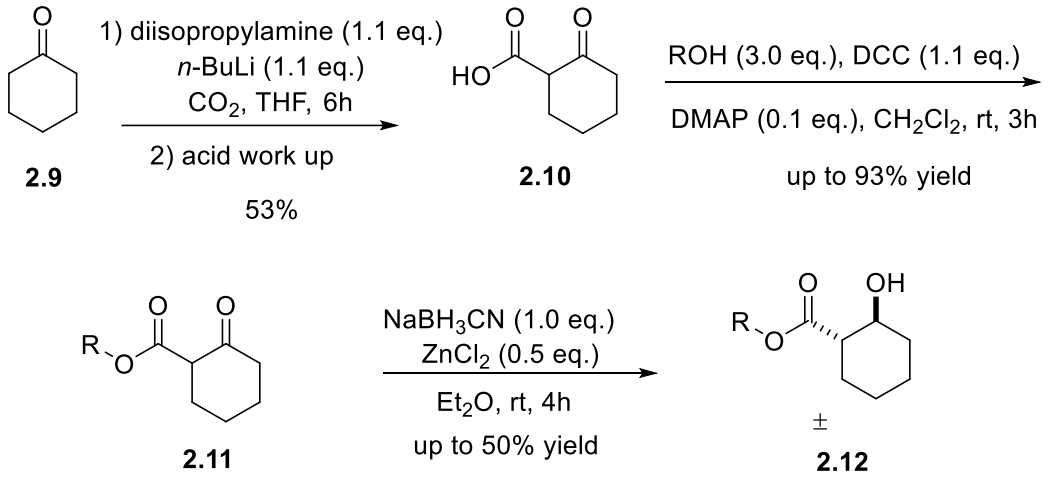

Scheme 2.6 Synthesis of *trans*-Alkyl-2-hydroxycyclohexanecarboxylates

2.3 Initial Investigations and Optimizations

With *trans*-alkyl-2-hydroxycyclohexanecarboxlateas in hand, our next focus was optimization of reaction conditions. The results are shown in Table 2.1. Chiral catalysts (**1.3** and **1.4**) were employed to activate a silyl chloride to preferentially silylate one alcohol enantiomer over the other, generating silyl ethers (**2.12a-b**) and recovering enantiomerically enriched alcohol ((+)-**2.9**). Similar to our previous work, the catalyst with the fused aromatic ring, (-)-benzotetramisole (**1.4**),[22] gave higher selectivity than the less conjugated version ((-)-tetramisole, **1.3**) (Table 2.1, Entry 1 vs 2, Entry 3 vs. 4). In a previous study, we noted that three phenyl groups on the silyl chloride are needed in order to obtain useful levels of selectivity,[1] and electron-donating isopropyl groups in the para position also resulted in improved selectivity.[4] These factors were also important in obtaining good selectivity with this substrate. When tris(4-isopropylphenyl)silyl chloride

(**1.9**) was utilized, selectivity increased versus employing the unsubstituted triphenylsilyl chloride (**1.8**) (entry 2 versus 4). Electron donating groups on the silyl group are hypothesized to stabilize the reactive silicon/catalyst intermediate.[4]

Absolute stereochemistry (+/-) of recovered starting material of **2.9** was determined by testing the optical rotation of recovered starting material and compared the data to the existing literature (for details please check section 2.6). Absolute stereochemistry (+/-) of recovered starting material of other derivatives were determined by reducing the ester with $LiAlH_4$ in diethyl ether to give the diol 2-(hydroxymethyl)cyclohexan-1-ol. The optical rotation of that compound was compared to literature values, suggesting that we obtained the same major enantiomers.

Table 2.1 Optimization of Reaction Conditions for Resolution of *trans*-Ethyl-2-hydroxycyclohexanecarboxylate

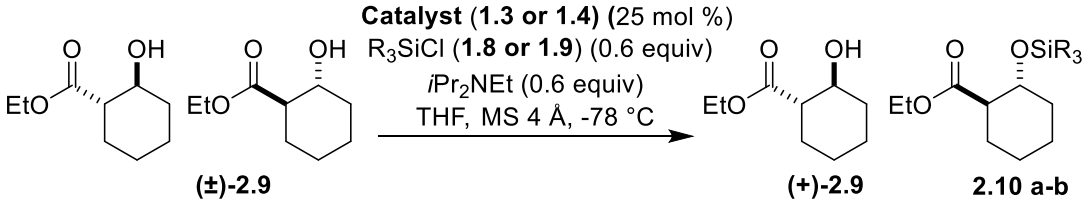

Entry[b]	catalyst	R	*t* (h)	conv (%)[a]	*s*[a]
1	**1**	Ph (**1.8**)	24	47	3
2	**2**	Ph (**1.8**)	24	44	11
3[c]	**1**	*p*-*i*Pr-Ph (**1.9**)	48	18	3
4	**2**	*p*-*i*Pr-Ph (**1.9**)	48	36	14

[a]Conversions and selectivity factors are based on the ee of the recovered starting materials and products. See ref [23]. [b]Selectivity factors are an average of two runs. Conversions are from a single run. [c]Conversion and selectivity factor is based on the ee of the recovered starting material and 1H NMR conversion.

2.4 Kinetic Resolution of Various *trans*-Alkyl 2-hydroxycyclohexanecarboxylates

With the optimized reaction conditions obtained, the effect of altering the sterics on the ester group was explored (Table 2.2). When the ethyl group of *trans* ethyl 2-hydroxycyclohexanecarboxylate (**2.9**) was changed to an isopropyl group, a decrease in the selectivity factor was observed (from s = 14 to 10) presumably from an increase in steric hindrance of the ester (Table 2.2, entry 2). In order to provide evidence that sterics on the ester correlate to the selectivity factor, multiple 2-ester cyclohexanol derivatives were synthesized through the esterification of 2-hydroxycyclohexanecarboxylate and tested under the optimized conditions. As predicted, substrates with cyclohexyl and *t*-butyl groups also followed the same trend of decreasing selectivity as the alkyl group on the ester increased in size (Table 2.2, entry 3 and 4). The sensitivity of these selectivity factors (Table 2.2, entries 1-4) to steric hindrance was then investigated using Charton (υ) values in a linear free energy relationship[24-26] to establish if there is a correlation between the steric effect and selectivity. Charton values are substituent parameters that use the van der Waals radius of the substituent to study sterics.[27-29] The log of the selectivity factors for the different substrates were plotted against the Charton values associated with each alkyl group (Figure 2.2). Indeed, there is a strong linear correlation between the steric effect near the π-system and the selectivity factors (Ψ = -0.7), showing that as sterics increase selectivity decreases. The sterics obviously have a negative impact regarding how the substrate and the reactive intermediate organize in the transition state to obtain selectivity. The sterics also play a negative effect on reactivity, with the conversion of the reaction

decreasing as sterics increase. In fact, the t-butyl substrate has very little conversion over a 24-hour period (Table 2.2, entry 4).

Table 2.2 Substrate Scope of the Silylation-Based kinetic Resolution of *trans*-Alkyl-2-hydroxycyclohexanecarboxylate

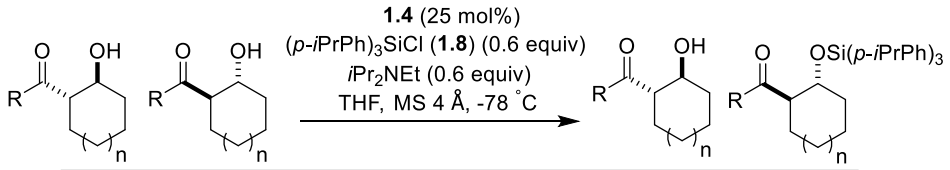

entry[b]	recovered alcohol	er of recovered alcohol	conv (%)[a]	*s*[a]
1	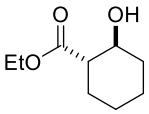	72:28	36	14
2	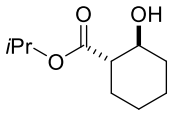	55:45	35	10
3	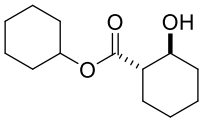	66:34	30	8.4
4[c]	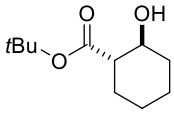	52:48	6	4.7
5[c]	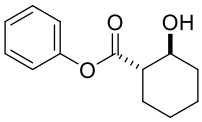	64:36	41	3
6[c]	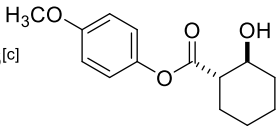	58:42	20	4.4
7[c]	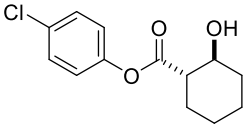	82.5:17.5	43	27
8[c]	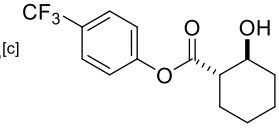	69:31	29	34

9	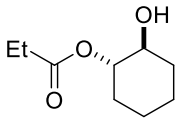	60:40	38	3
10	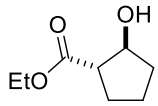	61:39	45	2.7

[a]Conversions and selectivity factors are based on the ee of the recovered starting materials and products. See ref [23]. Selectivity factors are an average of two runs. Conversions are from a single run. [b]Reactions were run for 48 h at a concentration of 0.42 M with respect to alcohol on a 0.4 mmol scale. [c]Conversion and selectivity factor is based on the ee of the recovered starting material and ^{1}H NMR conversion.

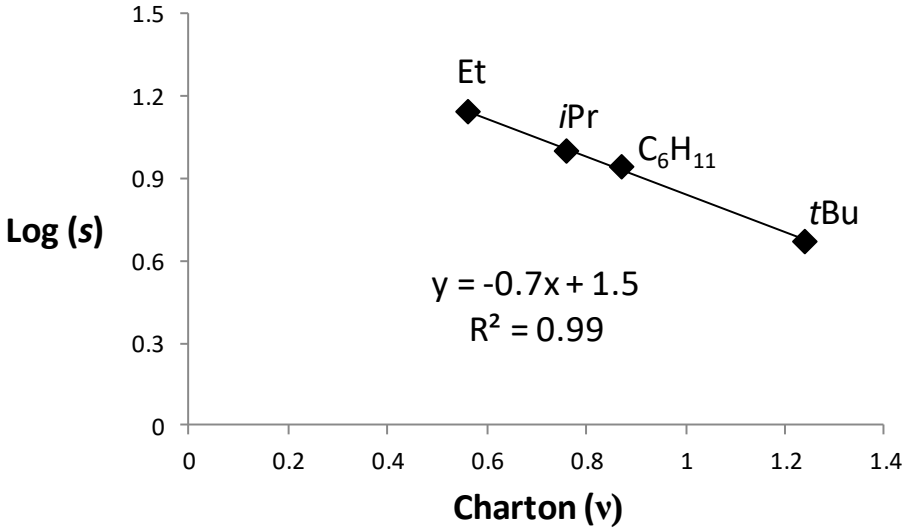

Figure 2.2 LFER Employing Charton Values to Selectivity for the Sterics of the Ester Substituent

In order to modulate the electronics of the ester with the intention of altering the strength of the electrostatic interaction controlling selectivity, phenyl esters were synthesized with either a hydrogen or an electron withdrawing group in the para position on the phenyl ring (Table 2.2, Entries 5-8). It is known that the phenyl group on a phenyl ester is not in resonance with the ester group, but is rotated such that the plane of the phenyl

group is perpendicular to the plane of the s-*trans* ester.[30] Since Neuvonen and coworkers have shown that electron donating and withdrawing substitutents on these phenyl groups affect the polarity of the carbonyl,[31-32] we hypothesized that the selectivity of the kinetic resolution would also be affected with different substituents. When just a phenyl group was employed, the selectivity was pretty low (Table 2.2, Entry 5). By adding a methoxy group, which is inductively a mild electron withdrawing group, the selectivity slightly increased to $s = 4.4$ (Table 2.2, Entry 6), therefore only weakly enhancing the electrostatic interaction. When the para position was substituted with stronger electron withdrawing groups such as a chloro or a trifluoromethyl group, the selectivity significantly increased to $s = 27$ and 34 respectively (Table 2.2, Entries 7 and 8). While stronger electron withdrawing groups increase the electron density on the carbonyl carbon which would help promote a cation- π interaction, methoxy is considered an electron donating group regarding polarization of the carbonyl and decreases the electron density on the carbonyl carbon which would ultimately decrease the strength of the interaction with the cationic catalyst which does not support the data.

A linear free energy relationship (LFER) was found for the four substrates when sigma meta (σ^m) substituent parameters[33] were plotted against the log of the selectivity factor showing that as electron withdrawing groups become stronger selectivity increased, resulting in a significant sensitivity constant (ρ) of 2.6 (Figure 2.3). Edge to face π-π interactions are enhanced when one π system is electron deficient,[34] suggesting that the selectivity defining interaction for the phenyl esters is a π interaction with one of the aryl groups on the catalyst or silicon.

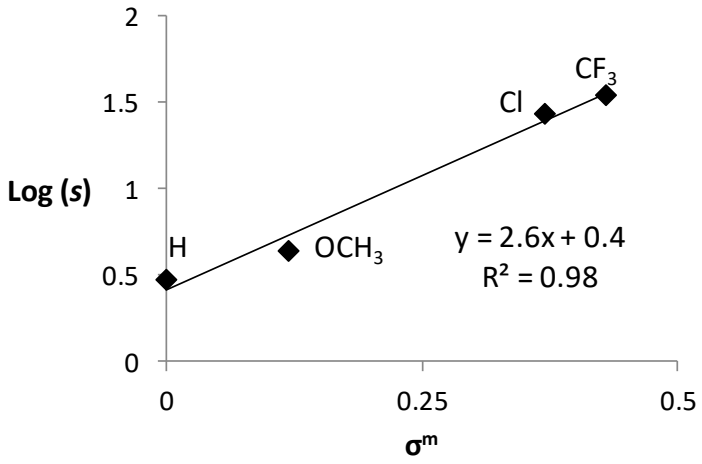

Figure 2.3 LFER Employing σ^m to Selectivity for the Induction of the Ester Substituent

In order to provide more evidence that the substituents are contributing to the interaction through induction, not resonance the Swain-Lupton dual parameter approach was used to determine the percent contribution of each effect, by using substituent constants for both field effects and resonance.[35-36] The log of the selectivity factor is set equal to the sum of the substituent constants for field effects (F) and resonance (R), with sensitivity factors for each (*f* and r respectively) (Equation 2.1). The experimental data is plotted against the predicted data and the sensitivity factors are solved for, ultimately looking for a slope of one. As expected, the sensitivity factor for field effects was about 2.5 times higher than the sensitivity factor for resonance, indicating that the field effects contribute more significantly towards controlling selectivity (Figure 2.4).

$$\log(s) = fF + rR$$

Equation 2.1

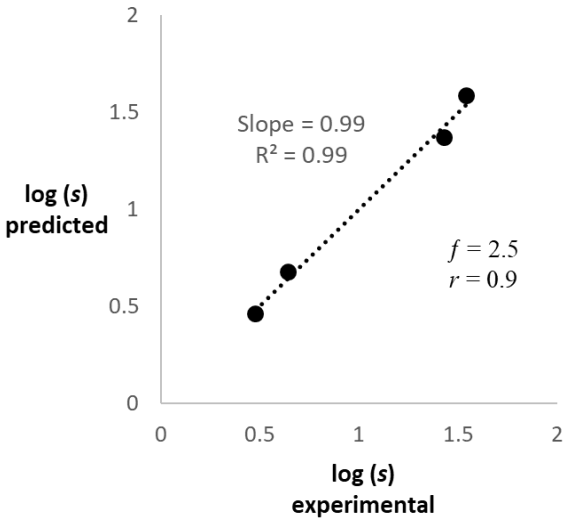

Figure 2.4 Comparison of Experimental log(s) Using Selectivity Factors from Table 2.2 vs Predicted log(*s*)

The last two entries in Table 2.2 highlight the importance of ring size and positioning of the π system. A six membered ring is needed in order to obtain selectivity, as seen in Table 2.2 entry 10 (vs. Table 2.2, entry 1) where the selectivity factor dropped to 2 when a cyclopentanol substrate was employed. When the orientation of the ester on the cyclohexanol was reversed, the selectivity of the reaction was very low (Table 2.2, entry 9, s = 3). We hypothesize that the intramolecular hydrogen bonding between the ester carbonyl and hydroxyl group of **2.9** forms a stable six-membered ring which aids in controlling selectivity, by favoring a chair conformation with both the hydroxyl and ester group in an equatorial position and prevents free rotation of the ester. When the orientation of the ester is switched in Table 2.2, entry 9, the intramolecular hydrogen bond forms a less energetically favorable seven membered ring, weakening that interaction (Figure 2.5). Ultimately, the π system is moved further from the reacting alcohol, and the

ester is more likely to be freely rotating. This prevents optimal electrostatic interactions, reducing the selectivity of the kinetic resolution.

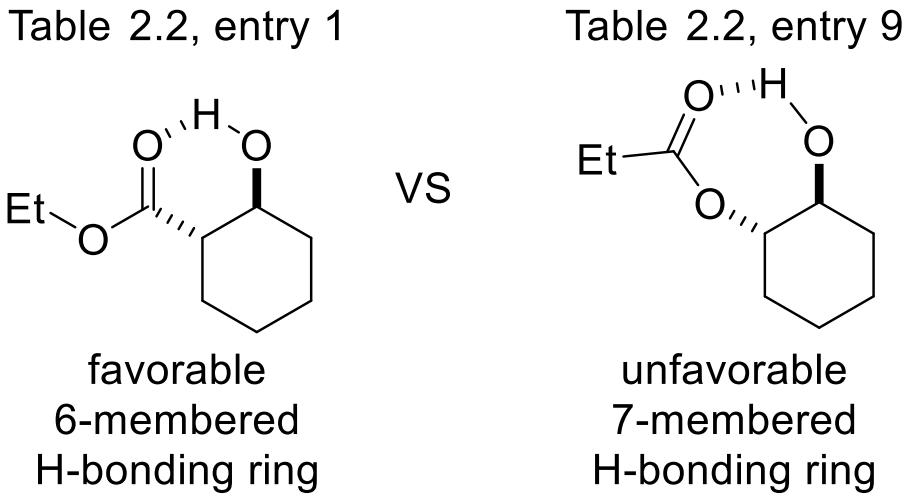

Figure 2.5 Comparison between 6- and 7-Membered Rings Formed from Intramolecular Hydrogen Bonding

2.5 Conclusions and Outlook

In conclusion, we have investigated potential electrostatic interactions between the proposed, reactive catalytic species and *trans* 2-ester substituted cyclohexanols by varying sterics and electronics on the ester π system. The electrostatic attraction helps align the substrate to the catalyst in an orientation that allows for increased selectivity. An increase in sterics adjacent to the π-system affects the ability to orient favorable, resulting in a decrease in selectivity which correlates well with Charton substituent constants. Substituting the ester with aryl groups affects the selectivity, mainly through field effects deduced from a Swain-Lupton analysis. The data suggests that an edge to face π-π interaction is dominating given that electron withdrawing groups dramatically increase the selectivity of the reaction. Finally, the ability of the hydroxyl group to form a favorable

hydrogen bond to the carbonyl of the ester (6- vs 7-membered rings) is an aspect that promotes an increase in selectivity. Future work will focus on computational modelling of these and similar systems and looking at other systems to see if similar trends are followed.

2.6 Experimental

General Information

All the reactions were carried out under a nitrogen atmosphere using oven-dried glassware. Molecular sieves were activated in an oven at 170 °C before use. Tetrahydrofuran (THF), diethyl ether, methanol and dichloromethane (CH_2Cl_2) were dried by passing through a column of activated alumina before use and stored over molecular sieves. Carbon tetrachloride (CCl_4) was distilled and degassed prior to use. Sulfuryl chloride (SO_2Cl_2) was distilled before use. *n*-BuLi was titrated prior to use.[34] Unless otherwise stated, all the other chemicals were obtained from major commercial sources and used without further purification. High resolution mass spectrometry (HRMS) was conducted by the mass spectrometry facility in the Department of Chemistry and Biochemistry at the University of South Carolina. Infrared spectroscopy (IR) was conducted using a Perkin Elmer Spectrum 100 FT-IR ATR spectrophotometer, ν_{max} in cm^{-1}. ^1H NMR was taken on a Bruker Avance (400 or 300 MHz). Chemical shifts were reported in ppm with TMS or chloroform as an internal standard (TMS: 0.00 ppm for ^1H and ^{13}C; $CHCl_3$: 7.26 ppm and 77.16 for ^1H and ^{13}C respectively). ^{13}C NMR spectra were taken on a Bruker Avance (101 or 75 MHz) with complete proton decoupling. Enantiometic ratios were determined via HPLC using an Agilent 1200 series employing the following chiral

stationary phases, Daicel Chiralcel OD-H, OJ-H, AD, AD-H or Daicel Chiralpak IC columns, monitored by a diode array detector in comparison with the racemic materials. Optical rotations were obtained utilizing a JASCO P-1010 polarimeter.

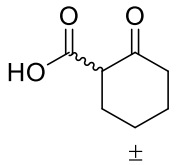

±

2-Oxocyclohexane-1-carboxylic acid

The compound 2-oxocyclohexane-1-carboxylic acid was prepared optimized based on a literature procedure.[19] A solution of diisopropylamine in 210 mL of dry THF in three-neck round bottom flask was cooled to -78 ^{o}C under a N_2 atmosphere. Then *n*-BuLi (29.7 mmol) was added drop wise to the three-neck round bottom flask. After the addition was completed, the solution was stirred at -78 ^{o}C for an hour. Then a solution of cyclohexanone (27 mmol) in 45 mL of THF was added drop wise to the mixture. The reaction mixture was stirred at -78 ^{o}C for an hour and warmed to 0 ^{o}C for another hour. Ultimately, the reaction was cooled back to -78 ^{o}C and pumped in fresh CO_2 (CO_2 was generated from the sublimation of dry ice) through a drying tube. The conversion of final product is highly depended on the reaction time, normally a yield around 50% could be obtained in 4 hours of reaction time. Once the desired conversion was reached, the three-neck round bottom flask was moved to the room temperature and quenched with 100 mL of deionized water. 100 mL of diethyl ether was then added to the mixture and extraction of aqueous layer was applied. Once the aqueous layer was isolated, It was treated with 1 M HCl solution until the pH value is below 2. At the end, the mixture was extracted with 100 mL of diethyl ether

for three times. The organic layers were combined, dried with magnesium sulfate and concentrated, affording a white solid. (1.86g, 13.1 mmol, yield 48.5%)

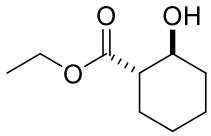

±

***Trans*-ethyl-2-hydroxycyclohexane-1-carboxylate**

To a 50 ml round bottom flask was added the ethyl 2-oxocyclohexanecarboxylate (3.19 g, 18.8 mmol) and dried methanol (30 ml). The solution was treated with $NaBH_4$ (0.2 g, 5.3 mmol) and stirred at room temperature for 3 hours. After quenching with saturated NH_4Cl, the aqueous layer was extracted with diethyl ether (3 x 10 ml), and the organic dried over anhydrous Na_2SO_4, filtered and concentrated. The crude was purified via silica gel chromatography (starting at 5% EtOAc in hexanes to 25% EtOAc) giving a colorless transparent oil (808 mg, 4.7 mmol, yield 25%). **^{1}H NMR** (400 MHz, $CDCl_3$) δ ppm 4.18 (q, J = 7.1 Hz, 2H), 3.77 (dd, J = 10.1, 5.4 Hz, 1H), 2.90 (s, 1H), 2.25 (ddd, J = 12.4, 9.9, 3.8 Hz, 1H), 2.11 – 1.93 (m, 2H), 1.83 – 1.62 (m, 2H), 1.39 – 1.17 (m, 7H). **^{13}C NMR** (101 MHz, $CDCl_3$) δ ppm 175.3, 70.9, 60.6, 51.3, 33.6, 28.1, 25.1, 24.3, 14.2.

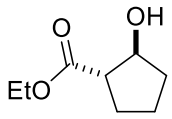

±

***Trans*-ethyl-2-hydroxycyclopentane-1-carboxylate**

To a 50 ml round bottom flask fitted with a Teflon coated stir-bar was added the commercially available ethyl 2-oxocyclopentanecarboxylate (2.93 g, 18.8 mmol) and dried

methanol (30 ml). The solution was treated with $NaBH_4$ (0.2 g, 5.3 mmol) and stirred at room temperature for 3 hours. The reaction was then quenched with saturated NH_4Cl, the aqueous layer was extracted with diethyl ether (3 x 10 ml) and the organic layers were then combined, dried over anhydrous Na_2SO_4, filtered and concentrated. The crude was purified via silica gel chromatography (starting at 5% EtOAc in hexanes and gradually increasing to 10% and 25% EtOAc) giving a transparent oil, 822 mg, 5.2 mmol, yield 28%. **^{1}H NMR** (400 MHz, $CDCl_3$) δ 4.38 (q, J = 6.4 Hz, 1H), 4.16 (q, J = 7.1 Hz, 2H), 2.81 – 2.52 (m, 1H), 2.32 (s, 1H), 2.14 – 1.91 (m, 2H), 1.89 – 1.49 (m, 4H), 1.27 (t, J = 7.1 Hz, 3H). **^{13}C NMR** (101 MHz, $CDCl_3$) δ ppm 175.0, 76.3, 60.6, 52.7, 34.1, 27.2, 22.0, 14.3.

General Procedure for the Preparation of *trans*-alkyl 2-hydroxycyclohexanecarboxylates[20-21] (GP1)

The starting carboxylic acid, 2-oxocyclohexane-1-carboxylic acid (1.0 equiv.) and CH_2Cl_2 (0.5 M) were added to a 25 mL round bottom flask equipped with a stir bar. Next, 4-dimethylaminopyridine (0.1 equiv.) was added, followed by the alcohol (3.0 equiv.) to be coupled. The solution was stirred and cooled in an ice bath at 0 °C. Then the solid dicyclohexylcarbodiimide (1.1 equiv.) was slowly added to the mixture. The reaction mixture was stirred for 3 hours at room temperature. The reaction was then quenched with water, extracted with diethyl ether three times, and dried over anhydrous $MgSO_4$. Concentration of the reaction mixture via reduced pressure afforded an oil, which was taken on without further purification. This oil was dissolved in diethyl ether to prepare a 1.25 M solution and was added to a suspended solution of sodium cyanoborohydride (1 equiv.) and zinc chloride (0.5 equiv.) in diethyl ether (0.04 M) at room temperature. The

reaction was stirred at room temperature for 4 hours. It was then diluted with the same volume of diethyl ether that was used to make the original solution and quenched with a 0.1 M potassium iodate solution. The aqueous layer was extracted with diethyl ether three times, then the ether layers were combined, washed with water and brine, and dried over anhydrous $MgSO_4$. The *trans* isomer was purified via silica gel chromatography (5% EtOAc in hexanes increasing to 5% EtOAc in hexanes, then to 25% EtOAc in hexanes).

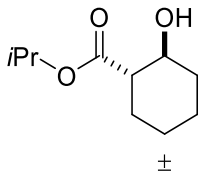

±

***Trans*-isopropyl-2-hydroxycyclohexane-1-carboxylate**

The product was prepared from 2-propanol (11 mmol) according to **GP1.** The desired product was obtained as a transparent colorless oil, 242 mg, 1.3 mmol, 35.5 % yield. **^{1}H NMR** (400 MHz, $CDCl_3$) δ 5.06 (hept, J = 6.2 Hz, 1H), 3.76 (td, J = 10.0, 4.6 Hz, 1H), 2.88 (s, 1H), 2.21 (ddd, J = 13.1, 10.3, 4.2 Hz, 1H), 2.10 – 1.93 (m, 2H), 1.82 – 1.65 (m, 2H), 1.46 – 1.11 (m, 10H). **^{13}C NMR** (101 MHz, $CDCl_3$) δ ppm 174.8, 71.0, 68.0, 51.4, 33.6, 78.0, 25.1, 24.4, 21.8.

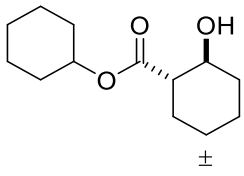

±

***Trans*-cyclohexyl-2-hydroxycyclohexane-1-carboxylate**

The product was prepared from cyclohexanol (42 mmol) according to **GP1.**The desired product was obtained as a transparent colorless oil, 980 mg, 4.3 mmol, 31.1 % yield. **^{1}H**

NMR (400 MHz, $CDCl_3$) δ ppm 4.85-4.79 (m, 1 H), 3,79-3.72 (m, 1 H), 2,95-2.94 (m, 1 H), 2.08-2.01 (m, 2 H), 1.85-1.71 (m, 6 H), 1.56-1.19 (m, 10 H). **^{13}C NMR** (101 MHz, $CDCl_3$) δ ppm 174.7, 77.2, 72.8, 71.0, 51.4, 33.6, 31.6, 31.5, 28.1, 25.4, 25.2, 24.4, 23.6. In order to prove that product is *trans* isomer instead of *cis* isomer, crystal structure analysis could be done. The absolute stereochemistry of the isomer can be obtained through a test of optical rotation.

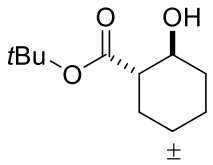

***Trans*-*tert*-butyl-2-hydroxycyclohexane-1-carboxylate**

The product was prepared from *t*-butyl alcohol (25.3 mmol) according to **GP1.** The desired product was obtained as a transparent colorless oil, 780 mg, 3.9 mmol, 46.2 % yield.**^{1}H NMR** (400 MHz, $CDCl_3$) δ ppm 3.80 – 3.62 (m, 1H), 3.05 – 2.90 (m, 1H), 2.23 – 2.07 (m, 1H), 2.06 – 1.93 (m, 2H), 1.81 – 1.62 (m, 2H), 1.46 (s, 9H), 1.33 – 1.13 (m, 4H).**^{13}C NMR** (101 MHz, $CDCl_3$) δ ppm 174.7, 81.0, 77.2, 71.0, 52.0, 33.5, 28.1, 25.2, 24.4.

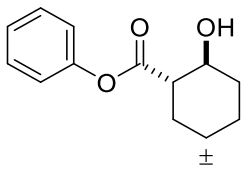

***Trans*-phenyl-2-hydroxycyclohexane-1-carboxylate**

The product was prepared from phenol (21.6 mmol) according to **GP1.** The desired product was obtained as a transparent colorless oil, 704 mg, 3.2 mmol, 44.4 % yield. **^{1}H NMR** (400 MHz, $CDCl_3$) δ ppm 7.38 (dd, J = 11.0, 4.6 Hz, 2H), 7.25 (d, J = 7.0 Hz, 1H), 7.14 – 6.95

(m, 2H), 3.98 – 3.76 (m, 1H), 2.68 (d, J = 3.8 Hz, 1H), 2.62 – 2.43 (m, 1H), 2.26 (dd, J = 9.5, 5.9 Hz, 1H), 2.14 – 2.00 (m, 1H), 1.93 – 1.69 (m, 2H), 1.50 – 1.12 (m, 4H).**^{13}C NMR** (101 MHz, $CDCl_3$) δ ppm 173.9, 150.6, 129.5, 126.0, 121.5, 71.0, 51.6, 33.7, 28.2, 25.1, 24.3.

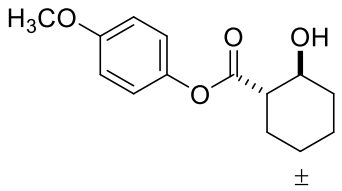

***Trans*-4-methoxyphenyl-2-hydroxycyclohexane-1-carboxylate**

The product was prepared from 4-methoxyphenol (23.2 mmol) according to **GP1.** The desired product was obtained as a transparent colorless oil, 900 mg, 3.6 mmol, 46.6 % yield. **^{1}H NMR** (400 MHz, $CDCl_3$) δ ppm 7.00 (d, J = 9.1 Hz, 2H), 6.89 (d, J = 9.1 Hz, 2H), 3.87 (td, J = 10.1, 4.9 Hz, 1H), 3.80 (s, 3H), 2.67 (d, J = 3.8 Hz, 1H), 2.57 – 2.42 (m, 1H), 2.25 (dd, J = 20.6, 5.1 Hz, 1H), 2.11 – 2.01 (m, 1H), 1.86 – 1.72 (m, 2H), 1.46 – 1.21 (m, 3H).**^{13}C NMR** (101 MHz, $CDCl_3$) δ ppm 174.3, 157.3, 144.0, 122.3, 114.5, 100.0, 71.0, 55.6, 51.5, 33.7, 28.2, 25.1, 24.3.

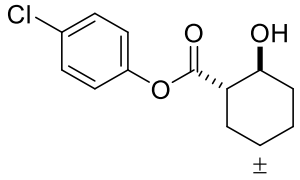

***Trans*-4-chlorophenyl-2-hydroxycyclohexane-1-carboxylate**

The product was prepared from 4-chlorophenol (27.5 mmol) according to **GP1.** The desired product was obtained as a transparent colorless oil, 1.042 g, 4.1 mmol, 44.7 % yield.

^{1}H NMR (400 MHz, $CDCl_3$) δ ppm 7.38 – 7.30 (m, 2H), 7.08 – 6.98 (m, 2H), 3.88 (s, 1H), 2.59 (s, 1H), 2.56 – 2.45 (m, 1H), 2.21 (dd, J = 13.2, 3.0 Hz, 1H), 2.12 – 2.01 (m, 1H), 1.89 – 1.71 (m, 2H), 1.53 (dd, J = 12.8, 3.3 Hz, 1H), 1.39 – 1.23 (m, 3H). **^{13}C NMR** (101 MHz, $CDCl_3$) δ ppm 173.7, 149.1, 131.3, 129.5, 122.9, 71.0, 51.6, 33.9, 28.3, 25.0, 24.3.

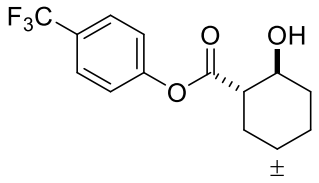

***Trans*-4-(trifluoromethyl)phenyl-2-hydroxycyclohexane-1-carboxylate**

The product was prepared from 4-(trifluoromethyl)phenol (30.6 mmol) according to **GP1.** The desired product was obtained as a transparent colorless oil, 1.284 g, 4.5 mmol, 44.1 % yield. **^{1}H NMR** (400 MHz, $CDCl_3$) δ ppm 7.59 (d, J = 8.5 Hz, 2H), 7.15 (d, J = 8.4 Hz, 2H), 3.90 – 3.76 (m, 1H), 2.48 (ddd, J = 12.5, 9.9, 3.8 Hz, 1H), 2.39 (d, J = 4.2 Hz, 1H), 2.22 – 2.09 (m, 1H), 2.06 – 1.93 (m, 1H), 1.81 – 1.71 (m, 2H), 1.34 – 1.16 (m, 4H). **^{13}C NMR** (101 MHz, $CDCl_3$) δ ppm 173.4, 153.1, 128.4, 128.1, 126.9, 122.1, 71.0, 51.7, 33.9, 28.3, 24.9, 24.3.

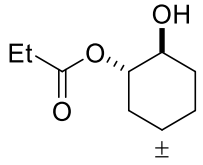

***Trans*-2-hydroxycyclohexyl propionate**

The compound *trans*-2-hydroxycyclohexyl propionate was prepared following a literature procedure.[38] The product was prepared from *trans*-cyclohexane-1,2-diol (10 mmol). The desired product was obtained as a transparent colorless oil, 1.308 g, 7.6 mmol, 76.0 % yield.

^{1}H NMR (400 MHz, $CDCl_3$) δ ppm 4.58 (td, J = 9.0, 4.7 Hz, 1H), 3.56 (td, J = 9.8, 4.4 Hz, 1H), 2.45 – 2.25 (m, 2H), 2.08 – 1.99 (m, 2H), 1.80 – 1.62 (m, 2H), 1.33 (qt, J = 12.6, 5.0 Hz, 4H), 1.16 (t, J = 7.6 Hz, 3H).**^{13}C NMR** (101 MHz, $CDCl_3$) δ ppm 174.8, 78.1, 72.9, 33.1, 30.0, 27.9, 23.9, 23.8, 9.2.

General procedure for the kinetic resolution of *trans*-alkyl-2-hydroxycyclohexanecarboxylate (GP2)

To an oven dried 1-dram vial with an oven dried Teflon coated stir bar and activated 4Å molecular sieves, the racemic alcohol substrate (0.4 mmol) and catalyst (0.1 mmol) were added. The vial was then purged with argon and sealed with a septa. N, N-diisopropylethylamine (0.24 mmol) was added via syringe and the resulting mixture was dissolved in 0.55 ml of THF to make a 0.72 M concentration solution with respect to the alcohol. The vial was then cooled to -78 ^{o}C for 30 mins. The cooled mixture was then treated with a 0.65 M solution of silyl chloride in THF (0.4 ml, 0.26 mmol) and was left to react for 48 h at -78 ^{o}C. The resulting solution was 0.42 M with respect to the alcohol. After 48 hours, the reaction was quenched with 0.3 ml of methanol. The solution was allowed to warm to room temperature and the crude contents were diluted with diethyl ether and transferred to a 4-dram vial. Solvent was removed by rotary evaporator and the crude mixture was purified via silica gel chromatography (5% EtOAc in hexanes increasing to 10% and 25% EtOAc in hexanes). The silylated alcohol was concentrated and saved for analysis and the unreacted alcohol could either be analyzed directly by HPLC or be converted to the benzoate ester for HPLC analysis.

General procedure for deprotection of silyl ether products (GP3)

The silyl-protected alcohol (0.1 mmol) was weighed into a 4-dram vial. The vial was then equipped with a stir bar and a septa, and the solid was dissolved in 1 mL of THF with stirring. To this solution TBAF (1 mL) was added. The reaction was monitored via TLC (25% EtOAc in hexanes). The reaction was generally complete in less than 2 h. The reaction was then quenched with 2 mL of brine, extracted with 3 mL of diethyl ether three times, dried through a pad of silica gel in a pipet. The reaction was concentrated via rotary evaporator which afforded an oil. Subsequent purification via silica gel column chromatography (10% EtOAc in hexanes gradient to 50% EtOAc in hexanes) afforded the deprotected products suitable for conversion to the benzoate ester or direct separation on chiral stationary phase HPLC.

General procedure for benzoylation of alcohols for HPLC analysis (GP4)

A 4-dram vial containing the alcohol (1 equiv) was fitted with a stir bar and a septa. The catalyst, 4-dimethylaminopyridine (DMAP, 0.1 equiv.) was added, followed by the addition of triethylamine (2.0 equiv) via syringe. The mixture was then dissolved in dichloromethane to make a 0.06 M solution. The vial was cooled to 0 °C in an ice bath and benzoyl chloride (1.4 equiv.) was added to the mixture through a syringe. The reaction was allowed to stir for 2 h and quenched with sat. sodium bicarbonate and extracted three time with dichloromethane. The crude mixture was then concentrated via rotary evaporator and purified by silica gel chromatography (5% EtOAc in hexanes) to obtain the desired benzoylated alcohols. The benzoate esters could then be analyzed by HPLC.

Analytical Data and HPLC Traces for Kinetic Resolutions

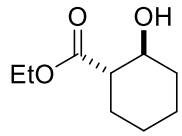

Table 2.2, Entry 1. Recovered starting material: 41 mg, 60 %, colorless oil. **^{1}H NMR** (400 MHz, $CDCl_3$) δ ppm 4.18 (q, J = 7.1 Hz, 2H), 3.77 (dd, J = 10.1, 5.4 Hz, 1H), 2.90 (s, 1H), 2.25 (ddd, J = 12.4, 9.9, 3.8 Hz, 1H), 2.11 – 1.93 (m, 2H), 1.83 – 1.62 (m, 2H), 1.39 – 1.17 (m, 7H). **^{13}C NMR** (101 MHz, $CDCl_3$) δ ppm 175.3, 70.9, 60.6, 51.3, 33.6, 28.1, 25.1, 24.3, 14.2. **Optical Rotation** $[\alpha]^{25}D$: +14.4 (c = 0.04) $CHCl_3$. Absolute stereochemistry of (+)-(1*S*,2*S*)-ethyl-2-hydroxycyclohexane-1-carboxylate was determined by comparing to a literature reference[39-40] $[\alpha]^{25}D$: +43° (c = 1.0, $CHCl_3$) for (1*S*,2*S*)-ethyl-2-hydroxycyclohexane-1-carboxylate). HPLC separation for the starting material was as follows using the corresponding benzoate ester of the starting material through **GP4**.

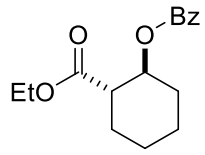

The product was prepared from recovered starting material (0.05 mmol) according to **GP4**. The desired product was isolated after column chromatography (10% EtOAc in hexane) as a colorless oil, 11 mg, 80 % yield. **^{1}H NMR** (400 MHz, $CDCl_3$) δ ppm 8.01 (d, J = 7.2 Hz, 2H), 7.54 (t, J = 7.3 Hz, 1H), 7.42 (t, J = 7.6 Hz, 2H), 5.22 (td, J = 10.1, 4.4 Hz, 1H), 4.21 – 3.90 (m, 2H), 2.79 – 2.56 (m, 1H), 2.22 (dd, J = 10.5, 5.6 Hz, 1H), 2.11 – 1.96 (m, 1H), 1.77 – 1.22 (m, 6H), 1.13 (t, J = 7.1 Hz, 3H). **^{13}C NMR** (101 MHz, $CDCl_3$) δ ppm 173.5,

165.6, 132.8, 129.6, 128.9, 128.3, 73.9, 60.5, 48.9, 30.9, 28.4, 24.5, 23.9, 14.1. HPLC condition[41] Chiralpak OD-H Column 5% isopropyl alcohol in hexane, flow rate: 1 mL/min, 25 °C t_s 6.4 min for (*S*)-enantiomer (major) and t_R 7.8 min for (*R*)-enantiomer (minor). (er = 71.6:28.4) In order to prove that product is *trans* isomer instead of *cis* isomer, crystal structure analysis could be done. The absolute stereochemistry of the isomer can be obtained through a test of optical rotation.

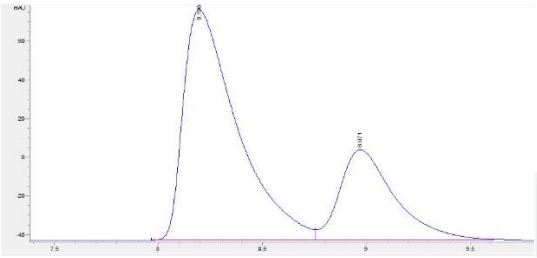

#	Time	Area	Height	Width	Area%	Symmetry
1	8.196	2154	119.2	0.2678	71.595	0.387
2	8.971	854.6	46.8	0.2711	28.405	0.564

Figure 2.6 HPLC Data of SM of Table 2.2 Entry 1

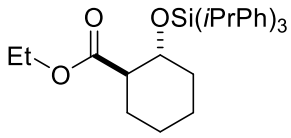

Recovered Product: 67 mg, 30 %, colorless oil. **^{1}H NMR** (400 MHz, $CDCl_3$) δ ppm 7.52 (d, J = 8.0 Hz, 6H), 7.20 (d, J = 7.9 Hz, 6H), 4.10 – 3.75 (m, 3H), 2.89 (dt, J = 13.8, 6.9 Hz, 3H), 2.50 (ddd, J = 13.3, 9.6, 3.8 Hz, 1H), 1.93 – 1.76 (m, 2H), 1.62 – 1.38 (m, 4H), 1.35 – 1.14 (m, 18H), 1.13 – 1.06 (m, 3H), 1.03 – 0.68 (m, 2H).**^{13}C NMR** (101 MHz, $CDCl_3$) δ ppm 175.0, 150.3, 135.6, 132.2, 125.8, 73.1, 60.2, 52.5, 35.0, 34.1, 28.4, 24.5, 24.1, 23.9, 14.1. **Optical Rotation** $[\alpha]^{25}D$: -7.2 (c = 0.023) $CHCl_3$. **IR** (neat, cm^{-1}) 2960, 2931, 2868, 1728, 1599, 1462, 1394, 1181, 1117, 1049, 879, 771. Calculated for ($C_{27}H_{33}O_3Si$) (M-*i*PrPh): 437.2512 Observed: 437.2509. The same conditions as the

benzoate ester of the starting material were utilized. The same conditions as the recovered starting materials were utilized. (er = 90.2: 9.8)

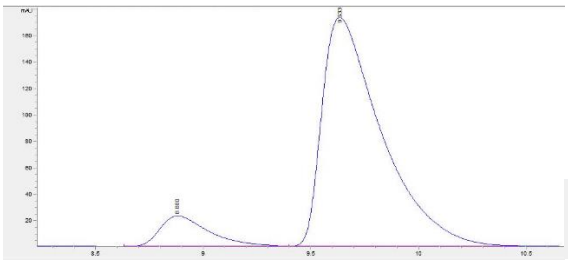

#	Time	Area	Height	Width	Area%	Symmetry
1	8.88	360.1	23	0.2357	9.765	0.532
2	9.633	3328	173.1	0.2843	90.235	0.396

Figure 2.7 HPLC Data of PR of Table 2.2 Entry 1

Table 2.3 Kinetic Resolution Data for Table 2.2, Entry 1

	er^{SM}	er^{PR}	% conv	*s*	*s average*
1	71.6: 28.4	90.2:9.8	35.5	13.8	14.0
2	67.0: 33.0	8.9: 91.1	29.3	14.1	

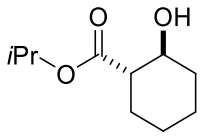

Table 2.2, Entry 2. Recovered starting material: 36 mg, 52 %, colorless oil. **^{1}H NMR** (400 MHz, $CDCl_3$) δ ppm 5.06 (s, 1H), 3.76 (td, J = 10.0, 4.6 Hz, 1H), 2.21 (ddd, J = 13.1, 10.3, 4.2 Hz, 1H), 2.08 – 1.96 (m, 2H), 1.83 – 1.66 (m, 2H), 1.38 – 1.19 (m, 9H).**^{13}C NMR** (101 MHz, $CDCl_3$) δ ppm 174.8, 71.0, 68.0, 51.4, 33.6, 78.0, 25.1, 24.4, 21.8. Absolute stereochemistry of (+)-(1*S*,2*S*)-isopropyl-2-hydroxycyclohexane-1-carboxylate was determined by reducing the ester with $LiAlH_4$ in diethyl ether to give the diol 2-(hydroxymethyl)cyclohexan-1-ol. The optical rotation of that compound was compared to literature values, which confirmed the stereochemistry (+)-(1*S*,2*R*)-2-

(hydroxymethyl)cyclohexan-1-ol. (synthetic, $[\alpha]^{25}D$: + 8.4 (c = 0.01) $CHCl_3$; lit [42] $[\alpha]^{25}D$: + 27.2. EtOH)

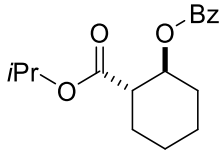

The product was prepared from recovered starting material (0.05 mmol) according to **GP4**. 12 mg, 80 % yield. **^{1}H NMR** (400 MHz, $CDCl_3$) δ ppm 8.05 – 7.98 (m, 2H), 7.54 (t, J = 7.4 Hz, 1H), 7.42 (t, J = 7.7 Hz, 2H), 5.22 (td, J = 10.3, 4.3 Hz, 1H), 4.95 (dt, J = 12.5, 6.3 Hz, 1H), 2.70 – 2.57 (m, 1H), 2.28 – 2.16 (m, 1H), 2.05 (dd, J = 8.8, 6.3 Hz, 1H), 1.86 – 1.71 (m, 2H), 1.60 (dd, J = 12.7, 9.1 Hz, 2H), 1.50 – 1.39 (m, 2H), 1.13 (d, J = 6.3 Hz, 3H), 1.09 (d, J = 6.2 Hz, 3H). **^{13}C NMR** (101 MHz, $CDCl_3$) δ ppm 173.0, 165.5, 132.8, 130.4, 129.6, 128.3, 74.0, 67.7, 49.2, 30.9, 28.4, 24.5, 23.9, 21.6. HPLC condition: Chiralpak IC Column pure hexane, flow rate: 1 mL/min, 25 °C; t_R 14.8 min for (R)-enantiomer (minor) and t_S 15.4 min for (S)-enantiomer (major). (er =82.5:17.5)

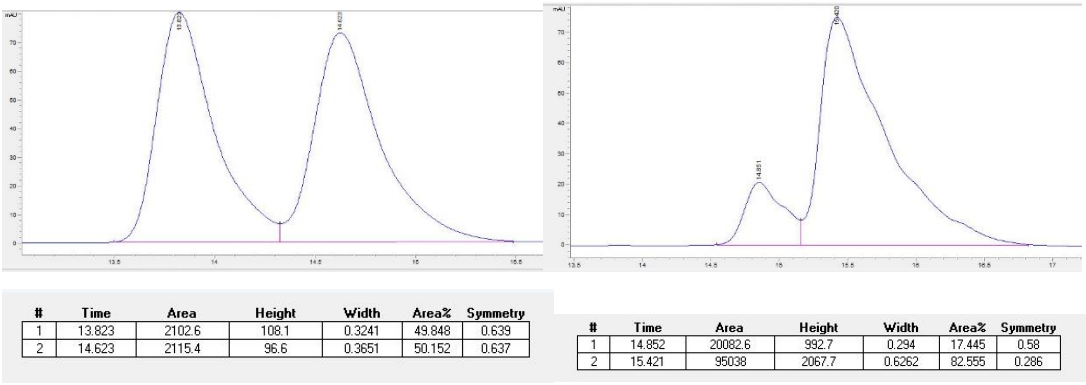

#	Time	Area	Height	Width	Area%	Symmetry
1	13.823	2102.6	108.1	0.3241	49.848	0.639
2	14.623	2115.4	96.6	0.3651	50.152	0.637

#	Time	Area	Height	Width	Area%	Symmetry
1	14.852	20082.6	992.7	0.294	17.445	0.58
2	15.421	95038	2067.7	0.6262	82.555	0.286

Figure 2.8 HPLC Data of SM of Table 2.2 Entry 2

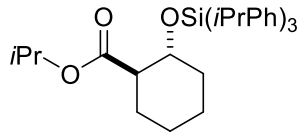

Recovered Product: 68 mg, 30 %, colorless oil. **^{1}H NMR** (400 MHz, $CDCl_3$) δ ppm 7.53 (d, J = 7.9 Hz, 6H), 7.20 (d, J = 7.9 Hz, 6H), 4.87 (dt, J = 12.5, 6.2 Hz, 1H), 4.03 (td, J = 10.0, 4.3 Hz, 1H), 2.89 (hept, J = 6.9 Hz, 3H), 2.47 (ddd, J = 11.8, 9.4, 3.8 Hz, 1H), 1.83 (ddd, J = 12.6, 10.0, 4.7 Hz, 2H), 1.65 – 1.56 (m, 2H), 1.43 – 1.34 (m, 2H), 1.24 (d, J = 6.9 Hz, 18H), 1.17 – 0.99 (m, 8H).**^{13}C NMR** (101 MHz, $CDCl_3$) δ ppm 174.5, 150.2, 135.6, 132.3, 125.8, 72.8, 67.4, 52.5, 34.9, 34.1, 28.4, 24.5, 23.6, 21.9, 21.6. **IR** (neat, cm^{-1}) 2959, 2930, 1731, 1600, 1554, 1460, 1394, 1264, 1182, 1118, 1050, 822. **HRMS** (EI^{+}) Calculated for (C28H39O3Si) (M-*i*PrPh): 451.2668. Observed: 451.2676. The same separation conditions as the benzoate ester of the starting material were utilized (er = 85.0:15.0)

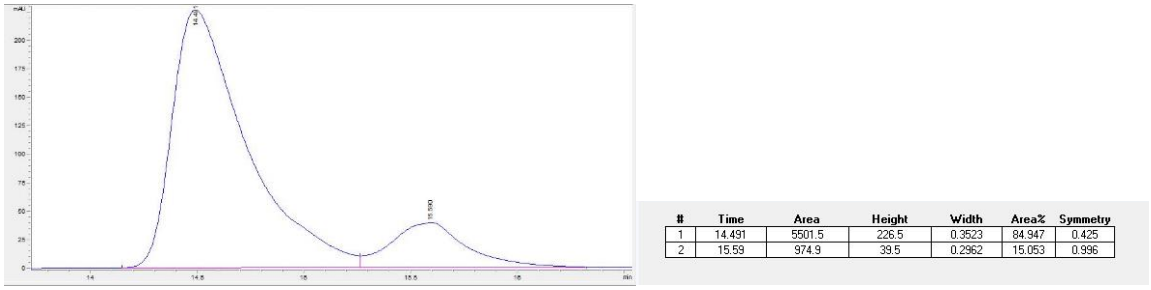

#	Time	Area	Height	Width	Area%	Symmetry
1	14.491	5501.5	226.5	0.3523	84.947	0.425
2	15.59	974.9	39.5	0.2962	15.053	0.996

Figure 2.9 HPLC Data of PR of Table 2.2 Entry 2

Table 2.4 Kinetic Resolution Data for Table 2.2, Entry 2

	er^{SM}	er^{PR}	% conv	*s*	*s average*
1	82.5: 17.5	85.0:15.0	47.8	10.8	10
2	66.4: 33.6	13.0: 87.0	30.7	9.2	

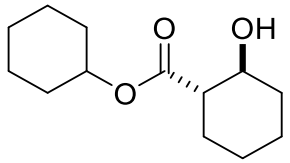

Table 2.2, Entry 3. Recovered starting material: 59 mg, 65 %, **^{1}H NMR** (400 MHz, $CDCl_3$) δ ppm 4.85-4.79 (m, 1 H), 3,79-3.72 (m, 1 H), 2,95-2.94 (m, 1 H), 2.08-2.01 (m, 2 H), 1.85-1.71 (m, 6 H), 1.56-1.19 (m, 10 H).**^{13}C NMR** (101 MHz, $CDCl_3$) δ ppm 174.7, 77.2, 72.8, 71.0, 51.4, 33.6, 31.6, 31.5, 28.1, 25.4, 25.2, 24.4,23.6. **Optical Rotation** $[\alpha]^{25}D$: +18.0 (c = 0.037) $CHCl_3$. **IR** (neat, cm^{-1}) 3443, 2930, 2858, 1726, 1450, 1250, 1122, 1038, 1017, 913, 892, 742. **HRMS** (EI^+) Calculated for (C13H22O3) (M^+): 226.1569 Observed: 226.1570. HPLC separation for the starting material was achieved by converting the alcohol into a benzoate ester through **GP4** in order to provide a chromophore.

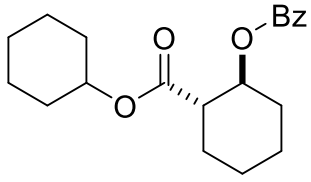

The product was prepared from recovered starting material (0.05 mmol) according to **GP4**. The desired product was isolated as a colorless oil, 13 mg, 80 % yield. **^{1}H NMR** (400 MHz, $CDCl_3$) δ ppm 8.00 (d, J = 7.1 Hz, 2H), 7.47 (dt, J = 37.6, 7.5 Hz, 3H), 5.22 (td, J = 10.2, 4.3 Hz, 1H), 4.72 (tt, J = 9.0, 4.4 Hz, 1H), 2.73 – 2.53 (m, 1H), 2.31 – 2.14 (m, 1H), 2.12 – 1.94 (m, 1H), 1.72 – 1.19 (m, 16H). **^{13}C NMR** (101 MHz, $CDCl_3$) δ ppm 172.9, 165.6, 132.8, 130.0, 128.8, 128.3, 74.0, 72.6, 49.3, 31.5, 31.4, 30.9, 30.4, 28.9, 28.5, 25.3, 24.5, 23.9. **Optical Rotation** $[\alpha]^{25}D$: +20.0 (c = 0.031) $CHCl_3$. **IR** (neat, cm^{-1}) 2936, 1722, 1451, 1316, 1266, 1181, 1109, 1070, 1029, 711. **HRMS** (EI^+) Calculated for: 330.1831 Observed:

330.1835. HPLC condition: IC Column pure hexane, flow rate: 1 mL/min, 25 °C; t_R 12.9 min for (R)-enantiomer (minor) and t_S 15.9 min for (S)-enantiomer (major). (er = 65.9:34.1)

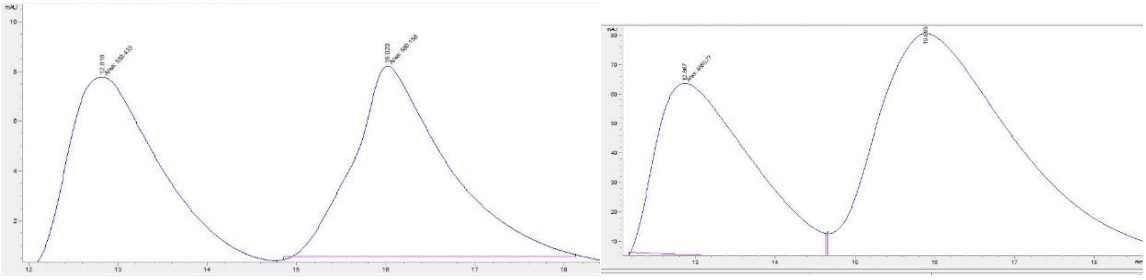

#	Time	Area	Height	Width	Area%	Symmetry
1	12.818	553.4	7.7	1.1963	49.698	0.574
2	16.02	560.2	7.7	1.2156	50.302	0.576

#	Time	Area	Height	Width	Area%	Symmetry
1	12.867	4880.8	58.1	1.3998	34.109	0.412
2	15.885	9428.5	77.5	1.7391	65.891	0.526

Figure 2.10 HPLC Data of SM of Table 2.2 Entry 3

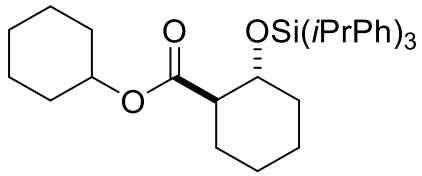

Recovered Product: 68 mg, 28 %, colorless oil. **^{1}H NMR** (400 MHz, $CDCl_3$) δ ppm 7.58-7.50 (m, 8H), 7.23-7.18 (m, 4H), 4.68-4.61 (m, 1H), 4.07-4.00 (m, 1H), 2.95-2.85 (m, 3 H), 2.53-2.45 (m, 1 H), 1.98-1.60 (m, 9H), 1.41-1.33 (m, 6H), 1.27-1.24 (t, 18H), 1.22-0.92 (m, 3H).**^{13}C NMR** (101 MHz, $CDCl_3$) δ ppm 150.4, 135.6, 129.2, 126.0, 123.1, 77.2, 52.6, 38.7, 35.0, 34.1, 30.4, 28.9, 28.5, 24.5, 24.0, 23.9, 23.0, 14.1, 11.0. **Optical Rotation** $[\alpha]^{25}D$: -22.0 (c = 0.014) $CHCl_3$. **IR** (neat, cm^{-1}) 2934, 2858, 1717, 1648, 1448, 1122, 1057, 984, 903, 864, 831, 771. **HRMS** (EI^+) Calculated for (C40H54O3Si) (M^+): 610.3842 Observed: 610.3852.

Table 2.5 Kinetic Resolution Data for Table 2.2, Entry 3

	er^{SM}	% conv (^{1}H NMR)	*s*	*s average*
1	65.9: 34.1	30.0	9.0	8.0
2	64.2: 35.8	29.2	7.1	

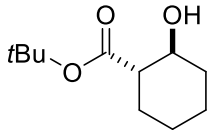

Table 2.2, Entry 4. Recovered starting material: 72 mg, 90%, colorless oil. **^{1}H NMR** (400 MHz, $CDCl_3$) δ ppm 3.80 – 3.62 (m, 1H), 3.05 – 2.90 (m, 1H), 2.23 – 2.07 (m, 1H), 2.06 – 1.93 (m, 2H), 1.81 – 1.62 (m, 2H), 1.46 (s, 9H), 1.33 – 1.13 (m, 4H).**^{13}C NMR** (101 MHz, $CDCl_3$) δ ppm 174.7, 81.0, 77.2, 71.0, 52.0, 33.5, 28.1, 25.2, 24.4. HPLC separation for the starting material was achieved by converting the alcohol into a benzoate ester through **GP4** in order to provide a chromophore.

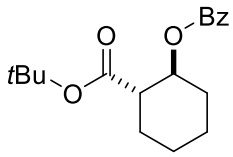

The product was prepared from recovered starting material (0.05 mmol) according to **GP4**. The desired product was isolated after column chromatography (10% EtOAc in hexane) as a colorless oil, 12 mg, 78 % yield. **^{1}H NMR** (400 MHz, $CDCl_3$) δ ppm 8.05 (d, J = 7.0 Hz, 2H), 7.57 (t, J = 7.4 Hz, 1H), 7.45 (t, J = 7.6 Hz, 2H), 2.64 – 2.48 (m, 1H), 2.28 – 2.13 (m, 1H), 2.08 (dd, J = 7.3, 5.4 Hz, 1H), 1.87 – 1.62 (m, 3H), 1.53 – 1.37 (m, 4H), 1.35 (s, 9H). **^{13}C NMR** (101 MHz, $CDCl_3$) δ ppm 132.8, 130.9, 130.5, 129.6, 128.8, 128.3, 50.2, 38.7,

30.9, 28.5, 27.9, 24.6, 24.0, 23.0. **Optical Rotation** $[\alpha]^{25}D$: +11.0 (c = 0.031) $CHCl_3$. **IR** (neat, cm^{-1}) 2860, 1718, 1602, 1458, 1388, 1316, 1181, 1108, 1070, 983, 804, 711. **HRMS** (EI^+) Calculated for (C18H24O4) (M^+): 304.1675 Observed: 304.1679. HPLC condition: Chiralpak AD Column 3% isopropyl alcohol in hexane, flow rate: 1 mL/min, 25 °C; t_R 5.1 min for (R)-enantiomer (minor) and t_S 6.5 min for (S)-enantiomer (major). (er = 51.6:48.4)

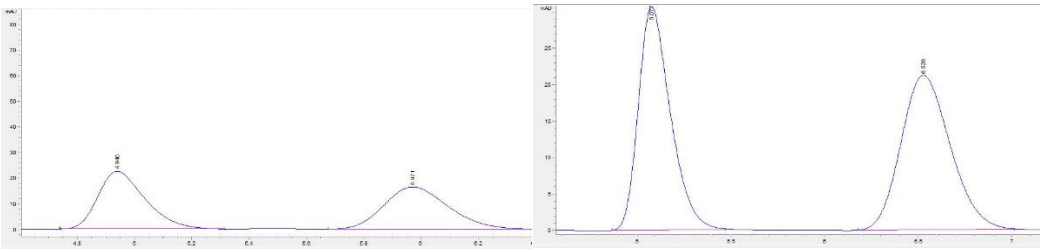

#	Time	Area	Height	Width	Area%	Symmetry
1	4.94	258	22.5	0.1745	49.942	0.665
2	5.971	258.6	16.5	0.2441	50.058	0.78

#	Time	Area	Height	Width	Area%	Symmetry
1	5.077	365.4	30.7	0.1809	48.359	0.67
2	6.526	390.2	21.2	0.2856	51.641	0.802

Figure 2.11 HPLC Data of SM of Table 2.2 Entry 4

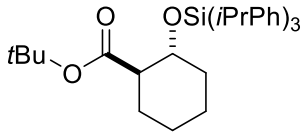

Recovered Product: 9 mg, 4%, colorless oil. **^{1}H NMR** (400 MHz, $CDCl_3$) δ ppm 7.57 (d, J = 8.0 Hz, 6H), 7.23 (d, J = 7.9 Hz, 6H), 4.06 (td, J = 9.9, 4.2 Hz, 1H), 2.92 (dt, J = 13.8, 6.9 Hz, 3H), 2.42 (ddd, J = 11.4, 9.2, 3.9 Hz, 1H), 1.87 (ddd, J = 16.5, 13.7, 3.4 Hz, 2H), 1.64 – 1.54 (m, 2H), 1.43 (dd, J = 16.9, 7.5 Hz, 2H), 1.35 (s, 9H), 1.27 (d, J = 6.9 Hz, 18H), 1.22 – 1.11 (m, 2H).**^{13}C NMR** (101 MHz, $CDCl_3$) δ ppm 174.3, 150.2, 135.7, 132.4, 125.8, 79.8, 72.8, 53.2, 34.8, 34.1, 28.4, 28.0, 24.5, 24.0, 23.9. **Optical Rotation** $[\alpha]^{25}D$: -4.6 (c = 0.018) $CHCl_3$. **IR** (neat, cm^{-1}) 2935, 2863, 1720, 1602, 1451, 1367, 1270, 1155, 1108, 1026, 978, 847, 864, 742.

Table 2.6 Kinetic Resolution Data for Table 2.2, Entry 4

	er^{SM}	% conv (^{1}H NMR)	*s*	*s average*
1	52.0:48.0	6.2	4.2	4.4
2	51.6:48:4	4.8	4.6	

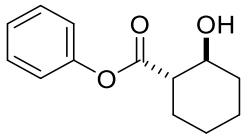

Table 2.2, Entry 5. Recovered starting material: 44 mg, 50 %. **^{1}H NMR** (400 MHz, $CDCl_3$) δ ppm 7.38 (dd, J = 11.0, 4.6 Hz, 2H), 7.25 (d, J = 7.0 Hz, 1H), 7.14 – 6.95 (m, 2H), 3.98 – 3.76 (m, 1H), 2.68 (d, J = 3.8 Hz, 1H), 2.62 – 2.43 (m, 1H), 2.26 (dd, J = 9.5, 5.9 Hz, 1H), 2.14 – 2.00 (m, 1H), 1.93 – 1.69 (m, 2H), 1.50 – 1.12 (m, 4H).**^{13}C NMR** (101 MHz, $CDCl_3$) δ ppm 173.9, 150.6, 129.5, 126.0, 121.5, 71.0, 51.6, 33.7, 28.2, 25.1, 24.3. **Optical Rotation** $[\alpha]^{25}D$: +42.0 (c = 0.034) $CHCl_3$. **IR** (neat, cm^{-1}) 3377, 2928, 1743, 1487, 1365, 1289, 1219, 1161, 1046, 970, 922, 798. HPLC conditions: Chiralpak AD-H Column 5% isopropyl alcohol in hexane, flow rate: 1 mL/min, 25 °C; tR 18.6 min for (R)-enantiomer (minor) and 24.1 min for (S)-enantiomer (major). (er = 62.9:37.1)

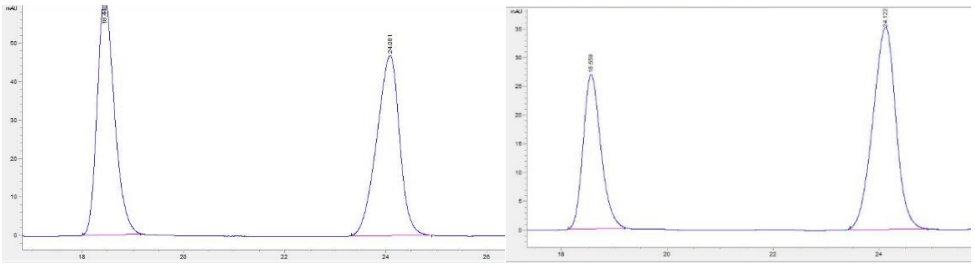

#	Time	Area	Height	Width	Area%	Symmetry
1	18.44	1472.3	62.1	0.3635	49.836	0.731
2	24.081	1482	46.9	0.4835	50.164	1.34

#	Time	Area	Height	Width	Area%	Symmetry
1	18.559	630.4	26.9	0.3586	37.090	0.774
2	24.122	1069.2	35.2	0.4727	62.910	1.18

Figure 2.12 HPLC Data of SM of Table 2.2 Entry 5

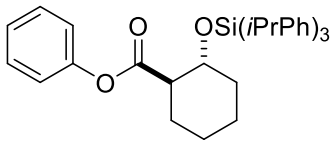

Recovered Product: 85 mg, 35%, colorless oil. **^{1}H NMR** (400 MHz, $CDCl_3$) δ ppm 7.55 (d, J = 7.7 Hz, 6H), 7.30 – 7.15 (m, 8H), 6.84 (dd, J = 8.3, 1.0 Hz, 1H), 4.29 – 4.04 (m, 1H), 2.91 (dt, J = 13.4, 6.8 Hz, 3H), 2.78 (ddd, J = 11.4, 9.4, 8.5 Hz, 1H), 2.18 – 1.87 (m, 2H), 1.71 – 1.52 (m, 2H), 1.49 – 1.31 (m, 2H), 1.25 (dd, J = 6.9, 3.6 Hz, 18H), 1.15 – 0.88 (m, 2H).**^{13}C NMR** (101 MHz, $CDCl_3$) δ ppm 172.1, 150.8, 150.4, 135.7, 132.0, 129.1, 126.1, 125.3, 121.7, 69.8, 48.5, 34.1, 32.9, 24.5, 23.9, 22.8, 20.2. **Optical Rotation** $[\alpha]^{25}D$: -32.2 (c = 0.014) $CHCl_3$. **IR** (neat, cm^{-1}) 3375, 2864, 1593, 1448, 1416, 1251, 1143, 1070, 952, 906, 887, 743. **HRMS** (EI^+) Calculated for (C40H48O3Si) (M^+): 604.3373 Observed: 604.3385. The selectivity factor of the kinetic resolution was obtained using the er of the recovered starting material and ^{1}H NMR conversion.

Table 2.7 Kinetic Resolution Data for Table 2.2, Entry 5

	er^{SM}	% conv (^{1}H NMR)	*s*	*s average*
1	62.9:37.1	41.0	2.8	3.0
2	64.2:35.8	41.2	3.1	

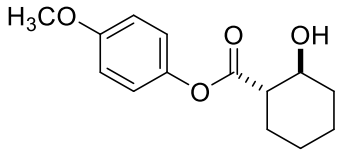

Table 2.2, Entry 6. Recovered starting material: 70 mg, 70%. **^{1}H NMR** (400 MHz, $CDCl_3$) δ ppm 7.00 (d, J = 9.1 Hz, 2H), 6.89 (d, J = 9.1 Hz, 2H), 3.87 (td, J = 10.1, 4.9 Hz, 1H), 3.80 (s, 3H), 2.67 (d, J = 3.8 Hz, 1H), 2.57 – 2.42 (m, 1H), 2.25 (dd, J = 20.6, 5.1 Hz, 1H),

2.11 – 2.01 (m, 1H), 1.86 – 1.72 (m, 2H), 1.46 – 1.21 (m, 3H).**^{13}C NMR** (101 MHz, $CDCl_3$) δ ppm 174.3, 157.3, 122.3, 114.5, 100.0, 71.0, 55.6, 51.5, 33.7, 28.2, 25.1, 24.3. **Optical Rotation** $[\alpha]^{25}D$: +12.0 (c = 0.033) $CHCl_3$. **IR** (neat, cm^{-1}) 2938, 2861, 1760, 1713, 1656, 1608, 1444, 1358, 1296, 1247, 1214, 1140, 1038, 898, 822, 793, 735. **HRMS** (EI^+) Calculated for (C14H18O4) (M^+): 250.1205 Observed: 254.1209. HPLC conditions for the starting material was as follows directly using the starting material: Chiralpak OD-H Column 5% isopropyl alcohol in hexane, flow rate: 1 mL/min, 25 °C; tR 4.4 min for (R)-enantiomer (minor) and 4.8 min for (*S*)-enantiomer (major). (er = 57.5:42.5)

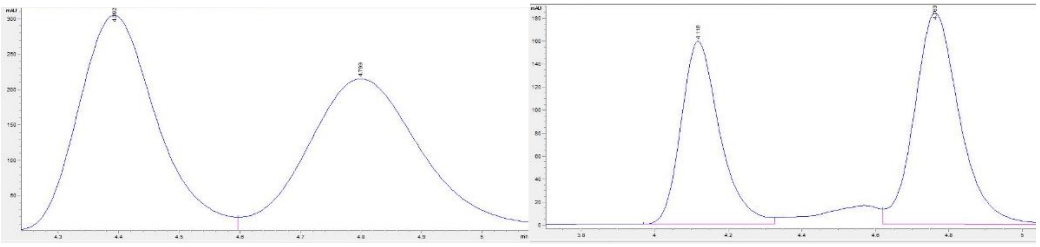

#	Time	Area	Height	Width	Area%	Symmetry
1	4.392	2748.2	305.3	0.139	49.122	0.794
2	4.799	2846.5	215.3	0.2032	50.878	0.832

#	Time	Area	Height	Width	Area%	Symmetry
1	4.118	1166.3	159.3	0.1114	42.540	0.723
2	4.763	1575.4	184.3	0.1297	57.460	0.803

Figure 2.13 HPLC Data of SM of Table 2.2 Entry 6

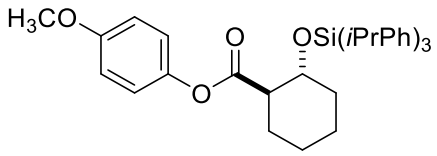

Recovered Product: 38 mg, 15%, colorless oil. **^{1}H NMR** (400 MHz, $CDCl_3$) δ ppm 7.56-7.54 (m, 6H), 7.21-7.18 (m, 6H), 6.79-6.71 (m, 4H), 4.16-4.08 (m, 1H), 3.78 (s, 3H), 2.94-2.85 (m, 3H), 2.75-2.71 (m, 1H), 2.10-2.04 (m, 1H), 1.93-1.87 (m, 1H), 1.68-1.64 (m, 2H), 1.49-1.38 (m, 2H), 1.25 (dd, J = 6.9, 3.6 Hz, 18H), 0.97-0.86 (m, 2H). **^{13}C NMR** (101 MHz, $CDCl_3$) δ ppm 173.8, 157.0, 150.3, 144.3, 135.7, 132.1, 125.9, 122.5, 114.2, 73.0, 55.5,

52.5, 35.0, 34.1, 31.6, 28.6, 24.5, 23.9. **Optical Rotation** $[\alpha]^{25}D$: -8.6 (c = 0.013) $CHCl_3$. **IR** (neat, cm^{-1}) 3440, 2935, 1748, 1722, 1448, 1296, 1247, 1147, 1065, 1030, 999, 972, 911, 868, 839, 819, 763. **HRMS** (EI^+) Calculated for (C41H50O4Si) (M^+): 634.3478 Observed: 634.3494.

Table 2.8 Kinetic Resolution Data for Table 2.2, Entry 6

	er^{SM}	% conv (^1H NMR)	*s*	*s average*
1	57.5:42.5	20.4	4.7	4.4
2	56.1:43.9	18.0	3.9	

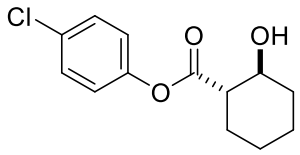

Table 2.2, Entry 7. Recovered starting material: 50 mg, 49 %. **^{1}H NMR** (400 MHz, $CDCl_3$) δ ppm 7.38 – 7.30 (m, 2H), 7.08 – 6.98 (m, 2H), 3.88 (s, 1H), 2.59 (s, 1H), 2.56 – 2.45 (m, 1H), 2.21 (dd, J = 13.2, 3.0 Hz, 1H), 2.12 – 2.01 (m, 1H), 1.89 – 1.71 (m, 2H), 1.53 (dd, J = 12.8, 3.3 Hz, 1H), 1.39 – 1.23 (m, 3H). **^{13}C NMR** (101 MHz, $CDCl_3$) δ ppm 173.7, 149.1, 131.3, 129.5, 122.9, 71.0, 51.6, 33.9, 28.3, 25.0, 24.3. **Optical Rotation** $[\alpha]^{25}D$: +22.0 (c = 0.033) $CHCl_3$. **IR** (neat, cm^{-1}) 2936, 1728, 1601, 1486, 1463, 1325, 1263, 1124, 1081, 1024, 960, 853, 778. **HRMS** (EI^+) Calculated for (C15H15ClO3) (M^+): 254.0710 Observed: 254.0716. The optical rotation of that compound was compared to literature values, which confirmed the stereochemistry (+)-(1S,2R)-2-(hydroxymethyl)cyclohexan-1-ol. (synthetic, $[\alpha]^{25}D$: + 6.2 (c = 0.01) $CHCl_3$; lit [42] $[\alpha]^{25}D$: + 27.2. EtOH) HPLC conditions for the starting material were as follows directly using the starting material:

Chiralpak OJ-H Column 10% isopropyl alcohol in hexane, flow rate: 1 mL/min, 25 °C; tR 25.7 min for (R)-enantiomer (minor) and 27.1 min for (S)-enantiomer (major). (er = 17.5:82.5)

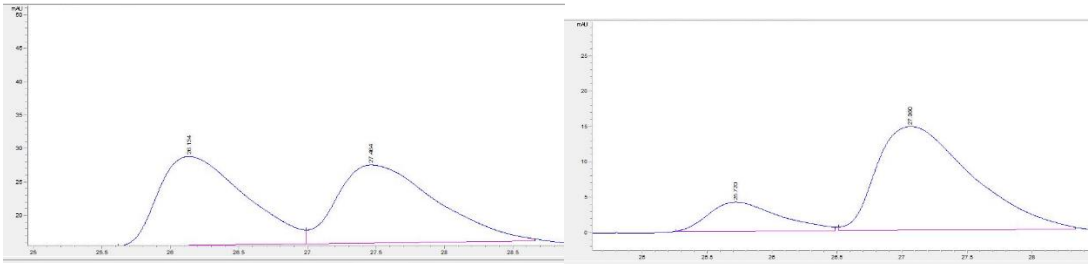

#	Time	Area	Height	Width	Area%	Symmetry
1	26.134	587.4	13.3	0.6059	49.714	0.514
2	27.464	594.2	11.8	0.7016	50.286	0.515

#	Time	Area	Height	Width	Area%	Symmetry
1	25.72	159	4.2	0.4681	17.570	0.601
2	27.06	746	14.7	0.6031	82.430	0.514

Figure 2.14 HPLC Data of SM of Table 2.2 Entry 7

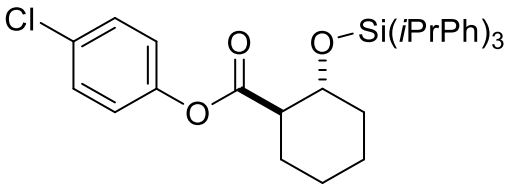

Recovered Product: 77 mg, 30 %, colorless oil. **^{1}H NMR** (400 MHz, $CDCl_3$) δ ppm 7.54 (t, J = 7.4 Hz, 8H), 7.23 – 7.17 (m, 8H), 6.73 (d, J = 8.8 Hz, 1H), 4.10 (td, J = 10.2, 4.2 Hz, 1H), 2.95 – 2.88 (m, 3H), 2.83 – 2.70 (m, 1H), 2.12 – 1.84 (m, 2H), 1.65 (t, J = 12.8 Hz, 2H), 1.26 – 1.22 (m, 19H), 1.04 – 0.83 (m, 2H).**^{13}C NMR** (101 MHz, $CDCl_3$) δ ppm 173.3, 150.4, 149.3, 135.6, 132.0, 129.2, 129.6, 125.9, 123.1, 73.1, 52.6, 35.0, 34.1, 28.5, 24.5, 24.0, 23.9. **Optical Rotation** $[\alpha]^{25}D$: -42.0 (c = 0.013) $CHCl_3$. **IR** (neat, cm^{-1}) 2859, 1601, 1584, 1450, 1371, 1352, 1286, 1068, 1044, 960, 913, 850, 752, 698. **HRMS** (EI) Calculated for (C40H47ClO3Si) (M-H): 637.2905 Observed: 637.2870.

Table 2.9 Kinetic Resolution Data for Table 2.2, Entry 7

	er^{SM}	% conv	*s*	*s average*
1	82.5:17.5	42.8	27.8	27
2	81.0:19.0	41.7	26.4	

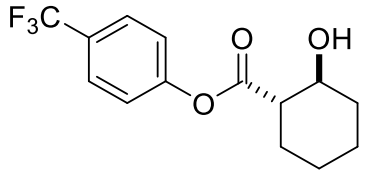

Table 2.2, Entry 8. Recovered starting material: 31 mg, 62 %. **^{1}H NMR** (400 MHz, $CDCl_3$) δ ppm 7.59 (d, J = 8.5 Hz, 2H), 7.15 (d, J = 8.4 Hz, 2H), 3.90 – 3.76 (m, 1H), 2.48 (ddd, J = 12.5, 9.9, 3.8 Hz, 1H), 2.39 (d, J = 4.2 Hz, 1H), 2.22 – 2.09 (m, 1H), 2.06 – 1.93 (m, 1H), 1.81 – 1.71 (m, 2H), 1.34 – 1.16 (m, 4H). **^{13}C NMR** (101 MHz, $CDCl_3$) δ ppm 173.4, 153.1, 128.4, 128.1, 126.9, 122.1, 71.0, 51.7, 33.9, 28.3, 24.9, 24.3. **Optical Rotation** $[\alpha]^{25}D$: +16.0 (c = 0.032) $CHCl_3$. **IR** (neat, cm^{-1}) 3503, 3080, 2939, 2863, 1733, 1610, 1514, 1451, 1415, 1322, 1248, 1204, 1106, 1017, 994, 979, 852, 745, 706. **HRMS** (EI^+) Calculated for ($C14H15F_3O3$) (M^+): 288.0973 Observed: 288.0978. The optical rotation of that compound was compared to literature values, that matched the reference. (synthetic, $[\alpha]^{25}D$: + 10.0 (c = 0.01) $CHCl_3$; lit [42] $[\alpha]^{25}D$: + 27.2. EtOH) HPLC conditions for the starting material was as follows directly using the starting material: Chiralpak OD-H Column 8 % isopropyl alcohol in hexane, flow rate: 1 mL/min, 25 °C; t_R 12.4 min for (*R*)-enantiomer (minor) and 13.3 min for (*S*)-enantiomer (major). (er = 68.8:31.2)

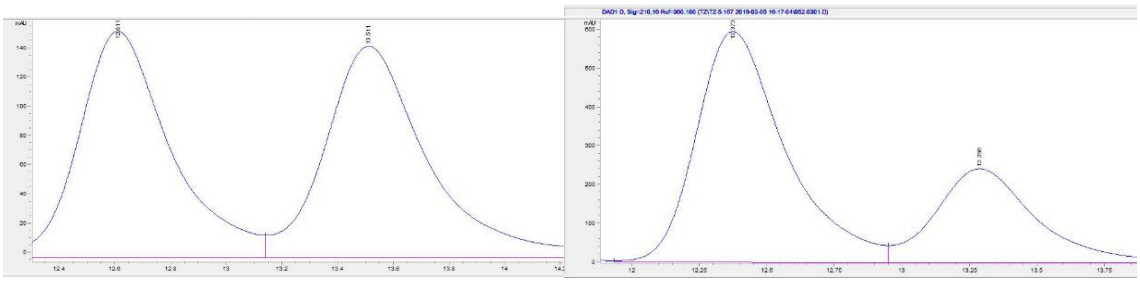

#	Time	Area	Height	Width	Area%	Symmetry
1	12.611	3628	155.1	0.3439	49.427	0.751
2	13.511	3712.1	145	0.3757	50.573	0.699

#	Time	Area	Height	Width	Area%	Symmetry
1	12.373	13751	596.2	0.3461	68.871	0.656
2	13.288	6215.2	242.2	0.3813	31.129	0.756

Figure 2.15 HPLC Data of SM of Table 2.2 Entry 8

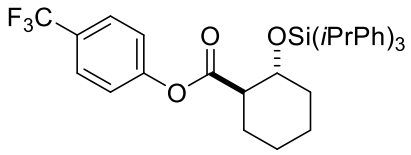

Recovered Product: 34 mg, 29 %, colorless oil. **^{1}H NMR** (400 MHz, $CDCl_3$) δ ppm 7.53 (d, J = 8.0 Hz, 8H), 7.20 (m, 6H), 6.90 (d, J = 8.4 Hz, 2H), 4.11 (td, J = 10.1, 4.4 Hz, 1H), 2.90 (d, J = 6.9 Hz, 3H), 2.77 (ddd, J = 11.2, 8.6, 2.6 Hz, 1H), 2.08 (dd, J = 13.1, 4.8 Hz, 1H), 1.92 (dd, J = 14.0, 2.8 Hz, 2H), 1.68 (dd, J = 12.3, 3.0 Hz, 2H), 1.52 – 1.36 (m, 3H), 1.25 (d, 18H). **^{13}C NMR** (101 MHz, $CDCl_3$) δ ppm 173.0, 153.3, 150.5, 150.3, 135.6, 133.2, 131.9, 126.5, 125.9, 122.2, 73.2, 60.2, 52.7, 35.0, 34.1, 28.5, 24.5, 23.8. **IR** (neat, cm^{-1}) 2960, 2954, 1763, 1734, 1600, 1460, 1395, 1324, 1167, 1093, 1050, 1018, 879, 822, 770. **HRMS** (EI^+) Calculated for ($C32H36F_3O3Si$) (M-*i*PrPh): 553.2386 Observed: 553.2381.

Table 2.10 Kinetic Resolution Data for Table 2.2, Entry 8

	er^{SM}	% conv (^{1}H NMR)	*s*	*s average*
1	69.6:30.4	30.0	33	35
2	68.9:31.2	29.0	37	

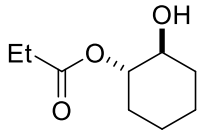

Table 2.2, Entry 9. Recovered starting material: 37 mg, 54%. **^{1}H NMR** (400 MHz, $CDCl_3$) δ ppm 4.58 (td, J = 9.0, 4.7 Hz, 1H), 3.56 (td, J = 9.8, 4.4 Hz, 1H), 2.45 – 2.25 (m, 2H), 2.08 – 1.99 (m, 2H), 1.80 – 1.62 (m, 2H), 1.33 (qt, J = 12.6, 5.0 Hz, 4H), 1.16 (t, J = 7.6 Hz, 3H).**^{13}C NMR** (101 MHz, $CDCl_3$) δ ppm 174.8, 78.1, 72.9, 33.1, 30.0, 27.9, 23.9, 23.8, 9.2. HPLC separation for the starting material was achieved by converting the alcohol into a benzoate ester through **GP4** in order to provide a chromophore.

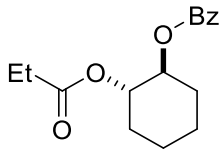

The product was prepared from recovered starting material (0.05 mmol) according to **GP4**. The desired product was isolated after column chromatography (10% EtOAc in hexane) as a colorless oil, 11 mg, 83 % yield. **^{1}H NMR** (400 MHz, $CDCl_3$) δ ppm 8.04 – 7.97 (m, 2H), 7.55 (s, 1H), 7.43 (t, J = 7.6 Hz, 2H), 5.04 (dd, J = 5.7, 3.7 Hz, 2H), 2.35 – 1.89 (m, 4H), 1.78 (d, J = 6.5 Hz, 2H), 1.43 (d, J = 10.3 Hz, 4H), 1.00 (t, J = 7.6 Hz, 3H). **^{13}C NMR** (101 MHz, $CDCl_3$) δ ppm 174.0, 166.0, 133.0, 130.0, 129.6, 128.4, 74.7, 73.3, 30.3, 30.2, 27.8, 23.6, 23.5, 9.2. HPLC conditions: Chiralpak AD-H Column 2% isopropyl alcohol in hexane, flow rate: 1 mL/min, 25 °C; t_R 10.6 min for (R)-enantiomer (minor) and t_S 11.3 min for (S)-enantiomer (major). (er = 60.3:39.7)

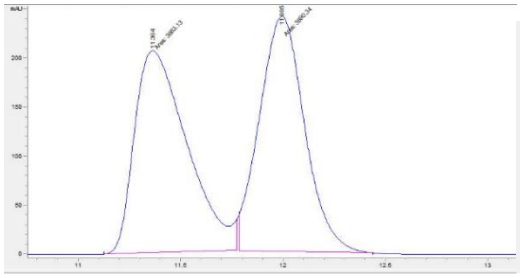

#	Time	Area	Height	Width	Area%	Symmetry
1	11.364	3683.1	205.6	0.2985	49.951	0.518
2	11.995	3690.3	240.1	0.2561	50.049	0.951

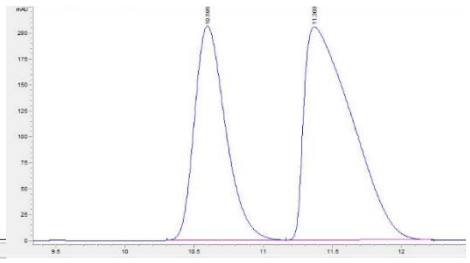

#	Time	Area	Height	Width	Area%	Symmetry
1	10.595	3236.1	206.4	0.2419	39.671	0.676
2	11.369	4921.2	205.3	0.3997	60.329	0.264

Figure 2.16 HPLC Data of SM of Table 2.2 Entry 9

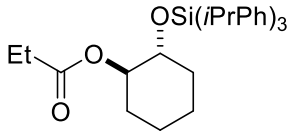

Recovered Product: 62 mg, 28%, colorless oil. **^{1}H NMR** (400 MHz, $CDCl_3$) δ ppm 7.51 (d, 6H), 7.21 (d, 6H), 4.80 (td , 1H), 3.76 (td, 1H), 3.00 – 2.79 (m, 3H), 2.12 – 1.83 (m, 3H), 1.77 – 1.30 (m, 7H), 1.25 (d, 18H), 0.90 (d, 3H). **^{13}C NMR** (101 MHz, $CDCl_3$) δ ppm 174.0, 150.3, 135.6, 132.2, 128.8, 125.9, 76.9, 73.4, 34.1, 33.9, 29.9, 27.4, 23.9, 23.5, 8.9. **Optical Rotation** $[\alpha]^{25}D$: -14.0 (c = 0.015) $CHCl_3$. **IR** (neat, cm^{-1}) 2957, 2870, 1736, 1599, 1459, 1394, 1263, 1191, 1097, 1049, 1019, 939, 914, 881, 872, 811, 770. **HRMS** (EI^+) Calculated for (C36H48O3Si) (M^+): 556.3373 Observed: 556.3383. The same separation conditions as the benzoate ester of the SM were utilized. (er = 66.7:33.3)

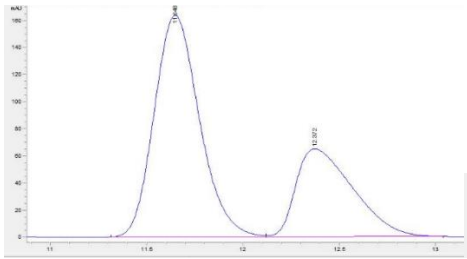

#	Time	Area	Height	Width	Area%	Symmetry
1	11.648	2675.7	163.8	0.2536	66.715	0.824
2	12.372	1335	64.9	0.3238	33.285	0.466

Figure 2.17 HPLC Data of PR of Table 2.2 Entry 9

Table 2.11 Kinetic Resolution Data for Table 2.2, Entry 9

	er^{SM}	er^{PR}	% conv	*s*	*s average*
1	60.3:39.7	66.7:33.3	38.1	2.4	3.0
2	61.0:39.0	73.8:26.2	31.5	3.5	

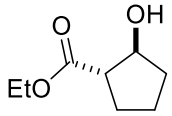

Table 2.2, Entry 10. Recovered starting material: 30 mg, 48%. **^{1}H NMR** (400 MHz, $CDCl_3$) δ ppm 7.53 (d, J = 7.9 Hz, 6H), 7.22 (d, J = 7.8 Hz, 6H), 4.61 (dd, J = 10.0, 5.0 Hz, 1H), 4.05 – 3.78 (m, 2H), 2.89 (td, J = 13.5, 6.7 Hz, 4H), 2.13 – 1.94 (m, 1H), 1.83 – 1.58 (m, 5H), 1.25 (d, J = 6.9 Hz, 18H), 1.12 (t, J = 7.1 Hz, 3H). **^{13}C NMR** (101 MHz, $CDCl_3$) δ ppm 175.0, 60.6, 52.7, 34.1, 27.2, 22.0, 14.3. HPLC separation for the starting material was achieved by converting the alcohol into a benzoate ester through **GP4** in order to provide a chromophore.[39]

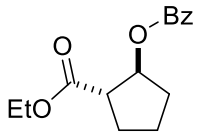

The product was prepared from recovered starting material (0.05 mmol) according to **GP4**. The desired product was isolated after column chromatography (10% EtOAc in hexane) as a colorless oil, 12 mg, 90 % yield. **^{1}H NMR** (400 MHz, $CDCl_3$) δ ppm 8.02 (d, J = 7.1 Hz, 2H), 7.56 (t, J = 7.4 Hz, 1H), 7.43 (t, J = 7.5 Hz, 2H), 5.58 (dt, J = 8.3, 4.1 Hz, 1H), 4.35 – 4.00 (m, 2H), 3.12 – 2.84 (m, 1H), 2.29 – 2.02 (m, 2H), 2.00 – 1.70 (m, 4H), 1.26 (t, J = 7.1 Hz, 3H). **^{13}C NMR** (101 MHz, $CDCl_3$) δ ppm 174.1, 166.0, 132.9, 130.4, 129.6,

128.3, 79.0, 60.8, 50.6, 32.7, 28.9, 23.7, 14.2. HPLC condition: Chiralpak OD-H Column 5% isopropyl alcohol in hexane, flow rate: 1 mL/min, 25 °C; t_s 6.4 min for (*S*)-enantiomer (major) and t_R 7.8 min for (*R*)-enantiomer (minor). (er = 60.6:39.4)

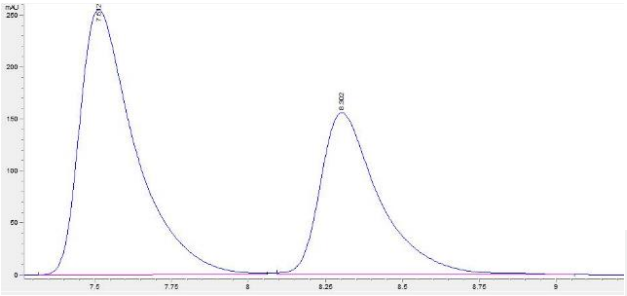

#	Time	Area	Height	Width	Area%	Symmetry
1	7.512	3211.2	255.5	0.1866	60.634	0.475
2	8.302	2084.9	156	0.1979	39.366	0.527

Figure 2.18 HPLC Data of SM of Table 2.2 Entry 10

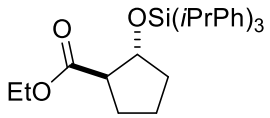

Recovered Product: 85 mg, 39 %, colorless oil. **^{1}H NMR** (400 MHz, $CDCl_3$) δ ppm 7.53 (d, J = 7.9 Hz, 6H), 7.22 (d, 6H), 4.61 (dd, J = 10.0, 5.0 Hz, 1H), 4.05 – 3.78 (m, 2H), 2.89 (td, 4H), 2.13 – 1.94 (m, 1H), 1.83 – 1.58 (m, 5H), 1.25 (d, 18H), 1.12 (t, 3H).**^{13}C NMR** (101 MHz, $CDCl_3$) δ ppm 175.3, 150.0, 135.6, 131.8, 125.9, 78.0, 60.2, 53.3, 35.5, 34.2, 28.3, 23.9, 23.1, 14.1. **Optical Rotation** $[\alpha]^{25}D$: -31.0 (c = 0.015) $CHCl_3$. As the product is not known compound, infrared spectrum and high-resolution mass spectrum had to be taken. **IR** (neat, cm^{-1}) 2960, 2871, 1731, 1600, 1394, 1188, 1092, 1018, 860, 821, 769. **HRMS** (EI^+) Calculated for (C35H46O3Si) (M^+): 542.3216 Observed: 542.3199. The infrared spectrum and high-resolution mass spectrum proved the product was the target product. HPLC data is of the desilylated products via **GP3** followed by conversion to the corresponding benzoate ester. The same separation conditions as the benzoate ester of the

starting material were utilized. (er = 63.2:36.8) In order to prove that product is *trans* isomer instead of *cis* isomer, crystal structure analysis could be done. The absolute stereochemistry of the isomer can be obtained through a test of optical rotation.

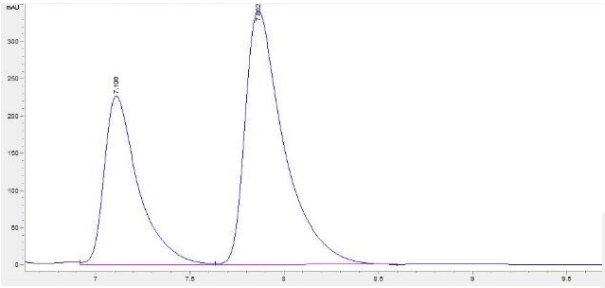

#	Time	Area	Height	Width	Area%	Symmetry
1	7.108	2842	226.6	0.1853	36.806	0.5
2	7.862	4879.5	341	0.2119	63.194	0.471

Figure 2.19 HPLC Data of PR of Table 2.2 Entry 10

Table 2.12 Kinetic Resolution Data for Table 2.2, Entry 10

	er^{SM}	er^{PR}	% conv	*s*	*s average*
1	60.6:39.4	63.2:36.8	44.5	2.0	2.7
2	65.6:34.4	70.2:29.8	43.6	3.1	

2.7 References

1. Sheppard, C. I.; Taylor, J. L.; Wiskur, S. L., Silylation-Based Kinetic Resolution of Monofunctional Secondary Alcohols. *Org. Lett.* **2011,** *13* (15), 3794-3797.
2. Wang, L.; Akhani, R. K.; Wiskur, S. L., Diastereoselective and Enantioselective Silylation of 2-Arylcyclohexanols. *Org. Lett.* **2015,** *17* (10), 2408-2411.
3. Clark, R. W.; Deaton, T. M.; Zhang, Y.; Moore, M. I.; Wiskur, S. L., Silylation-Based Kinetic Resolution of alpha-Hydroxy Lactones and Lactams. *Org. Lett.* **2013,** *15* (24), 6132-6135.
4. Akhani, R. K.; Moore, M. I.; Pribyl, J. G.; Wiskur, S. L., Linear Free-Energy Relationship and Rate Study on a Silylation-Based Kinetic Resolution: Mechanistic Insights. *J. Org. Chem.* **2014,** *79* (6), 2384-2396.
5. Wang, L.; Zhang, T.; Redden, B. K.; Sheppard, C. I.; Clark, R. W.; Smith, M. D.; Wiskur, S. L., Understanding Internal Chirality Induction of Triarylsilyl Ethers Formed from Enantiopure Alcohols. *J. Org. Chem.* **2016,** *81* (18), 8187-8193.
6. A. G. Doyle, E. N. Jacobsen, Small-Molecule H-Bond Donors in Asymmetric Catalysis. *Chem. Rev.* **2007**, 107 (1), 5713-5743.
7. X. Companyo, M. Viciano, R. Rios, Improving asymmetric organocatalysts via supramolecular interactions. *Mini-Rev. Org. Chem.* **2010**, 7 (1), 1-9.
8. R. R. Knowles, E. N. Jacobsen, Attractive noncovalent interactions in asymmetric catalysis: links between enzymes and small molecule catalysts. *Proc. Natl. Acad. Sci. U.S.A.* **2010**, 107 (48), 20678-20685.
9. C. R. Martinez, B. L. Iverson, Rethinking the term "pi-stacking". *Chem. Sci.,* **2012**, 3(7), 2191–2201.

10. D. A. Dougherty, The Cation-π Interaction. *Acc. Chem. Res.* **2013**, 46 (4), 885-893.
11. R. Thakuria, N. K. Nath, B. K. Saha, The nature and applications of π-π interactions: A perspective. *Cryst. Growth Des.* **2019**, 19 (2), 523−528.
12. S. Yamada, Intramolecular cation-π interaction in organic synthesis. *Org. Biomol. Chem.* **2007**, 5 (18), 2903-2912.
13. L. M. Salonen, M. Ellermann, F. Diederich, Aromatic rings in chemical and biological recognition: energetics and structures. *Angew. Chem. Int. Ed.* **2011**, 50 (21), 4808–4842.
14. C. R. Kennedy, S. Lin, E. N. Jacobsen, The Cation-π Interaction in Small-Molecule Catalysis. *Angew. Chem. Int. Ed.* **2016**, 55 (41), 12596-12624.
15. A. J. Neel, M. J. Hilton, M. S. Sigman, F. D. Toste, Exploiting non-covalent π interactions for catalyst design. *Nature* **2017**, 543 (7647), 637-646.
16. S. Yamada, Cation-π Interactions in Organic Synthesis. *Chem. Rev.* **2018**, 118 (23), 11353-11432.
17. M. Mohiti, C. Rampalakos, K. Feeney, D. Leonori, V. K. Aggarwal, Asymmetric addition of chiral boron-ate complexes to cyclic iminium ions. *Chem. Sci.* **2014**, 5 (2), 602−607.
18. S. Yamada, Y. Takahashi, Stereoselective synthesis of N,N-acetals by cyclization of an N-acyliminium ion through interaction with an N-sulfonyl group. *Tetrahedron Lett.* **2009**, 50 (38), 5395-5398.
19. Tirpak, R. E.; Olsen, R. S.; Rathke, M. W., Carboxylation of ketones using triethylamine and magnesium halides. *J. Org. Chem.* **1985**, 50 (24), 4877-4879.
20. Srikrishna, A.; Lakshmi, B. V.; Mathews, M., Construction of spiro[5.5]undecanes containing a quaternary carbon atom adjacent to a spirocentre via an Ireland ester

Claisen rearrangement and RCM reaction sequence. Total syntheses of (±)-α-chamigrene, (±)-β-chamigrene and (±)-laurencenone C. *Tetrahedron Lett.* **2006**, 47 (13), 2103-2106.

21. Lohr, T. L.; Li, Z.; Assary, R. S.; Curtiss, L. A.; Marks, T. J., Thermodynamically Leveraged Tandem Catalysis for Ester RC(O)O-R' Bond Hydrogenolysis. Scope and Mechanism. *ACS Catal.* **2015**, 5 (6), 3675-3679.
22. Birman, V. B.; Li, X. M., Homobenzotetramisole: An effective catalyst for kinetic resolution of aryl-cycloalkanols. *Org. Lett.* **2008**, 10 (6), 1115-1118.
23. Conversions and selectivity factors are based on the ee of the recovered starting materials and products. Percent conversion = $ee_s/(ee_s + ee_p) \times 100\%$ and $s = \ln[(1 - C)(1 - ee_s)]/\ln[(1 - C)(1 + ee_s)]$, where ee_s = ee of recovered starting material and ee_p = ee of product. See ref H. B. Kagan, J. C. Fiaud In Topics in Stereochemistry (Ed.: L. Ernest, S. H. Wilen), John Wiley and Sons: New York, 1988; Vol. 18, p 249.
24. M. Charton, Steric effects.I. Esterification and acid-catalyzed hydrolysis of esters. *J. Am. Chem. Soc.* **1975**, 97 (6), 1552-1556.
25. M. Charton, Steric effects. II. Base-catalyzed ester hydrolysis. *J. Am. Chem. Soc.* **1975**, 97 (13), 3691-3693.
26. M. Charton, Steric effects.III. Bimolecular nucleophilic substitution. *J. Am. Chem. Soc*. **1975**, 97 (13), 3694-3697.
27. J. H. Wu, G. Zhang, N. A. Porter, Substrate steric effects in enantioselective Lewis acid promoted free radical reactions. *Tetrahedron Lett.* **1997**, 38 (12), 2067-2070.

28. L. Mantilli, D. Gerard, S. Torche, C. Besnard, C. Mazet, Improved catalysts for the iridium-catalyzed asymmetric isomerization of primary allylic alcohols based on Charton analysis. *Chem. Eur. J.* **2010**, 16 (42), 12736-12745.

29. H. Huang, H. Zong, G. Bian, L. Song, Constructing a Quantitative Correlation between N-Substituent Sizes of Chiral Ligands and Enantioselectivities in Asymmetric Addition Reactions of Diethylzinc with Benzaldehyde. *J. Org. Chem.* **2012**, 77 (22), 10427-10434.

30. L. A. Cohen, S. Takahashi, Reexamination of electronic effects in ring-substituted phenyl esters. Correlation of spectral and kinetic properties with σ^{o}.. *J. Am. Chem. Soc.* **1973**, 95 (2), 443-448.

31. H. Neuvonen, K. Neuvonen, Correlation analysis of carbonyl carbon ^{13}C NMR chemical shifts, IR absorption frequencies and rate coefficients of nucleophilic acyl substitutions. A novel explanation for the substituent dependence of reactivity. *J. Chem. Soc., Perkin Trans. 2*. **1999**, (7), 1497-1502.

32. H. Neuvonen, K. Neuvonen, P. Pasanen, Evidence of Substituent-Induced Electronic Interplay. Effect of the Remote Aromatic Ring Substituent of Phenyl Benzoates on the Sensitivity of the Carbonyl Unit to Electronic Effects of Phenyl or Benzoyl Ring Substituents. *J. Org. Chem.* **2004**, 69 (11), 3794-3800.

33. M. Lewis, C. Bagwill, L. K. Hardebeck, S. Wireduaah, The use of hammett constants to understand the non-covalent binding of aromatics. *Comput. Struct. Biotechnol.* **2012**, 1, e201204004.

34. F. J. Carver, C. A. Hunter, D. J. Livingstone, J. F. McCabe, E. M. Seward, Substituent effects on edge-to-face aromatic interactions. *Chem. Eur. J.* **2002**, 8 (13), 2847-2859.

35. C. G. Swain, E. C. Lupton, Field and resonance components of substituent effects. *J. Am. Chem. Soc.* **1968**, 90 (16), 4328-4337.

36. C. Hansch, A. Leo, S. H. Unger, K. H. Kim, D. Nikaitani, E. J. Lien, Aromatic substituent constants for structure-activity correlations. *J. Med. Chem.* **1973**, 16 (11), 1207-1216.

37. Burchat, A. F.; Chong, J. M.; Nielsen, N., Titration of alkyllithiums with a simple reagent to a blue endpoint. *J. Organomet. Chem.* **1997**, 542 (2), 281-283.

38. Yoshida, M.; Ohno, S.; Shishido, K., Synthesis of Tetrasubstituted Furans by Palladium-Catalyzed Decarboxylative [3+2] Cyclization of Propargyl β-Keto Esters. *Chem. Eur. J.* **2012**, 18 (6), 1604-1607.

39. Kitamura, M.; Ohkuma, T.; Tokunaga, M.; Noyori, R., Dynamic kinetic resolution in BINAP-ruthenium(II)-catalyzed hydrogenation of 2-substituted 3-oxo carboxylic esters *Tetrahedron: Asymmetry* **1990**, 1(1), 1-4.

40. Buisson, D.; Azerad, R., Diastereoselective and enantioselective microbial reduction of cyclic α-alkyl β-keto esters. *Tetrahedron Lett.* **1986**, 27 (23), 2631-2634.

41. Ros, A.; Magriz, A.; Dietrich, H.; Lassaletta, J. M.; Fernández, R., Stereoselective synthesis of syn β-hydroxy cycloalkane carboxylates: transfer hydrogenation of cyclic β-keto esters via dynamic kinetic resolution. *Tetrahedron* 2007, 63 (32), 7532-7537.

42. Jung, M. E.; Cho, Y. M.; Jung, Y. H., Facile synthesis of optically active 2-hydroxymethyl-4-methylenecyclohexanol. De novo synthesis of dideoxycarbocyclic sugars. *Tetrahedron Lett.* 1996, 37 (1), 3-6.

CHAPTER 3

INVESTIGATION OF CATION-π INTERACTION BETWEEN ISOTHIOUREA CATALYST AND *trans*-2-PHENYLCYCLOHEXANOL

3.1 Introduction

Isothiourea catalysts[1] have successfully shown excellent selectivities in our silylation-based kinetic resolution system. Selectivity factors up to 100 were obtained when (-)-benzotetramisole **1.4** was used to resolve α-hydroxy lactones (Scheme 3.1).[2-4] An investigation on how isothiourea catalysts dictate the enantioselectivity in our system directed the progression of our research. Our group has performed mechanistic research to explore the mechanism of our silylation-based kinetic resolution system and to understand the intermediate formed when the isothiourea catalyst reacts with the silyl chloride.[5-6] This work suggested the isothiourea catalysts would serve as a nucleophile to attack the silyl chloride and a cationic intermediate is formed on the isothiourea. This provides the possibility of a cation-π[7-8] interaction between the cationic catalyst and a π system in the substrate which has been suggested to be a key factor to control the selectivity in other asymmetric reactions.[9-11] We wondered if that same electronic interaction between our cationic intermediate and a pi system around the alcohols control the selectivity of our kinetic resolution. Understanding the potential cation-π interaction in our system would

provide an efficient path to discover more substrate candidates without a time-consuming screen of substrates. This chapter will focus on exploration of cation-π interaction between *trans*-2-phenylcyclohexanol and (-)-benzotetramisole (**1.4**) (most suitable isothiourea catalyst for *trans*-2-phenylcyclohexanol) in our silylation-based kinetic resolution system.

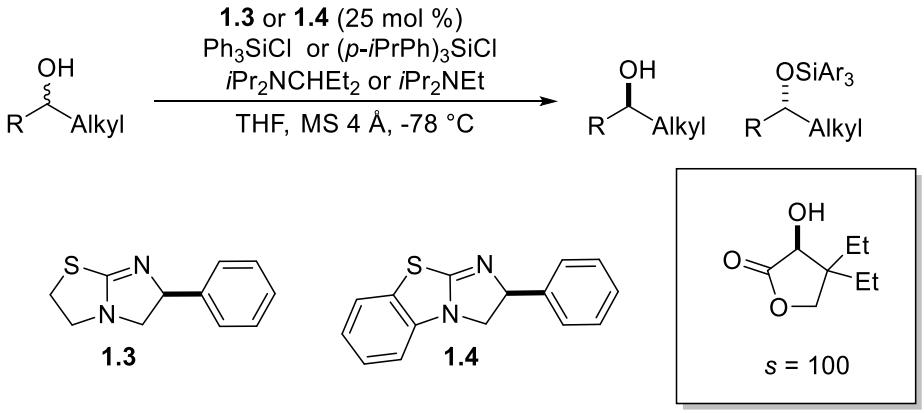

Scheme 3.1 Silylation-Based Kinetic Resolutions of Wiskur Group

In Chapter 2, *trans* alkyl-2-hydroxycyclohexanecarboxylate substrates were used to explore the electrostatic interactions between a π system adjacent to the resolving alcohol and an isothiourea catalyst (Scheme 3.2). It was discovered that electrostatic interactions between the π system of an ester group adjacent to the resolving alcohol and a cationic catalyst complex aid in controlling the selectivity. When the ester is derivatized with alkyl groups, an electrostatic attraction between the esters and the catalyst seem to dominate selectivity control. Electrostatic interactions are hypothesized to be controlled by a cation-π interaction between the ester and the cationic catalyst intermediate (Figure 3.1). However, when the ester is derivatized with phenyl groups, edge to face π-π interactions between the phenyl group on the ester and one of the aromatic groups on the catalyst intermediate predominant in controlling stereochemistry (Figure 3.2). In this case, we have

determined that depending on the nature of the substrate, different interactions aid in controlling the selectivity. We were interested in exploring whether the selectivity of our kinetic resolution with a different alcohol substrate would show control through a cation-pi interaction or if another interaction would again dominate controlling the selectivity. Our previous LFER study had too many pi systems (the phenyl group and the ester it was attached to) allowing for multiple interactions, therefore we decided to simplify the substrate to include only one π system, an aryl group. Since aromatic systems have been shown to provide a decent selectivity factor and the electronics on the phenyl system affect the selectivity, we decided to investigate the potential cation-π interaction between the phenyl ring of 2-aryl cyclohexanols and the cationic catalyst intermediate.[4] In this chapter, we will strive to understand this cation-π interaction through a linear free energy relationship.

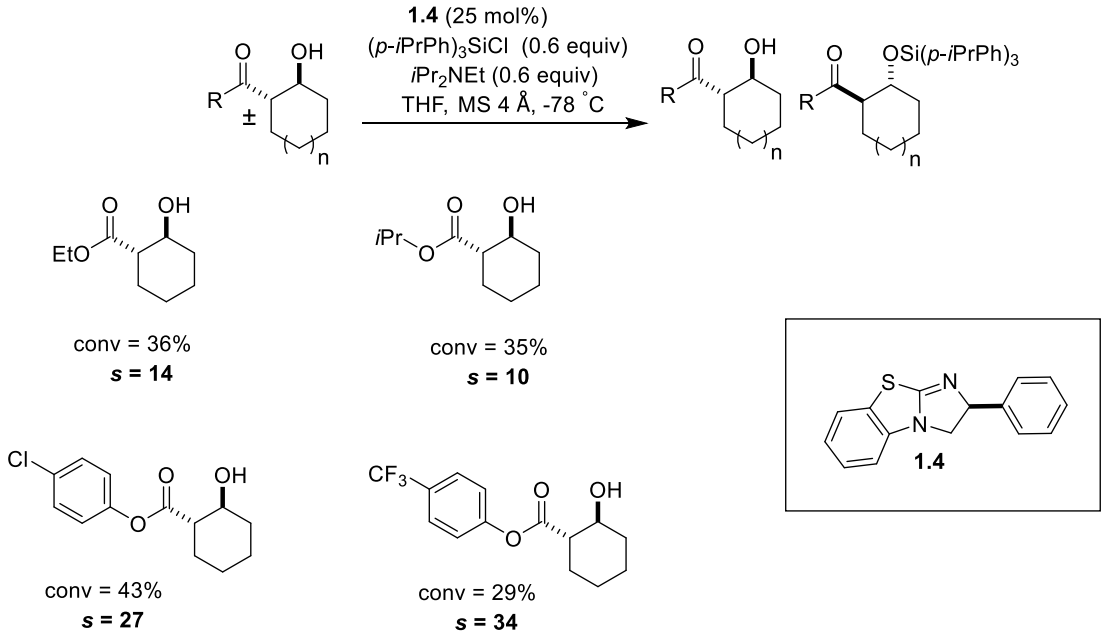

Scheme 3.2 Kinetic Resolution of *trans*-Alkyl-2-hydroxycyclohexanecarboxylate

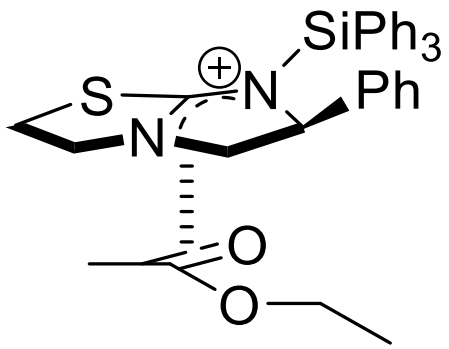

Figure 3.1 Cation-π Interaction

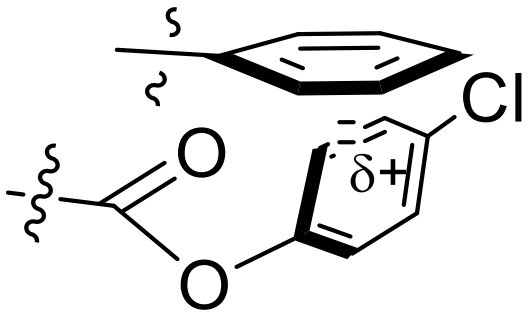

Figure 3.2 Edge to Face π-π Interaction

In order to investigate the cation-π interaction between the phenyl ring of the alcohol and the cationic catalyst intermediate, an appropriate alcohol model is needed. The alcohol must possess a phenyl ring near the hydroxyl group and this substrate class should be suitable for an easy synthesis of its derivatives. Ultimately, 2-phenyl cyclohexanol and its derivatives were picked as the substrate models for the investigation as the phenyl group is the only π system present in the substrate and the electronics of the phenyl ring could be controlled by various substituents on the *meta* position of the phenyl group (Figure 3.3). Previous studies[4] showed higher selectivity factors are achieved in the meta position, therefore our efforts were focused on designing *meta* substituted derivatives.[4] Linear free

energy relationship (LFER) studies were employed to explore what intermolecular interactions control selectivity.

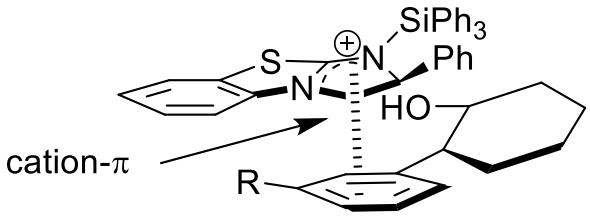

Figure 3.3 Potential Cation- π Interaction

Isothiourea catalysts were developed by Birman as an enantioselective acyl transfer catalyst and were successfully employed in a number of kinetic resolution reactions.[12-14] Even at room temperature, 2-phenyl cyclohexanol could be resolved via acylation with a selectivity factor of 25 and conversion of 48 percent in 6 hours (Scheme 3.3) under catalysis by (-)-benzotetramisole **1.4**. [14]

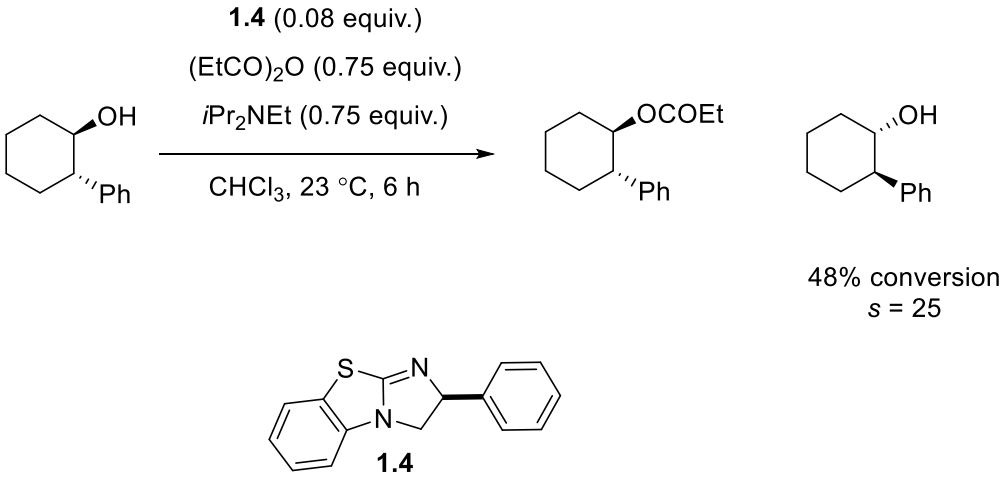

Scheme 3.3 Birman's Kinetic Resolution of *trans*-2-Arylcyclohexanol

Considering the excellent performance of the isothiourea catalysts in enantioselective acylation, Birman carried out computational studies on the origin of the enantioselectivity in benzotetramisole-catalyzed kinetic resolutions.[11, 14] It was observed that all of the substrates studied in Birman's kinetic resolution system share the same general patterns of having a π-system located adjacent to a nucleophilic atom and displayed the same absolute sense of chirality in the fast reacting enantiomers. A transition state was proposed to demonstrate how the enantioselectivity was obtained based on the kinetic resolution of secondary benzylic alcohols catalyzed by CF_3-PIP (**3.1**), his first generation of isothiourea catalysts (Scheme 3.4). The proposed transition state indicates how the faster enantiomer is more favorably attracted by strong cation-π interactions to the cationic catalyst, affording a selective acylation. The slower enantiomer has a weaker cation-π interaction to the cationic catalyst due to the unfavorable chiral recognition.

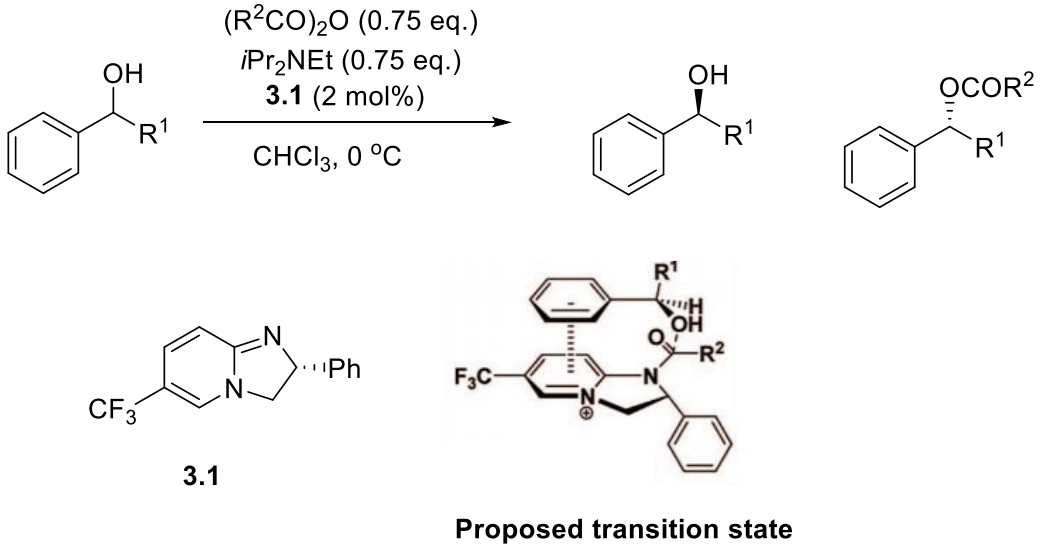

Scheme 3.4 BTM-Catalyzed Kinetic Resolution of Benzylic Alcohols

Density function theory (DFT) computations were performed to analyze if the origin of selectivity is the proposed transition state structure in Scheme 3.4. To start with, Birman succeeded in obtaining the crystal structure of the *N*-acetylated catalyst. Then computation studies of the intermediate associated with the *R* and *S* enantiomer of benzylic alcohol were conducted at the B3LYP/6-31G* level of theory. The distance between the center of the phenyl ring of the alcohol to the center cationic aromatic ring of the catalyst is different in the transition states of the two enantiomers. It is obvious that the faster enantiomer is closer to the cationic catalyst, suggesting strong cation-π interactions. In addition, the overall energy in the transition state of the faster enantiomer is lower than that of the slower enantiomer, suggesting a stabilization of the transition state by the cation-π interactions.

We use benzotetramisole as our catalyst and share the same general pattern of requiring a π-system at an adjacent position to the hydroxyl group. Our approach to exploring the interactions controlling the selectivity is twofold. First, we plan to apply a linear free energy relationship study employing 2-aryl cyclohexanols substituted with different electron donating and withdrawing groups to study how these groups affect the selectivity as a result of changing the strength of the potential cation-π interaction. Second, we would carry out a computational study on our proposed transition state to check for the existence of a cation-π interaction by recording the distance between the phenyl ring of tetralol and the aromatic moiety of (-)-benzotetramisole **1.4**. To be specific, spartan computation program would be used. A single point computation on the geometry optimization of cationic intermediate would be run plus a energy profile computation on the whole nucleophilic attack process.

3.2 Synthesis of *trans*-2-Arylcyclohexanol

The synthesis of *trans* 2-aryl cyclohexanols with different groups (X = H, CH_3, OCH_3, F) in the *meta* position share a general procedure (Scheme 3.5) and start with a substituted bromo benzene **3.2**.[15] Magnesium turnings were crushed overnight under vacuum then treated with a solution of **3.2** in THF. Temperature was carefully increased to 60 ^oC to afford a complete conversion to the Grignard reagent **3.3**. The temperature needs to be carefully controlled due to the vulnerability of the radical to temperature.[16] If the temperature is too low, no radical will be generated, while high temperature will kill radicals. The Grignard reaction of **3.2** is normally finished in 2 hours. Afterwards the resulting mixture was transferred to another round bottom flask containing a slurry mixture of copper oxide and cyclohexene oxide in THF. Copper oxide serves as the Lewis acid to activate the epoxide towards nucleophilic ring opening with the Grignard reagent. Since it is an S_N2 reaction, only *trans* 2-phenyl cyclohexanol is generated.

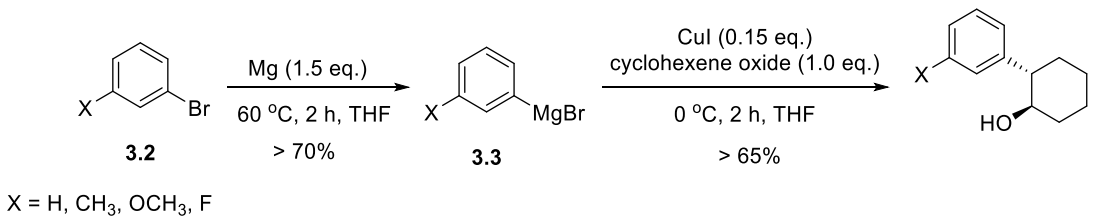

Scheme 3.5 Synthesis of *trans*-2-Arylcyclohexanol

Our plan was to synthesize a number of *trans*-2-arylcyclohexanols, that are substituted with groups that span a range of sigma meta (σ_m) constants.[17] However, when we analyzed the kinetic resolution data we obtained on the *trans*-2-arylcyclohexanol (X = H, CH_3, OCH_3, F) with a sigma meta linear free energy relationship (LFER) analysis, no

correlation was observed (discussed in more detail below). However, when asigma resonance (σ_R) constant was employed, a strong correlation was observed. Unfortunately, the *trans*-2-arylcyclohexanols we synthesized all share a negative σ_R constant. In order to have more convincible LFER plot, synthesis of a *trans*-2-arylcyclohexanol with a positive σ_R constant was required. Our next target was a *trans*-2-arylcyclohexanol with an ethyl ester in the meta position. Since a Grignard reagent, which is used to open the epoxide would attack and destroy an ester substituent, we needed to protect the electrophilic during the Grignard reaction. Initial attempt utilized a super "silyl group" to derivatize the 3-bromo benzoic acid **3.4** to the silyl ester **3.5** (Scheme 3.6).[18] The resulting ester **3.5** is tolerable to the Grignard reaction but would not need a series of oxidation and protection steps after the epoxide opening. However, the super "silyl" reagent is very expensive and low yields were obtained in preparing **3.5**. An alternative compound was then targeted.

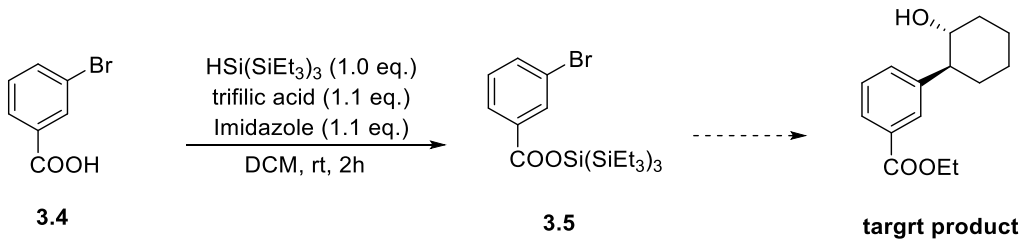

Scheme 3.6 Protection of Carboxylic Acid with Super "Silyl" Group

We then changed our target compound to **3.8**, which has an aldehyde in the meta position (Scheme 3.7). Inspired by undergraduate organic chemistry, we picked 2-(3-bromophenyl)-1,3-dioxolane **3.6** as starting material. The acetal protected aldehyde **3.6** is commercially available and with the protecting group, the substrate is tolerant to Grignard reagents. A similar synthesis procedure to the derivatives in Scheme 3.6 was applied.

Substantial amounts of *trans* 2-aryl cyclohexanol with the acetal on the meta position of phenyl group (**3.7**) was prepared. The reaction was low yielding (25 %) presumably due to the negative effect of an electron withdrawing group on the preparation of the Grignard reagent. The target product, 2-hydroxycyclohexyl benzaldehyde **3.8,** can be synthesized after a simple deprotection of the acetal protecting group. This is where we are currently at with this substrate.

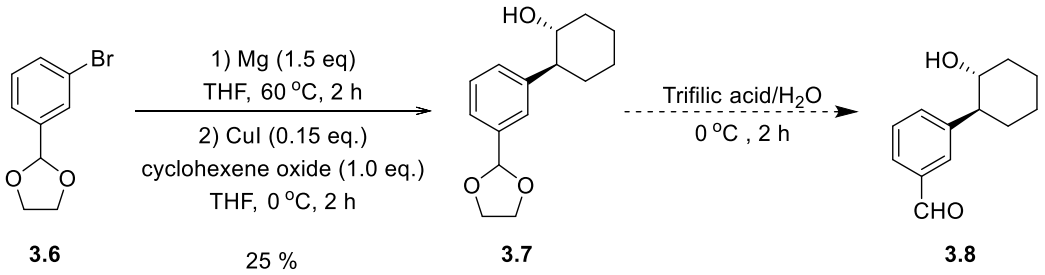

3.6 25 % **3.7** **3.8**

Scheme 3.7 Synthesis of 2-Hydroxycyclohexyl Benzaldehyde

3.3 Kinetic Resolution of *trans*-2-Arylcyclohexanol and LFER Studies

With some of the synthesized derivatives of *trans* 2-aryl cyclohexanol in hand, our next objective was the investigation of potential cation-π interactions between the phenyl ring of the alcohol and the cationic catalyst. Our experimental design used these substrates in our silylation-based kinetic resolution as well as Birman's acylation-based kinetic resolution. Since it is suggested in the literature that the acylation selectivity is dependent on a cation-π interaction,[11] we wanted to be able to compare our LFER data with data that supposedly comes from a similar interaction. The resulting kinetic resolutions would be used to explore a linear free energy relationship (LFER) using the log of the selectivity factors versus a substituent parameter that shows a linear relationship. The sigma parameter

that is usually identified with cation-π interactions is sigma meta. Correlation of the plots supportive of a cation-π interaction would involve more electron donating groups providing a stronger interaction.

Silylation-based kinetic resolutions of *trans* 2-aryl cyclohexanols were conducted by Dr. Wang from the Wiskur group for his substrate expansion study (Table 3.1).[4] The more selective (-)-benzotetramisole (**1.4**) was used as the chiral catalyst and an electron donating tris(4-isopropylphenyl) silyl chloride was used as the silyl source. When there is no substituent on the phenyl ring, a moderate selectivity (*s* = 10) was obtained (Table 3.1, Entry 1). When the phenyl ring was attached with substituents, higher selectivity factors were obtained (Table 3.1, Entry 2-4 vs Entry 1). In the presence of methoxy substituent which is strongly electron donating by resonance, but electron withdrawing by induction, the selectivity increased significantly (*s* = 53). The log of the selectivity factors of various *trans* 2-aryl cyclohexanols were plotted in Table 3.1 versus sigma meta (σ_m) parameters, but there was no linear correlation (Figure 3.4).[19] Interestingly, when we plotted our data vs sigma resonance (σ_R) parameters, a linear plot was observed with good correlation (Figure 3.5, $R^2 = 0.98$). With sigma resonance, all the substituents that we incorporated are all electron donating when just looking purely at resonance. A change in the electron density of the conjugated π system is highly relevant towards developing a strong cation-π interaction. Our data suggests that the resonance of a substituent with the π system is important in controlling the electrostatic interaction between the π system and the catalyst. We expect that compound **3.8** will show a decrease in selectivity, given the electron withdrawing nature of the aldehyde. However, we still couldn't conclude that this electrostatic interaction is a cation-π interaction. If employment of *trans*-2-

arylcyclohexanols in Birman's acylation-based system provided a similar LFER outcomes, we could probably draw an analogy of his explanation of mechanism into our silyl-based system.

Table 3.1 Silylation-Based Kinetic Resolution of *trans*-2-Arylcyclohexanols

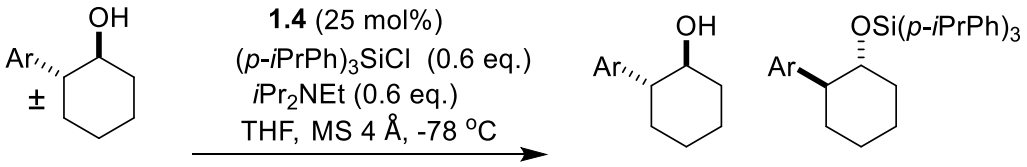

entry[a]	recovered alcohol	er of recovered alcohol	% conv[b]	*s*[b]
1	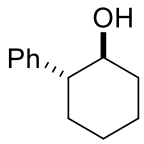	83:17	51	10
2	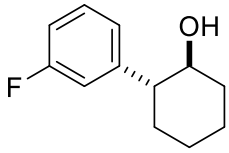	85:15	45	27
3	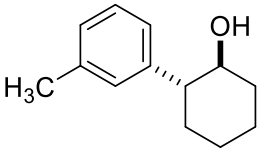	64:36	26	14
4	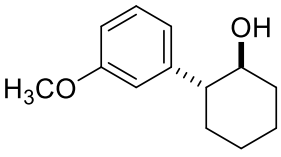	95:5	50	53

[a]Reactions were run for 48 hours at a concentration of 0.42 M with respect to alcohol on a 0.4 mmol scale. [b]See Ref[20]

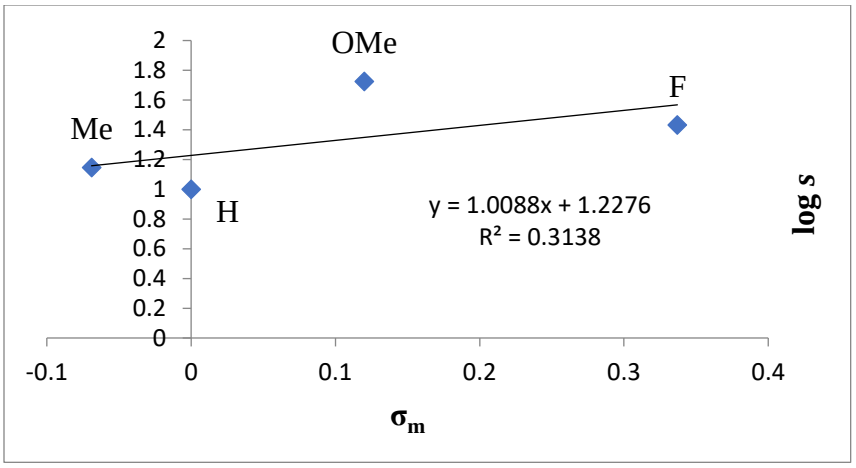

Figure 3.4 LFER Employing σ^m to log of Selectivity Factors

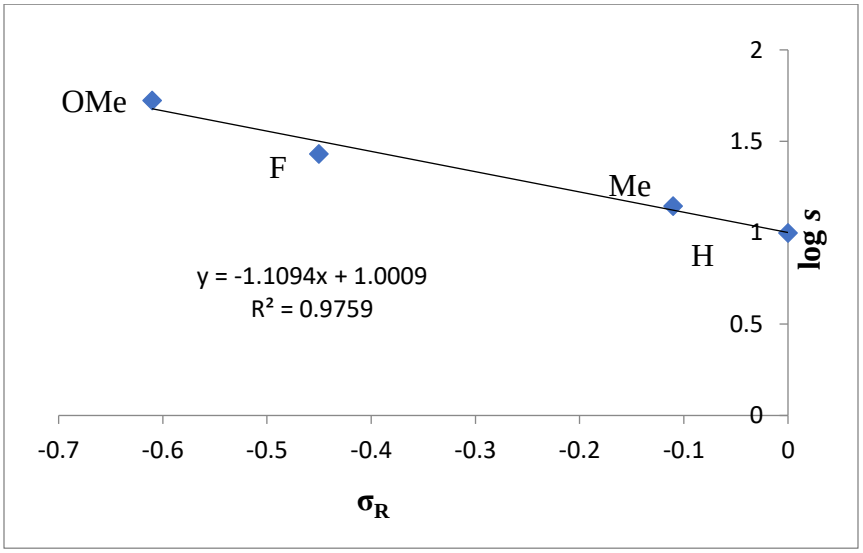

Figure 3.5 LFER Employing σ_R to log of Selectivity Factors

Acylation-based kinetic resolutions of *trans* 2-aryl cyclohexanol followed the procedure developed Birman with an exception of changing solvent from $CDCl_3$ to THF (Birman suggested replacement of solvent to THF has no significant effect on the selectivity factor) (Table 3.2).[14] The same 2-aryl cyclohexanols were resolved with Birman's system and moderate to high selectivity factors were obtained for all substrates. The log of the selectivity factors in Table 3.2 were plotted versus sigma meta (σ_m)

parameters and again, no correlation was obtained. However, no correlation (Figure 3.6, R^2 = 0.09) was obtained when a Hammett plot was generated sigma resonance (σ_R) substituent constants either, suggesting that not the induction nor resonance is predominant in controlling enantioselectivity.

Table 3.2 Acylation-Based Resolution of *trans*-2-Arylcyclohexanols

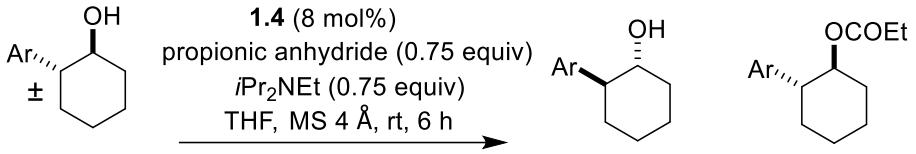

entry[a]	recovered alcohol	er of recovered alcohol	% conv[b]	s[b]
1	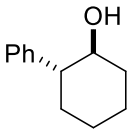	76:24	38	21
2	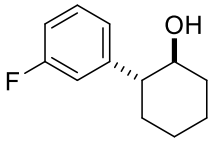	84:16	50	9
3	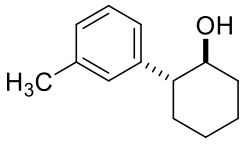	87:23	49	16
4	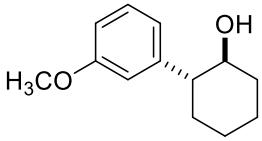	95:5	55	20

[a]Reactions were run for 48 hours at a concentration of 0.42 M with respect to alcohol on a 0.4 mmol scale. [b]See Ref[20]

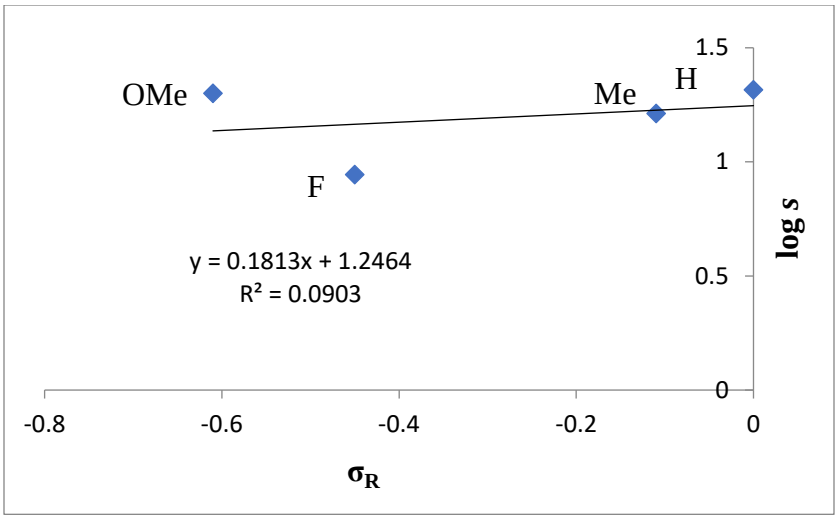

Figure 3.6 LFER Employing σ_R to log of Selectivity Factors

Future work will focus on finishing the kinetic resolution of **3.8** in silylation-based and acylation-based kinetic resolutions. Further research will focus on the computational study of the electrostatic interaction, especially the role it plays in the transition state.

3.4 Computation Study of Transition State

Based on the previous mechanistic study, we hypothesized that a cation-π interaction plays an important role in stabilizing and directing the alcohol in its approach to reacting with the activated silicon (Figure 3.7). In order to explore the possibility that a cation-π interaction makes a contribution towards controlling selectivity, Shelby Dickerson from our group conducted a series of computational studies of the transition state using Spartan's program.[21] The computation study started with a single point energy calculation followed by a geometry optimization of the potential intermediate **2.1** using Hartree Fock (HF) level of theory with the 6-31G* basis set in vacuum (Figure 3.8). We could easily observe a π-π stacking interaction between one phenyl ring on the silicon and

the phenyl ring of the catalyst. We hypothesize an occurrence of chirality transmission is controlled by this π-π stacking interaction.

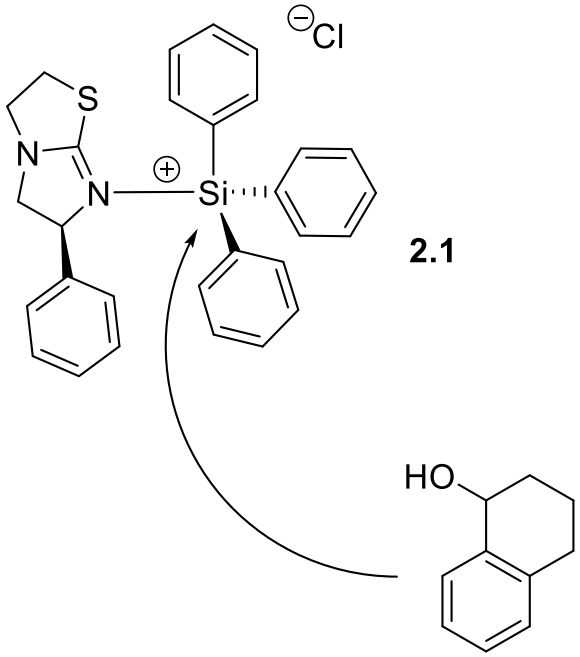

Figure 3.7 Tetralol Attacks Intermediate

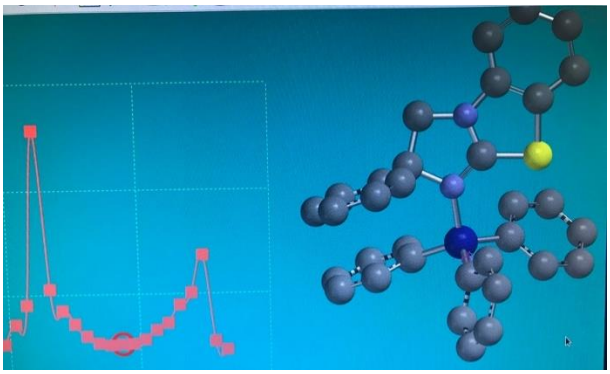

Figure 3.8 Single Point Energy Calculation

Once the structure of the intermediate **2.1** was determined, an energy profile computation of the nucleophilic attack to the cationic complex of intermediate was

conducted (Figure 3.9). Figure 3.9 shows the energy coordination diagram of the process highlighted in Figure 3.7 when the fast reacting enantiomer of the alcohol tetralol, serving as the replacement of trans-2-phenyl cyclohexanol to ease the complication of calculation ,attacks the cationic intermediate (**2.1**) to form the silyl ether. The peak of the energy coordination diagram suggests the structure of the transition state. We observed a close distance between the aromatic ring of alcohol and fused ring of cationic catalyst intermediate, suggesting a cation-π interaction between the π system of the alcohol and the cationic catalyst intermediate.

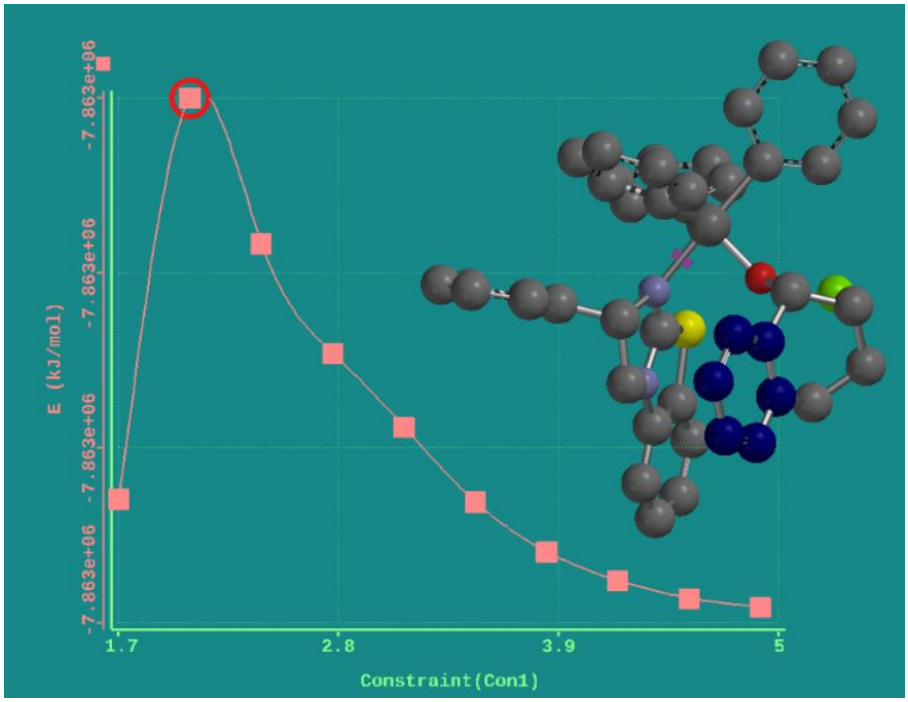

Figure 3.9 Energy Profile Computation of the Cationic Complex

3.5 Conclusion and Outlook

In conclusion, the mechanistic investigations on cation-π interactions in controlling enantioselectivity were carried out by performing LFER studies on *trans* 2-phenyl

cyclohexanol and its derivatives in our silylation-based kinetic resolution system and in Birman's acylation system. Linear free energy relationship (LEFR) plots suggest a different decisive electrostatic interaction in controlling the selectivity factors between the two systems even though the same catalyst was utilized. The importance of cation-π interactions in our system was suggested by strong correlation of log *s* to sigma resonance (σ_R). Kinetic resolutions under the same reaction conditions will be performed on 2-hydroxycyclohexyl benzaldehyde **3.8**. An additional data point with a negative σ_R is expected to perform worse by negatively impacted the hypothesized cation-π interaction.

Geometry optimization study of cationic intermediate **2.1** displayed a pi-pi stacking interaction between one phenyl ring on the silicon and the fused aromatic ring of the catalyst. We hypothesized that transmission of chirality is promoted by this interaction. More evidence will be collected to support our hypothesis. The energy profile computation was carried out to simulate the whole process of pseudo S_N2 attack of an alcohol onto the cationic catalyst intermediate resulting in silylation. A potential transition state was obtained according to the energy coordination diagram. The distance between the center of cationic catalyst to the phenyl ring of alcohol suggests a strong cation-π interaction. Our future work will continue the computational study of the transition state. We have explored one enantiomer attacking the silicon, but we also need to show the path of the slow reacting enantiomer to show that it does have a higher transition state. We also have performed these calculations lacking the presence of the chloride, but we know that may make a difference, therefore we are going to look at these calculations again in the presence of the chloride anion The structure will then undergo a transition state geometry calculation using DFT level of theory with the 6-31G* basis set in vacuum. Our long-term goal in the future

is the investigation of the whole mechanistic cycle of our silylation-based kinetic resolution, including computation study and kinetic study.

3.6 Experimental

General Information

All the reactions were carried out under a nitrogen atmosphere using oven-dried glassware. Molecular sieves were activated in an oven at 170 °C before use. Tetrahydrofuran (THF), diethyl ether and dichloromethane (CH_2Cl_2) were dried by passing through a column of activated alumina before use and stored over molecular sieves. Carbon tetrachloride (CCl_4) was distilled and degassed prior to use. Sulfuryl chloride (SO_2Cl_2) and tetramethylethylenediamine (TMDEA) were distilled before use. n-Butyl lithium was titrated prior to use. Unless otherwise stated, all the other chemicals were obtained from major commercial sources and used without further purification. High resolution mass spectrometry (HRMS) was submitted to and conducted by the Department of Chemistry and Biochemistry's mass spectrometry facility at the University of South Carolina. Infrared spectroscopy (IR) was conducted using a Perkin Elmer Spectrum 100 FT-IR ATR spectrophotometer, νmax in cm-1. ^{1}H NMR was taken on a Bruker Avance (300 or 400 MHz). Chemical shifts were reported in ppm with TMS or Chloroform as an internal standard (TMS 0.00 ppm for ^{1}H and ^{13}C or $CHCl_3$ 7.26 ppm and 77.16 for ^{1}H and ^{13}C respectively). ^{13}C NMR spectra were taken on a Bruker Avance (101 or 75 MHz) with complete proton decoupling. Enantiomeric ratios were determined via HPLC using an Agilent 1200 series. The chiral stationary phases were Daicel Chiralcel OD-H, OJ-H, AD, AD-H or Daicel Chiralpak IC columns, and the enantiomers were measured by a diode

array detector in comparison with the racemic materials. Optical Rotations were obtained utilizing a JASCO P-1010 polarimeter. Uncorrected melting points (mp) were taken with a Laboratory Devices Mel-Temp.

General procedure to prepare racemic substituted 2-aryl cyclohexanols (GP1)

Procedure was adapted from reported literature.[15] A 250 mL Schlenk flask was equipped with stir bar and charged with Mg turnings (1.8 equiv.). The flask was then flame dried fitted with septa. The apparatus was then purged with argon and fitted with an argon balloon. The turnings were crushed under vacuum overnight before use. Before activation of Grignard reagent started, 5 mL of THF was added to the Schlenk tube via syringe. The mixture was warmed to 60 °C in oil bath and a few drops of meta-substituted bromo benzene was added and allowed to stir for 5 min. The remaining solution of meta-substituted bromo benzene (1.5 equiv.) in THF (5 mL) was added slowly (10 min in total) and the mixture was allowed to react for 1 hour. The mixture was then cooled to room temperature. A mixture of cyclohexene oxide (1.0 equiv.) and copper iodide (0.15 equiv.) was prepared THF (2mL / 1mmol cyclohexene oxide) under argon. The mixture was added slowly to the Grignard solution producing an exothermic reaction and allowed to react at room temperature overnight. Once the reaction was done, it was quenched with saturated NH_4Cl (20 mL). Organic layer was washed with water (20 mL, 2 times) and Brine (20 mL). Then organic layer was dried with sodium sulfate anhydrous concentrated by Rotary Evaporator. The residue was purified through a silica gel chromatography with 5% ethyl acetate in hexane to 25% ethyl acetate in hexane to yield white soild.

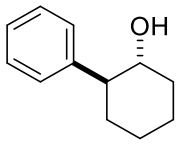

(±)

***trans*-2-(3-Phenyl)cyclohexan-1-ol**

The product was prepared from bromobenzene (15.6 mmol) according to **GP1.** The desired product was obtained as white solid, 1.972 g, 11.2 mmol, 71.8 % yield. **^{1}H NMR** (400 MHz, $CDCl_3$): δ ppm 7.38 – 7.29 (m, 2H), 7.29 – 7.21 (m, 3H), 3.67 (ddd, *J* = 10.1, 6.3, 2.5 Hz, 1H), 2.43 (ddd, *J* = 13.2, 10.0, 3.5 Hz, 1H), 2.16 – 2.06 (m, 1H), 1.85 (dt, *J* = 12.5, 6.6 Hz, 2H), 1.80 – 1.71 (m, 1H), 1.62 – 1.28 (m, 4H). **^{13}C NMR** (101 MHz, $CDCl_3$) δ ppm 143.2, 128.8, 127.9, 126.8, 74.4, 53.2, 34.4, 33.3, 26.1, 25.1.

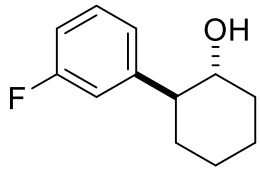

(±)

***trans*-2-(3-Fluorophenyl)cyclohexan-1-ol**

The product was prepared from 1-bromo-3-fluorobenzene (14.0 mmol) according to **GP1.** The desired product was obtained as white solid, 1.999 g, 10.3 mmol, 73.6 % yield. **^{1}H NMR** (400 MHz, $CDCl_3$): δ ppm 7.33 – 7.27 (m, 1H), 7.03 (d, *J* = 7.7 Hz, 1H), 6.99 – 6.90 (m, 2H), 3.68 – 3.59 (m, 1H), 2.50 – 2.38 (m, 1H), 2.15 – 2.06 (m, 1H), 1.92 – 1.72 (m, 3H), 1.55 – 1.26 (m, 4H), **^{13}C NMR** (101 MHz, $CDCl_3$) δ ppm 164.4, 161.9, 146.2, 146.2, 130.2, 130.1, 123.7, 123.6, 114.7, 114.5, 113.8, 113.6. 74.3, 53.0, 34.6, 33.2, 25.9, 25.0.

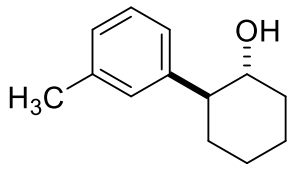

(±)

***trans*-2-(3-Methylphenyl)cyclohexan-1-ol**

The product was prepared from 1-bromo-3-methylbenzene (17.0 mmol) according to **GP1.** The desired product was obtained as white solid, 2.359 g, 12.4 mmol, 72.9 % yield. **^{1}H NMR** (400 MHz, $CDCl_3$): δ ppm 7.22 (t, *J* = 7.5 Hz, 1H), 7.06 (d, *J* = 7.9 Hz, 3H), 3.70 – 3.61 (m, 1H), 2.44 – 2.36 (m, 1H), 2.35 (s, 3H), 2.15 – 2.07 (m, 1H), 1.89 – 1.71 (m, 3H), 1.60 – 1.27 (m, 4H), **^{13}C NMR** (101 MHz, $CDCl_3$) δ ppm 143.2, 138.8, 128.7, 128.6, 127.6, 124.9, 74.4, 53.2, 34.4, 33.3, 26.1, 25.1, 21.5.

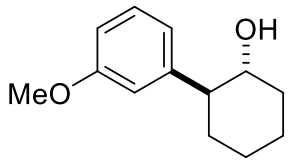

(±)

***trans*-2-(3-Methoxyphenyl)cyclohexan-1-ol**

The product was prepared from 1-bromo-3-methoxybenzene (15.8 mmol) according to **GP1.** The desired product was obtained as white solid, 1.979 g, 9.6 mmol, 60.8 % yield. **^{1}H NMR** (400 MHz, $CDCl_3$): δ ppm 7.30 – 7.22 (m, 1H), 6.88 – 6.76 (m, 3H), 3.81 (s, 3H), 3.70 – 3.60 (m, 1H), 2.48 – 2.35 (m, 1H), 2.18 – 2.07 (m, 1H), 1.94 – 1.19 (m, 7H). **^{13}C NMR** (101 MHz, $CDCl_3$) δ ppm 159.6, 144.8, 129.5, 120.0, 113.5, 111.8, 74.2, 55.1, 53.2, 34.3, 33.2, 26.0, 25.0.

General procedure for the silylation-based kinetic resolution of the alcohols (GP2)

To a 1-dram vial with an oven dried Teflon coated stir bar and activated 4Å molecular sieves, the racemic substrate (0.4 mmol) and catalyst (0.1 mmol) were added. The vial was then purged with argon and sealed with a septa. The *N*,*N*-diisopropylethylamine (0.26 mmol) was added via syringe and the starting materials were dissolved in 0.55 mL of THF to make a 0.42 M concentration solution. The vial was then cooled to -78 °C for 30 min. The cooled mixture was then treated with a 0.65 M solution of silyl chloride in THF (0.4 mL, 0.26 mmol) and was left to react for a set amount of time at -78 °C, then quenched with 0.3 mL of methanol. The solution was left to warm to room temperature and then the crude contents were extracted with diethyl ether and the organic layer was transferred to a 4-dram vial. The solvent was removed under vacuum and the residue was purified via silica gel chromatography (gradient of 5% to 10% to 25% EtOAc in hexanes). The silylated alcohol was concentrated under vacuum and saved for analysis and the unreacted alcohol could either be analyzed by HPLC.

General procedure for deprotection of silylated alcohols (GP3)

To a 4-dram vial with stir bar and a septum was added the silyl protected alcohol. The solid was then dissolved in 2 mL of THF with stirring. To this solution of tetra-*n*-butylammonium fluoride (TBAF) (1 mL) was added and stir for 2 h for full deprotection. The reaction was then quenched with brine and extracted with diethyl ether three times. The crude organic layers were combined, then concentrated under vacuum, and purified by silica gel chromatography (gradient of 10 to 25% EtOAc in hexanes). The isolated, deprotected alcohol was then analyzed by HPLC.

General procedure for the acylation-based kinetic resolution of the alcohols (GP4)

To a 1-dram vial with an oven dried Teflon coated stir bar and activated 4Å molecular sieves, the racemic substrate (0.4 mmol) and catalyst (0.032 mmol) were added. The vial was then purged with argon and sealed with a septa. The *N*,*N*-diisopropylethylamine (0.3 mmol) was added via syringe and the starting materials were dissolved in 1.6 mL of THF to make a 0.25 M concentration solution. The mixture was then treated with a 0.3 M solution of propionic anhydride in THF (1.0 mL, 0.3 mmol) and was left to react for 6 hours at room temperature, then quenched with 0.3 mL of methanol. The solution was left to warm to room temperature and then the crude contents were diluted with DCM (2 mL), washed with 1 M HCl (1 mL, 2 times) and saturated $NaHCO_3$ (1 mL, 2 times). After dying with anhydrous sodium sulfate, the solvent was removed under vacuum and the residue was purified via silica gel chromatography (gradient of 5% to 10% to 25% EtOAc in hexanes). The silylated alcohol was concentrated under vacuum and saved for analysis and the unreacted alcohol could either be analyzed by HPLC.

General procedure for deprotection of acylated alcohols (GP5)

To a 4-dram vial with stir bar and a septum was added the silyl protected alcohol. The solid was then dissolved in 3 mL of MeOH and 0.5 mL of water with stirring. Potassium carbonate (4 equiv.) was then added to the vial and stir for 1 h at room temperature for full deprotection. The reaction was extracted with diethyl ether three times. The crude organic layers were combined, then concentrated under vacuum, and purified by silica gel

chromatography (gradient of 10 to 25% EtOAc in hexanes). The isolated, deprotected alcohol was then analyzed by HPLC.

General Procedure Making a *p*-Substituted Triphenylsilane. (GP6)

In an oven-dried 250 mL three-neck round-bottom flask, p-substituted bromo/iodobenzene (1 equiv) was dissolved using diethyl ether (28 mL) under nitrogen at room temperature. To the stirred solution was slowly added n-BuLi (1.025 equiv) at room temperature. After addition of *n*BuLi, the resulting mixture formed a precipitate which was then allowed to stir for 1−1.5 h. After 1−1.5 h, a solution of $HSiCl_3$ (0.4 M in diethyl ether, 0.3 equiv) was added dropwise to the three-neck flask at -40 °C using dry ice/acetonitrile bath. The reaction mixture was then allowed to stir for another 2 h. After 2 h, the resulting suspension was then quenched with water and extracted with diethyl ether. Organic layer was dried with anhydrous Na_2SO_4 and concentrated under vacuum to yield the crude product. In most cases, purification of silane was done by recrystallization or silica gel chromatography using hexane.

General Procedure Making a *p*-Substituted Triphenylsilyl chloride. (GP7)

An oven-dried 50 mL three-neck round-bottom flask was charged with p-substituted triphenylsilane and the mixture dissolved using dry degassed carbon tetrachloride (CCl_4) under a nitrogen atmosphere. The mixture was allowed to stir for 10−15 min. Sulfuryl chloride (SO_2Cl_2) (2−6 equiv) was then added to the flask. The resulting mixture was then allowed to reflux for 2−10 h (conversion was monitored by disappearance of the silane

peak using 1 H NMR). After full conversion, the mixture was concentrated using vacuum. The final product was then recrystallized using pentane at -78 °C.

Analytical data and HPLC traces for kinetic resolutions

Data of silylation-based kinetic resolution (Table 3.1) see ref[4].

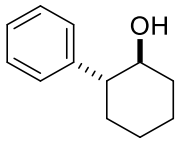

Table 3.2, Entry 1: GP4. Recovered starting material: 39 mg, 56%. **^{1}H NMR** (400 MHz, $CDCl_3$): δ ppm 7.38 – 7.29 (m, 2H), 7.29 – 7.21 (m, 3H), 3.67 (ddd, *J* = 10.1, 6.3, 2.5 Hz, 1H), 2.43 (ddd, *J* = 13.2, 10.0, 3.5 Hz, 1H), 2.16 – 2.06 (m, 1H), 1.85 (dt, *J* = 12.5, 6.6 Hz, 2H), 1.80 – 1.71 (m, 1H), 1.62 – 1.28 (m, 4H). **^{13}C NMR** (101 MHz, $CDCl_3$) δ ppm 143.2, 128.8, 127.9, 126.8, 74.4, 53.2, 34.4, 33.3, 26.1, 25.1. **HPLC** separation conditions: Chiralpak OD-H Column 2% isopropyl alcohol in hexane, flow rate: 1 mL/min, 25 °C; t_R 17.6 min for (*R*)-enantiomer (minor) and 18.9 min for (*S*)-enantiomer (major). (er = 76:24)

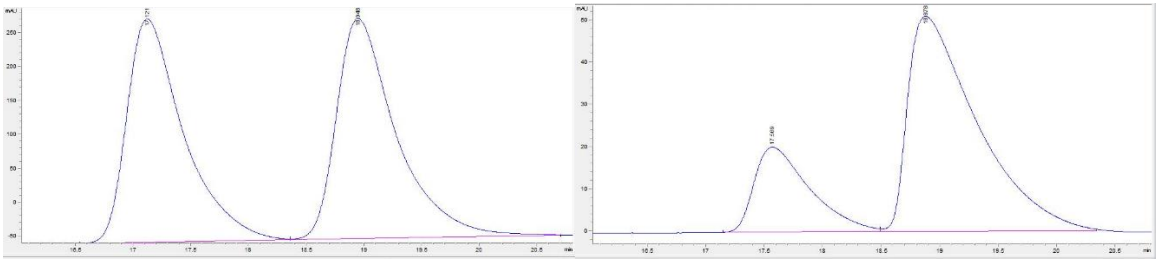

#	Time	Area	Height	Width	Area%	Symmetry
1	17.121	11299	329.5	0.5111	48.988	0.523
2	18.948	11766	325.1	0.5372	51.012	0.526

#	Time	Area	Height	Width	Area%	Symmetry
1	17.569	666.8	20.2	0.4919	24.089	0.458
2	18.878	2101.1	51	0.6048	75.911	0.322

Figure 3.10 HPLC Data of the SM of Table 3.2 Entry 1

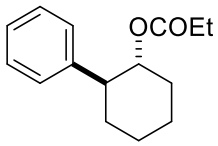

Table 3.2, Entry 1: GP5. Recovered product: 26 mg, 28%, white solid.**^{1}H NMR** (400 MHz, $CDCl_3$): 7.32 – 7.11 (m, 5H), 4.97 (td, J = 10.5, 4.4 Hz, 1H), 2.73 – 2.56 (m, 1H), 2.22 – 1.70 (m, 6H), 1.61 – 1.28 (m, 4H), 0.84 (t, J = 7.6 Hz, 3H); **^{13}C NMR** (101 MHz, $CDCl_3$) δ ppm 173.9, 143.3, 128.4, 127.7, 126.5, 75.9, 50.1, 34.0, 32.6, 27.9, 26.0, 25.0, 9.2 Same HPLC separation conditions as the starting materials were used. (er= 92:8)

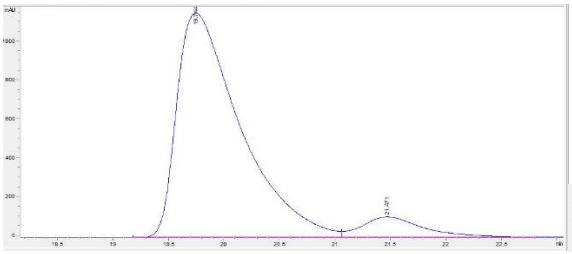

#	Time	Area	Height	Width	Area%	Symmetry
1	19.744	45948.4	1155.1	0.5911	91.968	0.394
2	21.471	4012.9	105	0.564	8.032	0.658

Figure 3.11 HPLC Data of the PR of Table 3.2 Entry 1

Table 3.3 Kinetic Resolution Data for Table 3.2, Entry 1

	er^{SM}	er^{PR}	% conv	*s*	*s average*
1	75.9:24.1	92.0:8.0	38.1	19.4	20.7
2	77.2:22.8	92.8:7.2	38.9	21.9	

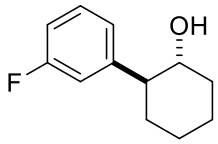

Table 3.2, Entry 2: GP4. Recovered starting material: 53 mg, 68 %. **^{1}H NMR** (400 MHz, $CDCl_3$): δ ppm 7.33 – 7.27 (m, 1H), 7.03 (d, *J* = 7.7 Hz, 1H), 6.99 – 6.90 (m, 2H), 3.68 –

3.59 (m, 1H), 2.50 – 2.38 (m, 1H), 2.15 – 2.06 (m, 1H), 1.92 – 1.72 (m, 3H), 1.55 – 1.26 (m, 4H), **^{13}C NMR** (101 MHz, $CDCl_3$) δ ppm 164.4, 161.9, 146.2, 146.2, 130.2, 130.1, 123.7, 123.6, 114.7, 114.5, 113.8, 113.6. 74.3, 53.0, 34.6, 33.2, 25.9, 25.0.

HPLC separation conditions: Chiralpak OD-H Column 2% isopropyl alcohol in hexane, flow rate: 1 mL/min, 25 °C; t_R 16.5 min for (*R*)-enantiomer (minor) and 19.0 min for (*S*)-enantiomer (major). (er = 59:41)

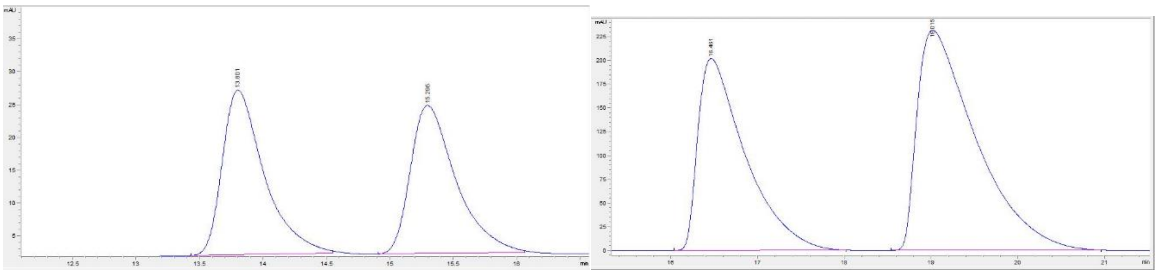

#	Time	Area	Height	Width	Area%	Symmetry
1	13.801	578.6	25.1	0.344	50.579	0.555
2	15.295	565.3	22.6	0.3784	49.421	0.561

#	Time	Area	Height	Width	Area%	Symmetry
1	16.461	7693.2	202.2	0.559	41.215	0.357
2	19.015	10972.8	232.2	0.7034	58.785	0.331

Figure 3.12 HPLC Data of the SM of Table 3.2 Entry 2

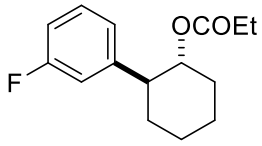

Table 3.2, Entry 2: GP5. Recovered product: 10 mg, 10 %, white solid. **^{1}H NMR** (400 MHz, $CDCl_3$): δ ppm 7.24 – 7.16 (m, 1H), 6.91 (dt, *J* = 17.6, 8.0 Hz, 3H), 4.92 (td, *J* = 10.5, 4.3 Hz, 1H), 2.66 (td, *J* = 11.6, 3.7 Hz, 1H), 2.22 – 1.65 (m, 6H), 1.50 – 1.25 (m, 4H), 0.87 (t, *J* = 7.6 Hz, 3H). **^{13}C NMR** (101 MHz, $CDCl_3$) δ ppm 173.7, 161.1, 145.9, 129.7, 123.1, 114.7, 113.4, 75.5, 49.6, 33.6, 32.3, 30.9, 27.2, 25.7, 24.7, 9.1. **HPLC** data is of the desilylated product formed by following GP5. The same HPLC separation conditions as the recovered starting materials were utilized. (er= 86:14)

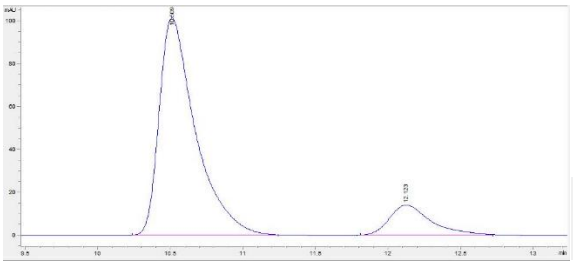

#	Time	Area	Height	Width	Area%	Symmetry
1	10.509	1767.7	101.4	0.2584	86.185	0.499
2	12.123	283.3	14.1	0.2941	13.815	0.628

Figure 3.13 HPLC Data of the PR of Table 3.2 Entry 2

Table 3.4 Kinetic Resolution Data for Table 3.2, Entry 2

	er^{SM}	er^{PR}	% conv	*s*	*s average*
1	58.8:41.2	86.2:13.8	19.6	7.3	8.8
2	83.6:16.4	83.8:16.2	49.9	10.2	

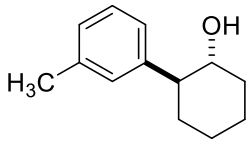

Table 3.2, Entry 3: GP4. Recovered starting material: 37 mg, 48 %. **^{1}H NMR** (400 MHz, $CDCl_3$): δ ppm 7.22 (t, *J* = 7.5 Hz, 1H), 7.06 (d, *J* = 7.9 Hz, 3H), 3.70 – 3.61 (m, 1H), 2.44 – 2.36 (m, 1H), 2.35 (s, 3H), 2.15 – 2.07 (m, 1H), 1.89 – 1.71 (m, 3H), 1.60 – 1.27 (m, 4H), **^{13}C NMR** (101 MHz, $CDCl_3$) δ ppm 143.2, 138.8, 128.7, 128.6, 127.6, 124.9, 74.4, 53.2, 34.4, 33.3, 26.1, 25.1, 21.5. **HPLC** separation conditions: Chiralpak OD-H Column 2% isopropyl alcohol in hexane, flow rate: 1 mL/min, 25 °C; t_R 11.3 min for (*R*)-enantiomer (minor) and 12.5 min for (*S*)-enantiomer (major). (er = 87:13) Absolute stereochemistry was obtained using optical rotation and the result of optical rotation matched the other substrate, indicating right major enantiomer was obtained.

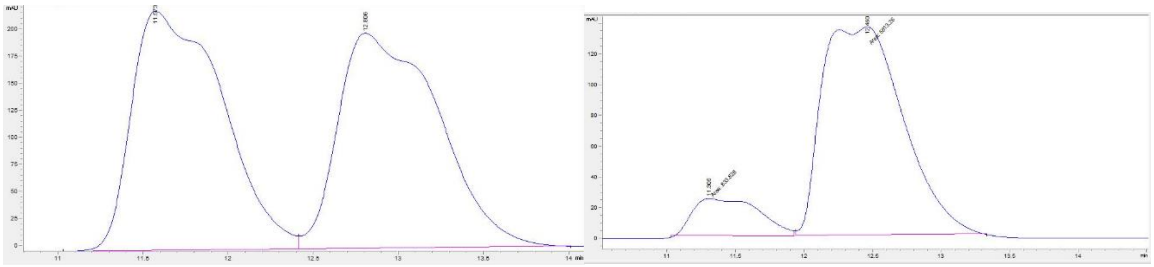

#	Time	Area	Height	Width	Area%	Symmetry
1	11.573	8217.4	221	0.5017	50.253	0.358
2	12.806	8134.6	198.8	0.5515	49.747	0.378

#	Time	Area	Height	Width	Area%	Symmetry
1	11.305	833.8	24.4	0.5704	12.933	0.34
2	12.46	5613.3	135.6	0.6898	87.067	1.136

Figure 3.14 HPLC Data of the SM of Table 3.2 Entry 3

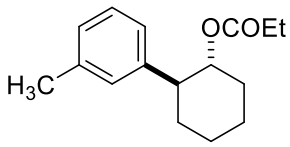

Table 3.2, Entry 3: GP5. Recovered product: 39 mg, 40 %, white solid.**^{1}H NMR** (400 MHz, $CDCl_3$): δ ppm 7.22 – 7.13 (m, 1H), 7.01 (d, J = 7.1 Hz, 3H), 4.97 (td, J = 10.5, 4.4 Hz, 1H), 2.71 – 2.58 (m, 1H), 2.33 (s, 3H), 2.21 – 1.70 (m, 6H), 1.54 – 1.22 (m, 4H), 0.88 (t, J = 7.6 Hz, 3H). **^{13}C NMR** (101 MHz, $CDCl_3$) δ ppm 173.1, 144.4, 138.1, 128.4, 128.3, 126.2, 123.5, 77.2, 40.7, 32.7, 32.4, 27.9, 25.4, 24.4, 21.6, 9.4. **HPLC** data is of the desilylated product formed by following GP5. The same HPLC separation conditions as the recovered starting materials were utilized. (er= 88:12)

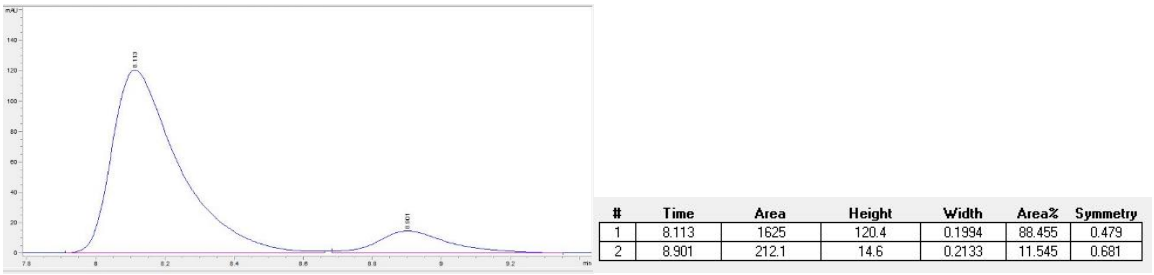

#	Time	Area	Height	Width	Area%	Symmetry
1	8.113	1625	120.4	0.1994	88.455	0.479
2	8.901	212.1	14.6	0.2133	11.545	0.681

Figure 3.15 HPLC Data of the PR of Table 3.2 Entry 3

Table 3.5 Kinetic Resolution Data for Table 3.2, Entry 3

	er^{SM}	er^{PR}	% conv	*s*	*s average*
1	87.1:22.9	88.5:11.5	49.1	16.9	16.3
2	77.4:22.6	90.1:9.9	40.6	15.7	

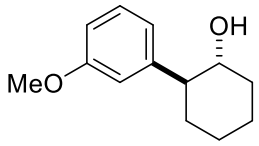

Table 3.2, Entry 4: GP4. Recovered starting material: 31 mg, 38 %. **^{1}H NMR** (400 MHz, $CDCl_3$): δ ppm 7.30 – 7.22 (m, 1H), 6.88 – 6.76 (m, 3H), 3.81 (s, 3H), 3.70 – 3.60 (m, 1H), 2.48 – 2.35 (m, 1H), 2.18 – 2.07 (m, 1H), 1.94 – 1.19 (m, 7H). **^{13}C NMR** (101 MHz, $CDCl_3$) δ ppm 159.6, 144.8, 129.5, 120.0, 113.5, 111.8, 74.2, 55.1, 53.2, 34.3, 33.2, 26.0, 25.0.

HPLC separation conditions: Chiralpak AD-H Column 7% isopropyl alcohol in hexane, flow rate: 1 mL/min, 25 °C; t_R 22.4 min for (*S*)-enantiomer (major) and 26.9 min for (*R*)-enantiomer (minor). (er = 95:5)

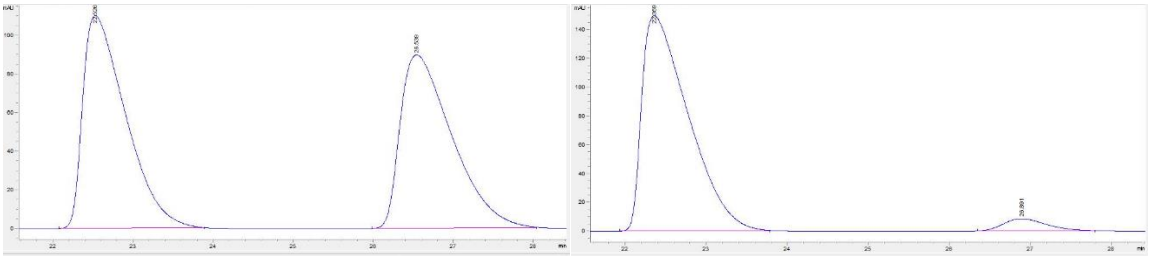

#	Time	Area	Height	Width	Area%	Symmetry
1	22.526	4112.1	110.2	0.5704	50.424	0.382
2	26.539	4043	89.8	0.6812	49.576	0.433

#	Time	Area	Height	Width	Area%	Symmetry
1	22.359	5964.1	149.7	0.5908	94.936	0.341
2	26.891	318.2	8.6	0.5261	5.064	0.71

Figure 3.16 HPLC Data of the SM of Table 3.2 Entry 4

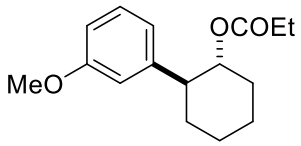

Table 3.2, Entry 4: GP5. Recovered product: 49 mg, 47 %, white solid.**^{1}H NMR** (400 MHz, $CDCl_3$): δ ppm 7.17 (t, J = 7.9 Hz, 1H), 6.90 – 6.58 (m, 3H), 4.96 (td, J = 10.5, 4.3 Hz, 1H), 3.78 (s, 3H), 2.81 – 2.46 (m, 1H), 2.22 – 1.63 (m, 6H), 1.53 – 1.20 (m, 4H), 0.87 (dd, J = 10.3, 4.8 Hz, 3H).**^{13}C NMR** (101 MHz, $CDCl_3$) δ ppm 1173.8, 159.5, 144.9, 129.2, 119.9, 113.3,111.7, 75.6, 55.2, 49.9, 33.9, 32.4, 27.8, 25.8, 24.8, 9.1. **HPLC** data is of the desilylated product formed by following GP5. The same HPLC separation conditions as the recovered starting materials were utilized. (er= 87:13) Absolute stereochemistry was obtained using optical rotation and the result of optical rotation matched the other substrate, indicating right major enantiomer was obtained.

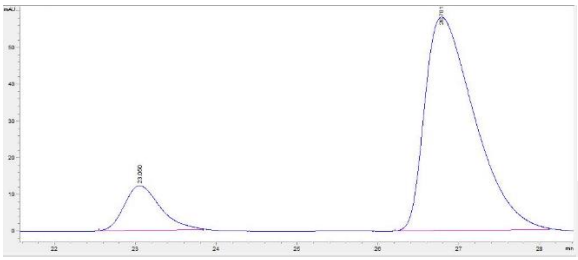

#	Time	Area	Height	Width	Area%	Symmetry
1	23.05	385.2	12.3	0.4694	13.366	0.704
2	26.781	2497	58.2	0.6453	86.634	0.477

Figure 3.17 HPLC Data of the PR of Table 3.2 Entry 4

Table 3.6 Kinetic Resolution Data for Table 3.2, Entry 4

	er^{SM}	er^{PR}	% conv	*s*	*s average*
1	94.9:5.1	86.6:13.4	55.1	19.3	19.6
2	97.6:2.4	84.6:15.4	57.9	19.9	

Transition State Geometry

Coordinates (Angstroms)

ATOM	X	Y	Z				
1	Si	-1.866264	-0.833701	0.228148	21 H	-5.130161	-4.541376	-0.770565
2	C	-2.487263	0.035142	-1.338721	22 H	-5.104071	-3.194175	3.313754
3	C	-3.643725	1.267034	-3.611898	23 H	-5.995784	-4.709063	1.554545
4	C	-3.832039	0.460738	-1.339992	24 C	-1.626249	0.393908	1.639252
5	C	-1.743916	0.259147	-2.504941	25 C	-1.535646	2.273700	3.751417
6	C	-2.311460	0.853563	-3.634195	26 C	-0.998922	0.087753	2.861282
7	C	-4.399880	1.080392	-2.453802	27 C	-2.199859	1.673536	1.505157
8	H	-4.455677	0.301988	-0.462858	28 C	-2.163708	2.598344	2.548634
9	H	-0.695933	-0.001677	-2.509104	29 C	-0.948344	1.018001	3.901325
10	H	-1.710385	0.998190	-4.529278	30 H	-0.544900	-0.883283	3.016646
11	H	-5.436954	1.404584	-2.420295	31 H	-2.667585	1.965407	0.570238
12	H	-4.088808	1.732694	-4.487626	32 H	-2.613329	3.577959	2.411945
13	C	-3.229811	-2.083522	0.674686	33 H	-0.449432	0.754592	4.830631
14	C	-5.228540	-3.978795	1.309713	34 H	-1.501247	2.995121	4.564360
15	C	-3.740742	-2.193843	1.979212	35 N	0.682153	1.344158	-0.536340
16	C	-3.758320	-2.945475	-0.306465	36 C	0.856554	2.519820	-1.445014
17	C	-4.740794	-3.885869	0.004703	37 H	0.568477	2.217594	-2.456542
18	C	-4.729108	-3.128534	2.295473	38 C	1.805174	1.223116	0.068758
19	H	-3.359125	-1.547895	2.764592	39 N	2.830921	2.091205	-0.276717
20	H	-3.410720	-2.877646	-1.335431	40 C	2.393004	2.874608	-1.422475

41	H	2.580047	3.943214	-1.283084	64	H	5.306158	3.370684	-0.586960
42	H	2.904140	2.538957	-2.334624	65	O	-0.442767	-1.790114	0.014249
43	C	-0.034881	3.680619	-1.032644	66	H	-0.303380	-2.617866	1.274928
44	C	-1.678959	5.850322	-0.325313	67	C	-0.132089	-2.561536	-1.212909
45	C	-1.048536	4.119657	-1.890580	68	C	2.357519	-2.979524	-1.140886
46	C	0.139732	4.338542	0.193284	69	C	0.865992	-4.849738	-0.386002
47	C	-0.672180	5.417316	0.541474	70	C	2.074951	-3.959495	-0.034268
48	C	-1.869250	5.194165	-1.541126	71	C	-0.340754	-4.074876	-0.988867
49	H	-1.206975	3.605490	-2.835454	72	C	1.275232	-2.287914	-1.718867
50	H	0.902753	4.000898	0.890174	73	H	1.194384	-5.604954	-1.109884
51	H	-0.522407	5.917413	1.495012	74	H	1.877633	-3.418897	0.897179
52	H	-2.654261	5.517238	-2.220142	75	H	-1.240175	-4.221619	-0.383980
53	H	-2.311039	6.691290	-0.051776	76	H	-0.848370	-2.226400	-1.967492
54	S	2.341437	0.112002	1.339066	77	H	0.548374	-5.385167	0.512449
55	C	4.048306	1.878414	0.338562	78	H	2.955095	-4.585427	0.153234
56	C	3.973377	0.829600	1.281501	79	H	-0.568160	-4.489474	-1.978511
57	C	5.085354	0.468003	2.029649	80	C	1.516122	-1.464706	-2.824989
58	H	5.024009	-0.338292	2.754975	81	H	0.686374	-0.992016	-3.338172
59	C	6.287536	1.159063	1.829985	82	C	2.807292	-1.268813	-3.315846
60	H	7.164105	0.885926	2.409951	83	H	2.968027	-0.625929	-4.177448
61	C	6.362736	2.191677	0.893215	84	C	3.882039	-1.915884	-2.707437
62	H	7.300958	2.719550	0.746014	85	H	4.892891	-1.772457	-3.080480
63	C	5.246399	2.563863	0.137493	86	C	3.648790	-2.777705	-1.636065

87 H 4.478039 -3.316056 -1.182599 | 88 Cl -0.277473 -3.340583 2.460657

Point Group: c1 Number of degrees of freedom: 258

Energy is -2994.725626613

Starting Material Ring Rotation Energy Profile

Constraint (X-axis):

-13.06	49.94	112.94
-4.06	58.94	121.94
4.94	67.94	130.94
13.94	76.94	139.94
22.94	85.94	148.94
31.94	94.94	157.94
40.94	103.94	166.94

E(kJ/mol) y -axis:

-5436953.99 -5436952.11

-5436953.06

-5436950.46

-5436947.93

-5436925.74

-5436945.93

-5436948.76

-5436950.52

3.7 References

1. Birman, V. B.; Li, X., Benzotetramisole: A remarkably enantioselective acyl transfer catalyst. *Org. Lett.* **2006,** *8* (7), 1351-1354.

2. Sheppard, C. I.; Taylor, J. L.; Wiskur, S. L., Silylation-based kinetic resolution of monofunctional secondary alcohols. *Org. Lett.* **2011,** *13* (15), 3794-3797.

3. Clark, R. W.; Deaton, T. M.; Zhang, Y.; Moore, M. I.; Wiskur, S. L., Silylation-based kinetic resolution of α-hydroxy lactones and lactams. *Org. Lett.* **2013,** *15* (24), 6132-6135.

4. Wang, L.; Akhani, R. K.; Wiskur, S. L., Diastereoselective and enantioselective silylation of 2-arylcyclohexanols. *Org. Lett.* **2015,** *17* (10), 2408-2411.

5. Akhani, R. K.; Moore, M. I.; Pribyl, J. G.; Wiskur, S. L., Linear free-energy relationship and rate study on a silylation-based kinetic resolution: mechanistic insights. *J. Org. Chem.* **2014,** *79* (6), 2384-2396.

6. Wang, L.; Zhang, T.; Redden, B. K.; Sheppard, C. I.; Clark, R. W.; Smith, M. D.; Wiskur, S. L., Understanding internal chirality induction of triarylsilyl ethers formed from enantiopure alcohols. *J. Org. Chem.* **2016,** *81* (18), 8187-8193.

7. Dougherty, D. A., Cation-π interactions in chemistry and biology: a new view of benzene, Phe, Tyr, and Trp. *Science* **1996,** *271* (5246), 163-168.

8. Ma, J. C.; Dougherty, D. A., The cation− π interaction. *Chem. Rev.* **1997,** *97* (5), 1303-1324.

9. Companyo, X.; Viciano, M.; Rios, R., Improving asymmetric organocatalysts via supramolecular interactions. *MINI-REV ORG CHEM.* **2010,** *7* (1), 1-9.

10. Li, X.; Liu, P.; Houk, K.; Birman, V. B., Origin of enantioselectivity in CF3− PIP-catalyzed kinetic resolution of secondary benzylic alcohols. *J. Am. Chem. Soc.* **2008,** *130* (42), 13836-13837.

11. Liu, P.; Yang, X.; Birman, V. B.; Houk, K., Origin of enantioselectivity in benzotetramisole-catalyzed dynamic kinetic resolution of azlactones. *Org. Lett.* **2012,** *14* (13), 3288-3291.

12. Yang, X.; Lu, G.; Birman, V. B., Benzotetramisole-catalyzed dynamic kinetic resolution of azlactones. *Org. Lett.* **2010,** *12* (4), 892-895.

13. Birman, V. B.; Guo, L., Kinetic resolution of propargylic alcohols catalyzed by benzotetramisole. *Org. Lett.* **2006,** *8* (21), 4859-4861.

14. Birman, V. B.; Li, X., Homobenzotetramisole: an effective catalyst for kinetic resolution of aryl-cycloalkanols. *Org. Lett.* **2008,** *10* (6), 1115-1118.

15. Whitesell, J. K.; Lawrence, R. M.; Chen, H. H., Auxiliary structure and asymmetric induction in the ene reactions of chiral glyoxylates. *J. Org. Chem.* **1986,** *51* (25), 4779-4784.

16. NEWMAN, M. S.; SMITH, A. S., A STUDY OF REACTIONS OF GRIGNARD REAGENTS AT LOW TEMPERATURES1. *J. Org. Chem.* **1948,** *13* (4), 592-598.

17. Lewis, M.; Bagwill, C.; Hardebeck, L. K.; Wireduaah, S., The use of Hammett constants to understand the non-covalent binding of aromatics. *Comput. Struct. Biotechnol. J.* **2012,** *1* (1), e201204004.

18. Oda, S.; Yamamoto, H., Generation of Organolithium Compounds bearing Super Silyl Ester and their Application to Matteson Rearrangement. *Angew. Chem. Int. Ed.* **2013,** *125* (31), 8323-8326.

19. Hansch, C.; Leo, A.; Taft, R., A survey of Hammett substituent constants and resonance and field parameters. *Chem. Rev.* **1991,** *91* (2), 165-195.

20. a) Conversions and selectivity factors are based on the ee of the recovered starting materials and products. % Conversion = ees/(ees + eep) × 100% and s = ln[(1 − C)(1 − ees)]/ln[(1 − C)(1 + ees)], where ees = ee of recovered starting material and eep = ee of product. b) Selectivity factors are an average of two runs. Converions are from a single run.

21. Hehre, W. J.; Huang, W. W., *Chemistry with computation: An introduction to SPARTAN*. Wavefunction, Inc.: 1995.

CHAPTER 4

EXPLORING THE EFFECT OF THE POLYMER BACKBONE ON SILYLATION-BASED KINETIC RESOLUTIONS EMPLOYING A POLYMER-SUPPORTED TRIPHENYLSILYL CHLORIDE

4.1 Introduction

The preparation of enantiopure compounds is an important task in both industry and academia. Among a variety of methods[1] to obtain enantiopure compounds, kinetic resolutions[2-6] are commonly employed to provide highly enriched compounds by taking a racemic mixture or an enantioenriched mixture, and selectively reacting one enantiomer over the other based on a difference in reaction rates with a chiral catalyst. After the reaction is complete, the derivatized compound needs to be separated from the unreacted starting material, which commonly involves chromatography separation if the product or starting material isn't crystalline.

In order to solve this problem and to promote the application of our silylation-based kinetic resolution, we previously developed a polymer supported silyl chloride reagent that is soluble in our system but can be isolated by precipitation during the workup.[7] To be more specific, we incorporated the silyl chloride used to protect the alcohol into a polystyrene polymer. By controlling the molecular weight of the polymer supported silyl chloride, it is soluble in THF at -78 ºC and therefore able to undergo the reaction to selectively protect

one enantiomer of secondary alcohol over the other. The polymer is not soluble in methanol and can be "crashed out" at the end of the reaction when methanol is added to quench the reaction. Enantioenriched unreacted starting material can be isolated from the enantioenriched polymer product via filtration. This allows for facile separation of the unreacted starting material from the silyl ether polymer product. With this method, the need for chromatography is eliminated. However, the polymer supported silyl chloride was less selective and less reactive than just the small molecule silyl chloride, presumably due to the nonpolar microenvironment of the polymer backbone and steric crowding. In this chapter, we report a new silyl chloride copolymer that incorporates polarity into the polymer backbone, and spaces out the silyl chloride, providing a polar microenvironment and eliminating overcrowding of the reactive silyl chlorides. The polymers were able to resolve a variety of different substrates with selectivity factors and conversions that were comparable to the small molecule silyl chloride, thereby improving the selectivity and reactivity over our first-generation polymer.

4.2 Background

One of the main hurdles of application of transferring synthesis developed in the lab into industrial scale is the efficiency of product purification from the crude material. Many well-established syntheses in industry involve the isolation of target products by crystallization or distillation since these isolation methods are more economic than the costly and time-consuming chromatography. Scientists have developed another approach of isolating the target products by introducing polymers or solid support reagents to achieve a chromatography-free isolation of products.[8-11] Studies have been reported on the

application of polymer-supported or solid-supported reagents and catalysts in asymmetric reactions[12-19] and kinetic resolutions.[20-28] There is some research that involves the use of polymers for the selective removal of one enantiomer. In general, there are three main strategies that involve polymer-supported or solid-supported materials as a method to isolate enantioenriched products or starting materials in kinetic resolutions. These include selective polymerization of one enantiomer from a racemic mixture (Scheme 4.1a), selective removal of one enantiomer from a polymer derivatized with a racemic mixture (Scheme 4.1b), and derivatization of one enantiomer onto a polymer support from a racemic mixture (Scheme 4.1c). [29]

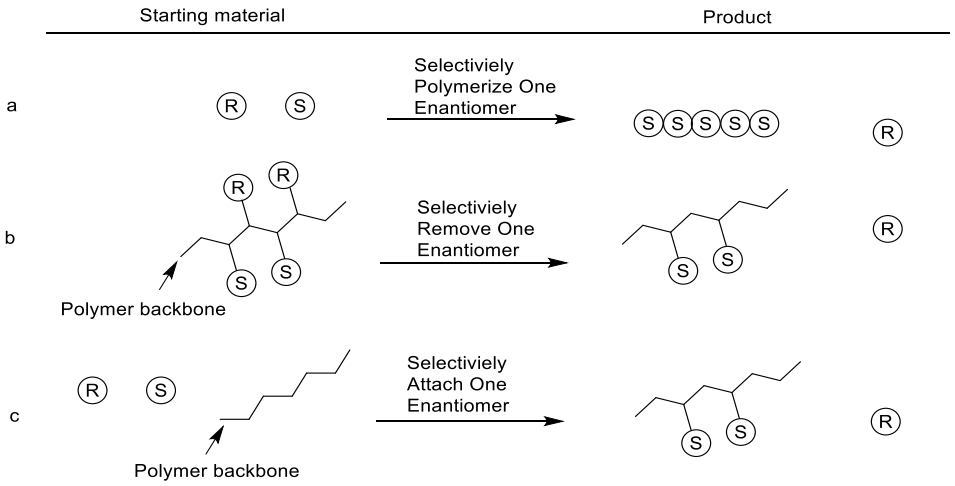

Scheme 4.1 Approaches to Kinetic Resolutions on Polymer Supports

A good example of polymer-formation kinetic resolution is the kinetic resolution of chiral α-olefins using an *ansa*-zirconocene polymerization catalyst (Scheme 4.2).[30] With the aid of the doubly bridged *ansa*-zirconocene **4.1** as catalyst and methylaluminoxane as activator, one enantiomer of a methylsubstituted olefin polymerized as an isotactic polymer while the other enantiomer remained unreacted in the solvent. The monomer polymerized

with high selectivity, resulting in a selectivity factor of almost 18. A facile isolation of the enantioenriched *R*-olefin can be achieved through a simple filtration and removal of the polymer. The main drawback of this method is the narrow scope of the catalysts and involvement of expensive and toxic transition metals.

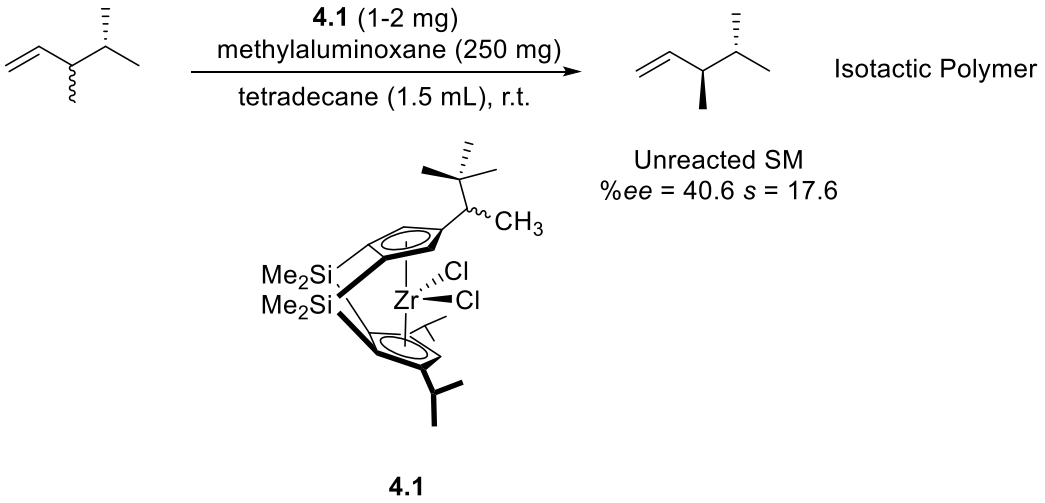

Scheme 4.2 Kinetic Resolutions of Chiral Methylsubstituted *R*-olefins Using an *Ansa*-Zirconocene Catalyst

The second approach to apply polymer-supported material in kinetic resolutions is the selective removal of one enantiomer from a polymer derivatized with a racemic mixture. As the kinetic resolution proceeds, one enantiomer is selectively cleaved from the polymer backbone and concentrated in the solvent while the other enantiomer remains attached to the polymer backbone. One example to demonstrate this strategy is Matsumoto's work utilizing an enzyme to selectively resolve secondary alcohols via a polymer-supported carbonate made from the alcohols (Scheme 4.3).[26] The polymer-supported carbonates **4.2** were prepared from a commercially available polymer MPEG5000 through a four-step

synthesis. The MPEG5000-supported carbonates **4.2** were then treated with porcine pancreas lipase (PPL) which is a hydrolytic enzyme that undergoes selective hydrolysis on the carbonate. When 1-phenylethanol was the target alcohol, one carbonate enantiomer was hydrolyzed, cleaving the alcohol from the polymer with an *ee* of 89%. The drawback of this approach is that the polymer needs to be derivatized with the racemic substrate, just to remove one enantiomer. A resolution where the small molecule is asymmetrically derivatized onto the polymer eliminates the first step which is more economical.

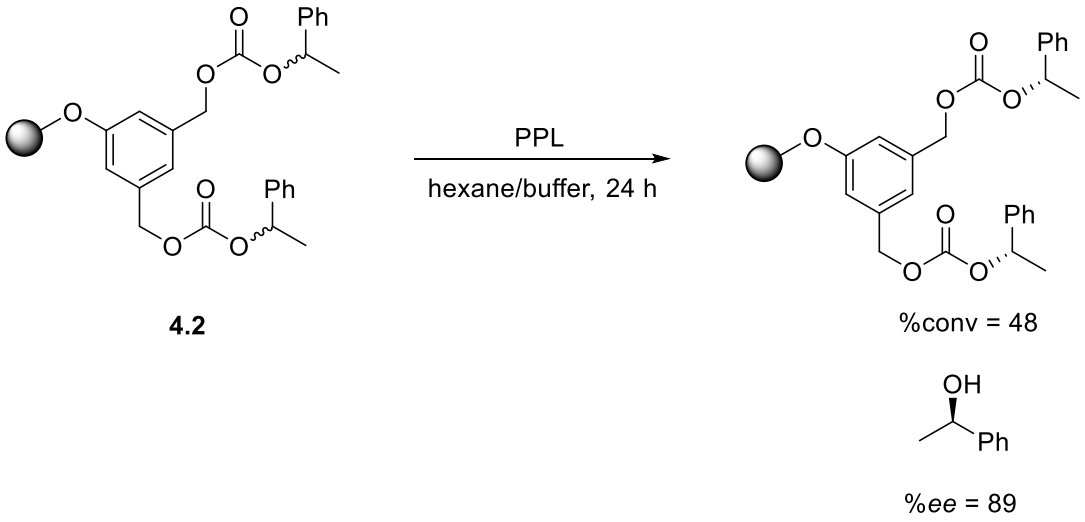

4.2

Scheme 4.3 Enantioselective Hydrolysis of MPEG5000-Supported Carbonates

The last approach to enantioenriched compounds through the use of polymer-supports is the derivatization of one enantiomer onto a polymer support. This strategy involves developing a polymer bound derivatizing reagent that reacts with the functional group being resolved to trap the product on the polymer. When employed in a kinetic resolution, one enantiomer will be bound to the polymer for facile removal. Actually, there

were only two non-enzymatic kinetic resolutions involving this technique. One developed by Vedejs and Rozners,[31] the other developed by our group.[7]

Vedejs and Rozners developed a parallel kinetic resolution for the separation of a racemic mixture of alcohols where one enantiomer was derivatized onto a solid support. A parallel kinetic resolution is when both enantiomers undergo different reactions at the same rate in the presence of a chiral catalyst, producing two different products. In Vedejs' work, one enantiomer becomes acylated, while the other enantiomer is benzoylated onto a polymer. To be specific, one enantiomer of the secondary alcohol reacted with vinyl acetate that was selectively catalyzed by the enzyme CALB, affording enantioenriched acylated product (*ee* = 98%). While the other enantiomer of alcohol interacted with a solid supported benzoyl chloride, leading to a chromatography-free isolation of the two enantiomers of alcohol. This method possesses advantages over the first two approaches. Compared to the first approach where one enantiomer is polymerized, neither enantiomer is polymerized and both enantiomers can be recovered. Compared to the second approach, this strategy only requires the derivatization of one enantiomer during the reaction instead of having to do an extra step to preform the racemic derivatized polymer. Ideally, an enantiopure unreacted starting material can be isolated directly after a simple filtration of the polymer-supported material which has covalently trapped the other enantiomer. In this enantioenriched unreacted starting material stays in the solution while the enantioenriched product attaches to the polymer backbone. Afterwards, selective deprotection could be applied to recover the enantioenriched deprotecting product from the polymer backbone handily.

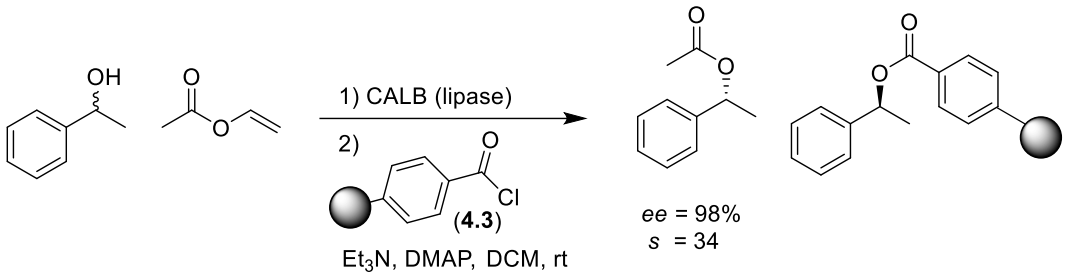

Scheme 4.4 Parallel Kinetic Resolution developed by Vedejs and Rozners

Since the ultimate goals of methodology development are their applications in the real world, Wiskur's group also reported an application of silylation-based kinetic resolution. One of the main drawbacks that restrained the application of an effective reaction was the large amount of chromatography associated with the isolation of the target product from the crude mixture. Recently, the Wiskur group proposed a chromatography-free polystyrene-supported triphenylsilyl chloride (**4.4**) to selectively silylate the secondary alcohol (Scheme 4.5).[7] The homogenous polymer selectively silylated the secondary alcohols in the solvent and could easily crash out after addition of methanol, affording an enantioenriched alcohol starting material in the solvent and enantioenriched silyl ether product as a precipitate. Successful kinetic resolutions on several substrates were achieved. While the polymer eliminated the need for chromatography, the reaction suffered from lower selectivity compared to triphenylsilyl chloride. The selectivity of the kinetic resolution is sensitive to the polarity of the solvent, with better selectivity being obtained in polar THF. The polystyrene backbone of **4.4** provided a very nonpolar microenvironment around the silyl chloride,[32] which we hypothesized was the reason for the decrease in selectivity. Therefore, our next objective was increasing the selectivity factor of the kinetic resolution by using a resin as the solid support as spacers of the resin provides a solvent-like microenvironment around the ending silylation active site.

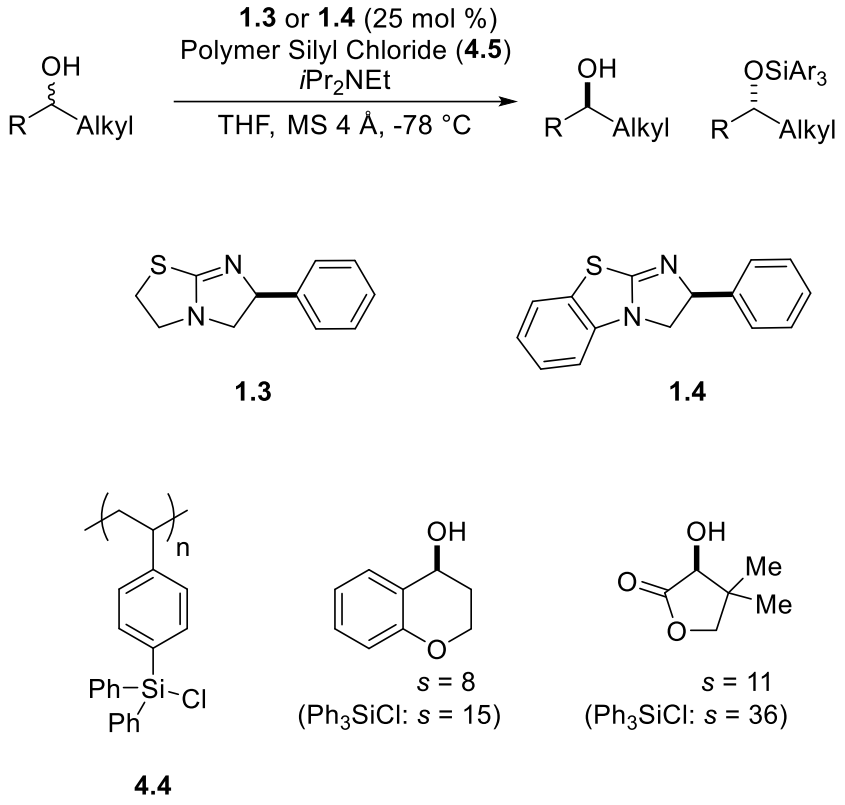

Scheme 4.5 Polystyrene-Supported Triphenylsilyl Chloride for the Silylation-Based Kinetic Resolution

4.3 Resin-Supported Triphenylsilyl Chloride

One of the most famous examples is the kinetic resolution of secondary alcohols using a resin supported proline-based catalyst developed by Janda (Scheme 4.6).[10] This kinetic resolution is based on a traditional kinetic resolution of secondary alcohol using a proline-based catalyst. One enantiomer of secondary alcohol converts to its benzoyl ester while the other enantiomer remains unreacted. Chromatography isolation is then applied to separate two enantiomers. Janda attached this proline-based catalyst to a resin though a few steps of synthesis. The distance between proline-based catalyst and resin backbone increases when a spacer is introduced, promoting a better conversion as active sites are away from the resin backbone. The same reaction condition was performed with 2-phenyl

cyclohexanol using this resin-supported diamine catalyst, affording an enantioselective benzoylation of the one enantiomer of alcohol over the other.

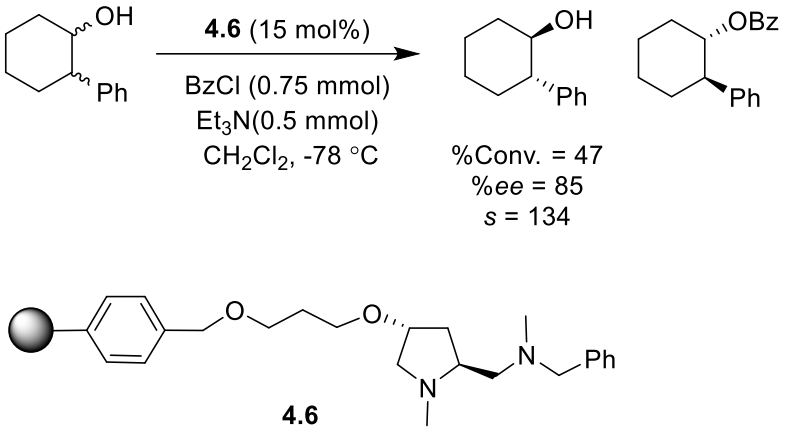

Scheme 4.6 Kinetic Resolution of Secondary Alcohols using a Polymer-Supported Proline-Based Catalyst

Research performed by Janda and coworkers has already proven the idea of introducing polarity to the reactive ending site by incorporating PEF spacers which provide similar microenvironment to THF between ending site and the resin backbone. We were wondering if we could connect triphenylsilyl chloride to the resin backbone through PEG spacers, affording a more polar microenvironment for the triphenylsilyl chloride attached to the resin. To be specific, triphenylsilyl chloride is connected to the resin through polar arms that isolate it from the non-polar resin backbone, obtaining a polar microenvironment as if it is surrounded by the solvent. We hypothesized that selectivity and conversion would increase with this change. Out of the different types of resin, we chose Tentagel as the solid support because it is commercially available and it possesses a polar spacer, leading to a microenvironment that is same as the solvent for the reaction. (Scheme 4.7). The goal of

the preliminary research is trying to synthesize the resin supported triphenylsilyl chloride and test its performance in our kinetic resolution.

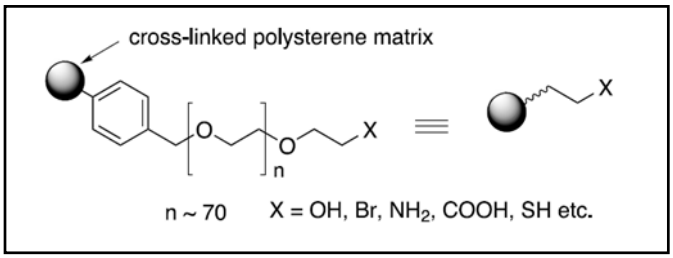

Scheme 4.7 Structure of Tentagel

The design of the resin supported silyl chloride is based on previous studies where we determined that three phenyl groups need to be attached to the silyl chloride to achieve high selectivity. Therefore, the final resin supported silyl chloride should also possess three phenyl groups.[33] Compound **4.10** shows the target resin supported silyl chloride, and Scheme 4.8 demonstrates the initial proposed synthetic route. In order to incorporate a silyl chloride onto the resin, a silane that could be coupled to the resin needed to be synthesized. A para substituted diiodobenzene (**4.6**) was reacted with chlorodiphenyl benzene (**4.7**) by performing a lithium halogen exchange on one of the iodo groups on **4.6**, followed by addition of the silyl chloride. Careful addition of only one equivalent of *n*-BuLi and reaction temperature needed to be optimized to avoid *n*-butyl substituted silicon or di-substituted side products which are very hard to separate from the product due to their similar polarity. Similar reaction conditions to the first step were followed to couple the silane to the resin to synthesize **4.8**. A lithium-halogen exchange reaction was performed on iodo substituted silane **4.8** and upon addition of the Tentagel-Br resin, a nucleophilic displacement took place with the primary alkyl halide to achieve the resin supported

triphenylsilane **4.9**. As the composition of Tentagel-Br resin was known, the composition of **4.9** could be obtained with the aid of ^{13}C solid-state NMR. Conversion from Tentagel-Br to Tentagel-silane can be calculated based on the integration of ^{13}C solid state NMR spectrum. Scheme 4.9 showed the solid state ^{13}C NMR for Tentagel-Br. The assignment is as follows: the chemical shift of 120 ppm-150 ppm indicates the aromatic carbons of polystyrene, 60 ppm-80 ppm indicates the aliphatic carbons of polyethylene glycol and 30 ppm-50 ppm shows the aliphatic backbone carbons of polystyrene. Comparing that spectra to the ^{13}C solid state NMR spectrum of Tentagel-Silane (Scheme 4.10), we found a broad peak at 135 ppm for the triphenylsilane carbons and the integration of polystyrene's aromatic and aliphatic stayed almost the same, which means the Tentagel resin was relatively stable under these conditions. The integration of the polyethylene glycol portion of the spectra did show some decrease indicating that some PEG may cleave. We could use the integration of aliphatic backbone carbons (30 ppm-50 ppm) to calculate the integration of aromatic backbone carbons (120 ppm-150 ppm). Then we can figure out how much triphenyl silane attached to the resin through the difference in the integration of the aromatic carbons (integration difference is aromatic carbon of phenyl groups on silicon). Then we consider if any spacers we lost based on the difference in PEG carbons (60 ppm-80 ppm) of **4.9** versus Tentagel-Br. We always used integration of aliphatic and aromatic carbons of the resin backbone as the calibration. Actually, it was always easy to prove the stability of resin backbone comparing the ration of aliphatic to aromatic carbons of resin backbone. In most cases, we wound obtain a same ratio of two types of carbons, suggesting the resin backbone was not destroyed. However, PEG spacers were not that stable, we may observe loss of PEG spacers up to 40%. Associating the number of PEG spacers per gram

of resin provided by the chemical company, we can figure out numbers of bromo active site per mole of resin. Number of bromo groups converted could be obtained through the calculation. Ultimately conversion of silane incorporation could be obtained.

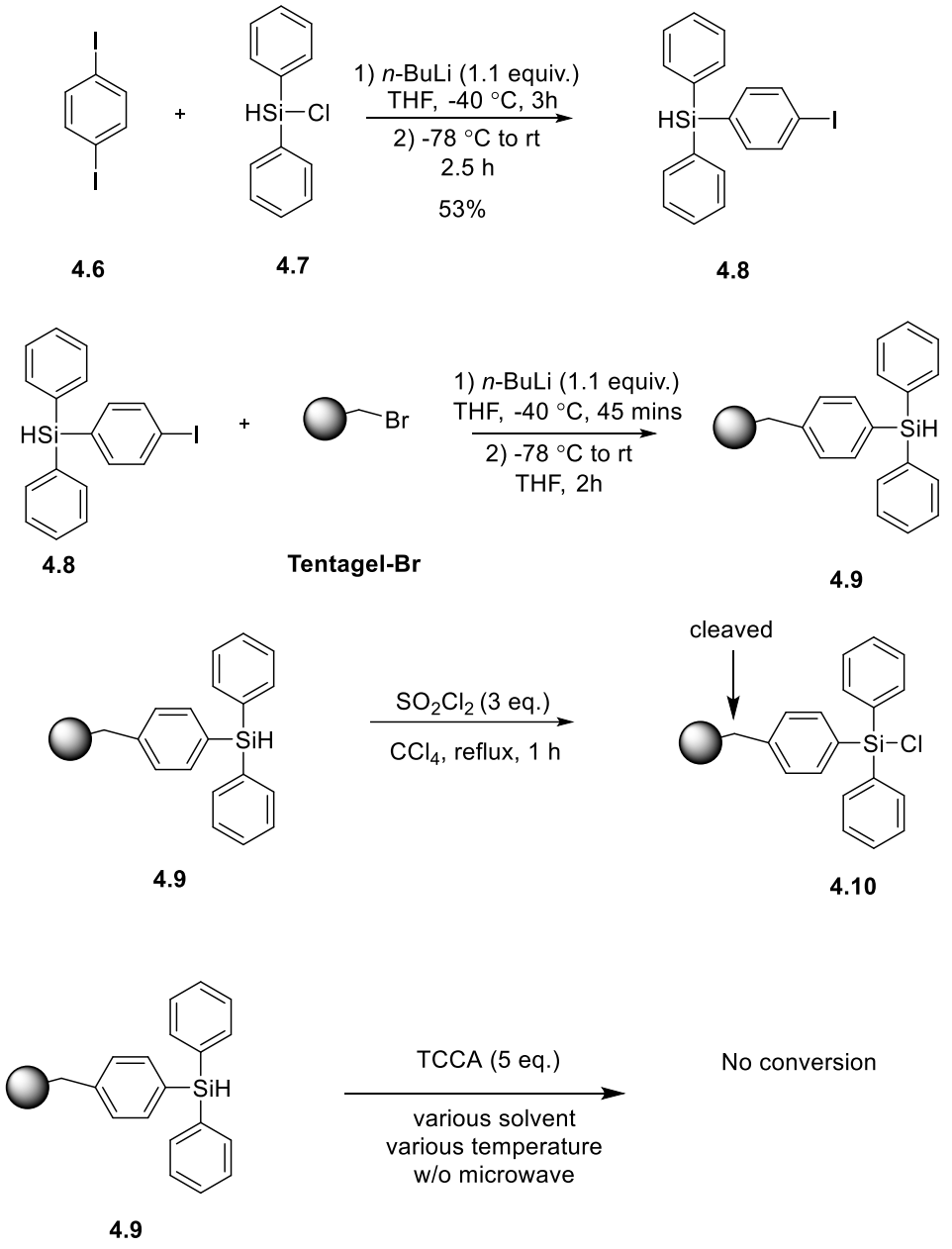

Scheme 4.8 Synthetic of Resin-Supported Material

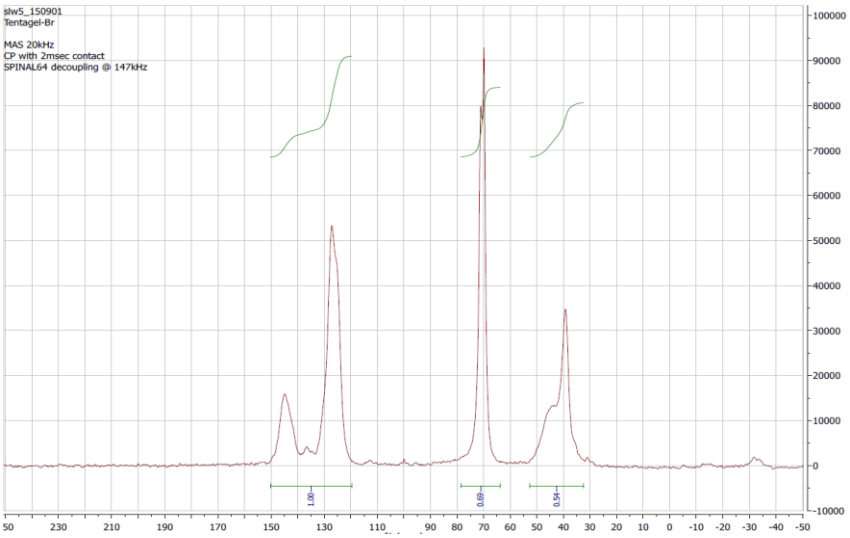

Scheme 4.9 Solid State ^{13}C NMR for Tentagel-Br

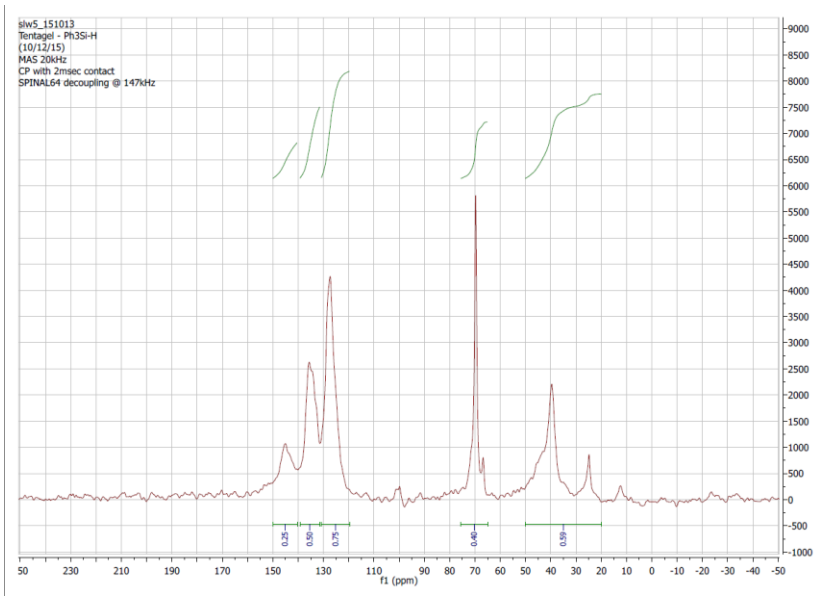

Scheme. 4.10 Solid State ^{13}C NMR for Tentagel-Silane

After obtaining **4.9**, different methods of chlorination were attempted. We started with the classic method of silane chlorination. Pure sulfuryl chloride was applied as both solvent and chlorine source to achieve a neat chlorination.[34-35] However, chlorination was too intense which caused decomposition of the resin. Solid state ^{13}C NMR showed the

inexistence of the spacers, suggesting that the structure of **4.9** was destroyed. Then we turned our attention to the mild chlorination routes due to how fragile the resin was. We applied trichloroisocyanuric acid (TCCA),[36] a mild chlorination reagent, as the source of chlorine. We tried to perfrom the chlorination at various temperatures (lower than boiling point of CCl_4, which is a typical solvent of the previous intense chlorination), we have used different solvents, and even attempted microwave chlorination. Unfortunately, the chlorination was not strong enough to afford any conversion, which was observed by comparing the ^{13}C solid state NMR of the starting material and product. After numerous attempts, the synthesis of resin-supported triphenylsilyl chloride **4.10** using TCCA was abandoned due to no conversion. In order to continue this project employing a resin, a different resin would need to be employed that can withstand more intense chlorination or can be chlorinated with TCCA.

4.4 2nd Generation of Polystyrene-Supported Triphenylsilyl Chloride

Since we failed to synthesize the resin-supported triphenylsilyl chloride, we turned our attention to an alternative approach to adjust polarity of the microenvironment of a solid-supported silyl chloride. Our design focuses on increasing the polarity of the microenvironment while simultaneously increasing the spacing between the silyl chlorides in the polymer. This was accomplished by copolymerizing our styrene silane monomer with the polar monomer methyl methacrylate. Since methyl methacrylate has a similar rate constant[37] compared to polystyrene, random copolymers could be prepared, efficiently spacing out the silicon reactive sites. This strategy has two advantages over the resin-supported triphenylsilyl chloride. The main strategy is the ease of characterization of the

material as the polymer-supported silane and silyl chloride has an appropriate *Mn* (3500-7000 g/mol) and are soluble in general solvents like THF or chloroform. The other advantage is the tolerance of the polystyrene backbone to simple chlorination conditions.

In order to explore the effects of polarity and spacing on the performance of the polymer-supported triphenylsilyl chloride in the kinetic resolution, copolymers with various compositions of methyl methacrylate were synthesized and their reactivity and selectivity were analyzed by employing them in a kinetic resolution.

Synthesis of the copolymers started with the preparation of silane monomer (**4.12**) from commercially available 4-bromo styrene (**4.11**). The synthesis started with a lithium-halogen exchange on commercially available 4-bromo styrene (**4.11)** using *n*-BuLi, the aryl lithium was then reacted with diphenylchlorosilane to prepare the silane monomer **4.12** (Scheme 4.11).[38] Next, three different polymers were synthesized with different amounts of methyl methacrylate incorporated into the copolymer. This was done via RAFT polymerization using 4-cyano-4-(phenylcarbonothioylthio)pentanoic acid （**CTP**） as the initiator,[39] to generate silane polymers **4.13a**, **4.13b**, and **4.13c** which have 30, 50, and 70% acrylate incorporation, respectively, as related to monomer unit. The polymers had decent dispersity (*Đ*) ranging from 1.1-1.5, and the number average molecular weights (*Mn*) were between 5600 and 8300 g/mol. Our previous work suggested that polymer supported silyl chlorides within this molecular weight range are homogeneous in THF but are easily precipitated after the kinetic resolution.[7] Finally, copolymers **(4.13a-4.13c**) were chlorinated through a radical chlorination with sulfuryl chloride to generate polymer supported silyl chlorides (**4.14a**-**4.14c**).[34-35]

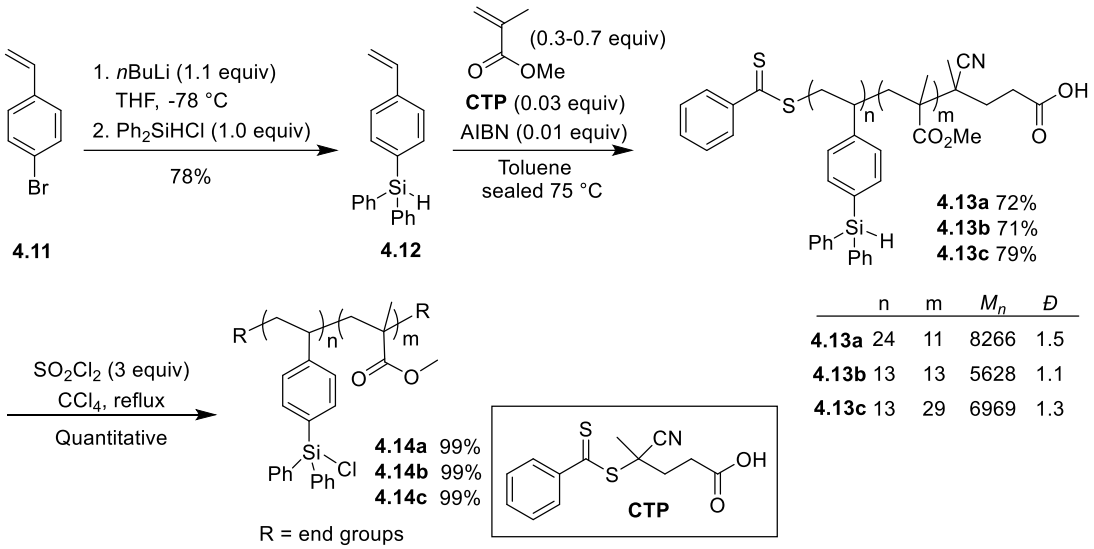

Scheme 4.11 Synthesis of Polymer Supported Silyl Chloride as a Styrene-Methacrylate Copolymer

Kinetic resolutions of alcohol **(±)-4.15** were performed using **1.3** as the catalyst and polymers **4.14a**-**4.14c** as the silyl source to explore the effect of increasing acrylate incorporation into the polymer backbone on the selectivity factors (Table 4.1, entries 1-3). All the polymers were homogeneous under the reaction conditions. Once the selective silylation was completed, enantioriched product **4.16** was precipitated out as a white solid after addition of methanol and removed from the reaction via filtration leading to an efficient chromatography-free separation of the alcohol enantiomers. Polymer **4.14a**, which contained the least amount of acrylate incorporation (31%), did not show an improvement over our first-generation polystyrene backbone polymer (Table 4.1, entry 1 vs entry 4). Upon increasing the acrylate incorporation to 50% and 70%, the selectivity factors increased to 12 and 13 respectively (Table 4.1, entries 2 and 3), which shows improvement over polymer silyl chloride **4.10** (Table 4.1, entry 4) and is competitive to the selectivity obtained when using triphenylsilyl chloride (Table 4.1, entry 5). Since

polymer **4.14c** was comprised of such a large percentage of acrylate, more polymer needed to be added to maintain the same concentration of silyl chloride resulting in a slurry like consistency and hurting conversion due to inefficient mixing of the reaction. Further studies were carried out with polymer **4.14b**, which had the best selectivity and conversion.

Table 4.1 Polymer-Supported Silylation-Based Kinetic Resolution Varying the Polar Composition

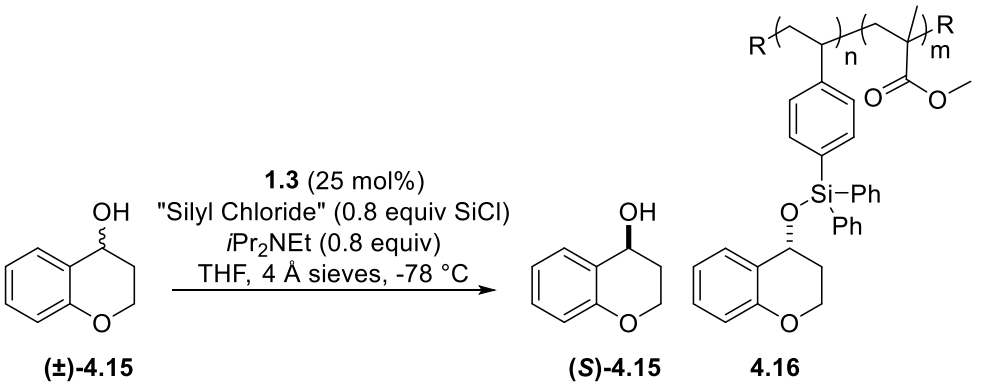

(±)-4.15 **(*S*)-4.15** **4.16**

Entry	Silyl Choride	% m	er of **(*S*)-4.15**	conv (%)[a]	*s*[a]
1	**4.14a**	31%	79:21	47	9
2	**4.14b**	50%	79:21	44	12
3	**4.14c**	70%	69:31	32	13
4[b]	**4.10**	0%	79:21	46	9
5[c]	Ph_3SiCl	----	85:15	49	15

Representative substrates that were previously resolved using our silylation-based kinetic resolution were chosen to test the versatility of polymer **4.14b** (Table 4.2), compared with resolutions employing the styrene backbone polymer **4.10** and triphenylsilyl chloride. The resolution of the secondary alcohols (Table 4.2, entries 1 and 2) and the lactone (Table 4.2, entry 3) with **4.14b** as the silyl chloride all had higher selectivities in the presence of the acrylate/styrene backbone versus using the silyl chloride

polymer **4.10** with just a styrene backbone. Specifically, the pantolactone (Table 4.2, entry 3) has a dramatic increase in selectivity from *s* = 11 with polymer **4.10** to *s* = 28 for **4.14b**. Excitingly all the selectivities were comparable to selectivities obtained when triphenylsilyl chloride is employed (Table 2, last column), showing that the polymer is behaving similarly to a small molecule silyl chloride. The last entry shows the resolution of an α-hydroxy lactam, with a selectivity factor of 12 when using **4.14b** compared with the 20 obtained when employing triphenylsilyl chloride. Ultimately, the sterically hindered lactam has trouble converting past 16%, even after 94 hours, and we presume the sterics on the substrate are also affecting the selectivity. To understand whether spacing out the silyl chlorides or incorporating polarity into the polymer was more important to obtain high selectivity, polymer **4.17** was synthesized. The polymer is synthesized with equal parts styrene and silane monomer **4.12**, providing it with the same ratio of silyl chloride to spacer as polymer **4.14b**. Since both monomers are styrene, they should have the same rate constant, again providing a random copolymer. When the polymer was employed in a kinetic resolution to resolve the alcohol chromanol (Scheme 4.12), it essentially performed the same as polymer **4.14b** giving the same selectivity factor, but lower conversion. The difference in selectivity arose when the α-hydroxy lactone was resolved. The polymer with the pure polystyrene backbone resulted in a much lower selectivity factor and lower conversion as compared to using the more polar **4.14b** silyl chloride. These results show that spacing out the silyl chlorides in the polymer improves selectivity, but it is still essential to incorporate polarity into the backbone to get higher selectivity and to get higher conversion.

Table 4.2 Substrate Scope for the Polymer-Supported Silylation-Based Kinetic Resolution

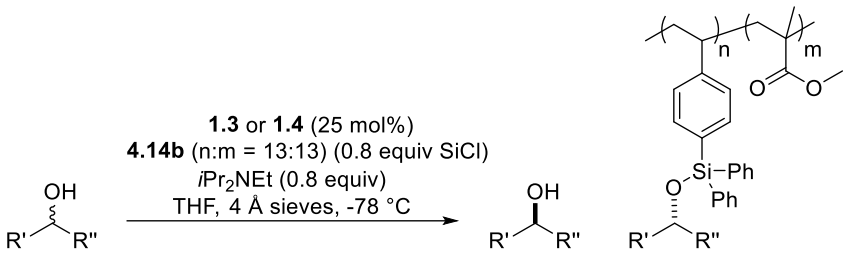

Entry	recovered alcohol	catalyst	er of recovered alcohol	conv (%)[a]	s^a **4.14b**	s^b **4.10**	s^c Ph_3SiCl
1	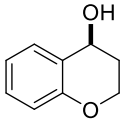	**1.3**	79:21	44	12	8	15
2	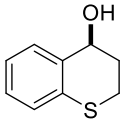	**1.3**	84:16	48	15	12	17
3	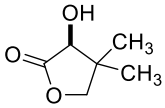	**1.4**	82:18	43	28	11	36
4	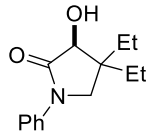	**1.4**	57:43	16	12	--	20

[a]Reactions were run at a concentration with respect to alcohol of: 0.2 M (entries 1 and 2) for 48h and 0.4 M (entries 3 and 4) for 94 h. Conversions and selectivity factors are calculated from the *ee* of the recovered starting materials and products. See ref [38] [b]See ref [7]. [c]Data for entry 1 was taken from ref. [41] and data for entries 3 and 4 was taken from ref. [42]. See references for full experimental details.

To understand whether spacing out the silyl chlorides or incorporating polarity into the polymer was more important to obtain high selectivity, polymer **4.17** was synthesized. The polymer is synthesized with equal parts styrene and silane monomer **4.12**, providing it with the same ratio of silyl chloride to spacer as polymer **4.14b**. Since both monomers

are styrene, they should have the same rate constant, again providing a random copolymer. When the polymer was employed in a kinetic resolution to resolve the alcohol chromanol (Scheme 4.12), it essentially performed the same as polymer **4.14b** giving the same selectivity factor, but lower conversion. The difference in selectivity arose when the α-hydroxy lactone was resolved. The polymer with the pure polystyrene backbone resulted in a much lower selectivity factor and lower conversion as compared to using the more polar **4.14b** silyl chloride. These results show that spacing out the silyl chlorides in the polymer improves selectivity, but it is still essential to incorporate polarity into the backbone to get higher selectivity and to get higher conversion.

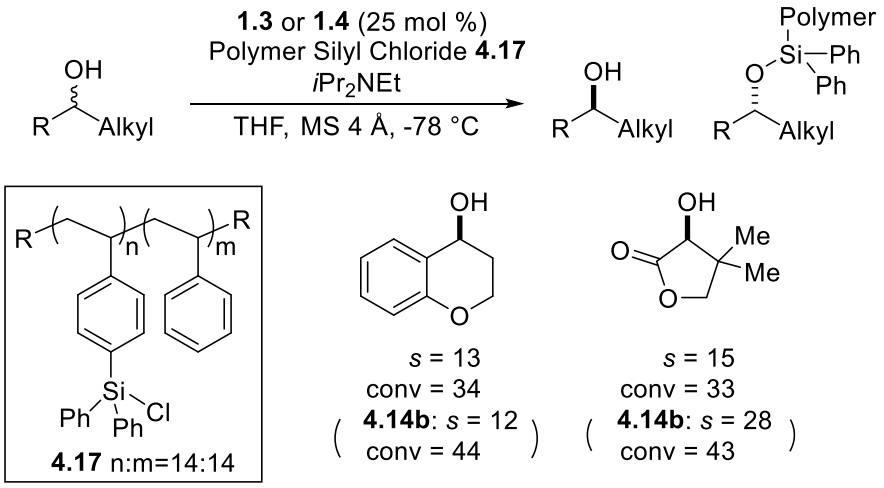

Scheme 4.12 Polymer-Supported Silylation-Based Kinetic Resolution with a Polystyrene Backbone

To further explore the importance of spacing and polarity, a copolymer was synthesized from butyl acrylate and the silane monomer **4.12** (Scheme 4.13), where the silane monomers polymerize faster than butyl acrylate causing the silane monomers to be grouped together. The silyl chloride polymer **4.18** was employed in the kinetic resolution

of chromanol resulting in a slightly lower selectivity factor (s = 10 versus 12 with **4.14b**) with dramatically decreased conversion. These last two polymers show the importance of spacing and the positioning of the polar groups to obtain the best selectivity and reactivity.

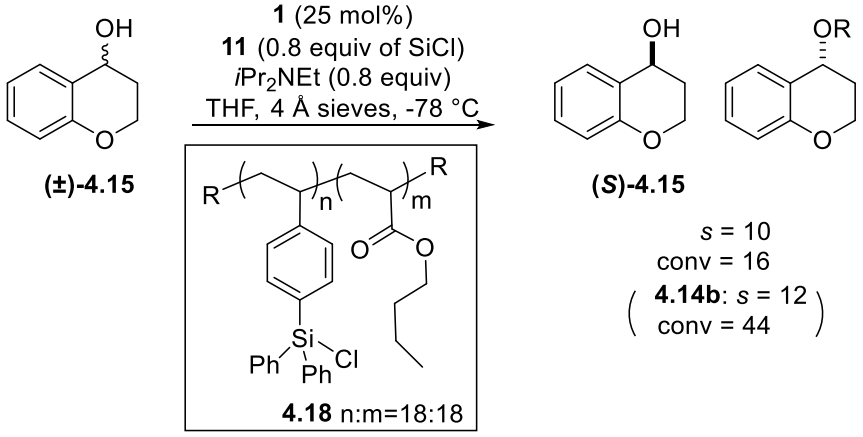

Scheme 4.13 Polymer-Supported Silylation-Based Kinetic Resolution with Butyl Acrylate as Monomer

4.5 Conclusions and Outlook

Our second-generation polymer-supported silyl chlorides were optimized by incorporating polar monomers to the backbone of the polymer adjacent to the silyl chlorides through a random copolymerization. Comparable selectivity factors and conversions to our small molecule silyl chloride were achieved by applying these novel copolymers. A favourable microenvironment around the active site can be obtained by spacing out the silyl chloride and introducing polarity around the silyl chloride. We have shown polarity contributes more to facilitate the selectivity factor over spacing in our system.

Future endeavours will focus on two directions. First, continue to optimize the silyl chloride polymer towards increased selectivity and conversion. Kinetic resolutions using

2nd generation polymer provided a performance closer to the monomer. However, there is still room to improve and push the reactivity same as the monomer. We will try to incorporate monomer which has similar polymerization to the methyl methacrylate but higher polarity. We also need to expand the substrate scope. The second direction is the recoverability of the polymer. In order to regenerate the silly ether derivatized polymer, the alcohol is cleaved through an LiAlH4 reduction, to generate the polymer-supported silane followed by rechlorination. Since methyl methacrylate is comprised of an ester group which is vulnerable to $LiAlH_4$ reduction. Therefore, we need to find a polar monomer that has a similar polymerization rate to methyl methacrylate but lacks a functional group that can be reduced. The last optimization of our polymer-supported triphenylsilyl chloride is the ease of precipitation and filtration, we will focus on increase the molecular weight of polymer chain without hurting its performance in kinetic resolution. Ultimately, we can combine the above two future works in one project by replacing the methyl methacrylate to a more polar monomer with similar polymerization rate and without carbonyl groups. Since polymerization rates of two monomers depends on temperature and pressure, we can try to optimize the polymerization condition to find a potential replacement of methyl methacrylate if we cannot directly find a suitable monomer for the replacement.

4.6 Experimental

General Information

All reactions were carried out under a N_2 atmosphere using oven dried glassware. Molecular sieves were activated for 48 h at 130 °C in an oven. Tetrahydrofuran (THF), toluene and dichloromethane were dried by passing through a column of activated alumina

before use and stored over molecular sieves. Carbon tetrachloride was distilled, degassed and stored over molecular sieves under argon. Sulfuryl chloride was distilled prior to use. 4,4-Diethyl-3-hydroxy-1-phenylpyrrolidin-2-one[1] was prepared according to known procedures. Methyl methacrylate (MMA, 99%, Aldrich), *tert*-butyl acrylate (*t*BA, 97%, Aldrich), and styrene (St, 99%, Aldrich) were passed through a basic alumina column before use. 2,2-Azobis (isobutyronitrile) (AIBN) was recrystallized from methanol. All other chemicals were obtained from commercial sources and used without further purification**.** ^{1}H NMR was taken on a Bruker Avance III (400 or 300 MHz). Chemical shifts are reported in ppm with TMS or chloroform as an internal standard. ^{13}C NMR spectra were taken on a Bruker Avance III (101 or 75 MHz) with complete proton decoupling. Enantiomeric ratios were determined via HPLC using an Agilent 1200 series using chiral stationary phases Daicel Chiralcel OD-H or chiral stationary phases Daicel Chiralcel AD-H (4.6 x 250 mm x 5 µm) columns, monitored by a diode array detector in comparison to racemic materials. Molecular weights and dispersity (Mw/Mn, *Đ*) were determined by GPC conducted on a Varian 390-LC system.

Synthesis of Resin-Supported Silane and Silyl Chlorides

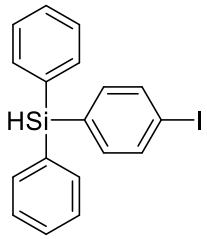

(4-iodophenyl)diphenylsilane (**4.8**)

A solution of **4.6** (990 mg, 3 mmol) in 6 mL THF was prepared in a four-dram vial with Teflon stir bar. The vial was put in -40 ℃ bath for 10 minutes until the starting material

fully cooled down for the following lithium halogen exchange reaction. After titration, an accurate 1.1 equivalent amounts of *n*-BuLi (2050 μL) was added into the vial drop by drop. After adding all the *n*-BuLi, reaction was arranged under nitrogen balloon and reacted for 3 hours. Then transferred the vial to –78 ℃ bath. A solution of **4.7** (656 mg, 3 mmol) in 3 mL THF was added drop by drop to the vail. After reacting under 78 ºC for 0.5 hour, the vial was transferred to room temperature for another 2 hours reaction. Reaction was then quenched with Deionized water (6 mL). Diethyl ether (6*3ml) was used for extraction and the organic layer was dried with sodium sulfate. Solvent was removed and the residue was purified by silica gel chromatography (pure Hexane) to give transparent oil (618 mg, 53% yield). ^{1}H NMR (400 MHz, $CDCl_3$, 25℃) δ 5.42 (s, 1H), 7.27-7.31 (d,2H), 7.35-7.46 (m,6H), 7.53-7.56 (d,2H), 7.70-7.74 (d,2H); ^{13}C NMR (75.46 MHz, $CDCl_3$, 25℃) δ 128.2, 130.0, 132.6, 135.7, 137.2, 137.4.

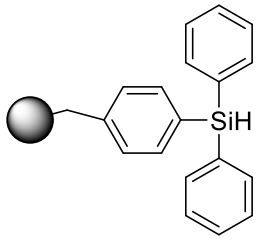

4.10

Tentagel-supported triphenyl silane (**4.10**)

A solution of **4.8** (268 mg, 0.7 mmol) in 3ml THF was prepared in a 4-dram vial with Teflon stir bar. The vial was put in 40 ºC baths until the starting materials fully cooled down. 1.1 equivalent of n-BuLi (475 μL) was added drop by drop to the vial. After adding all the n-BuLi. The reaction was arranged under nitrogen balloon and react for 45 minutes. In the meanwhile, **4.9** (276 mg, 0.07 mmol) in 9mL THF was prepared in a 25 mL round

bottom flask. The round bottom flask was set under room temperature for 20 minutes until resin was fully swollen then transferred to -78℃ bath. Once the lithium halogen exchange reaction was ready, the mixture was added drop by drop to the round bottom flask. It was transferred to shaker under room temperature for additional 2 hours followed by quenching with deionized water (6 mL). Crude product was obtained though the filtration, THF (2*6mL) was used to wash the crude product until the color turned white from yellow.

Synthesis of monomer 1-diphenylsilyl-4-ethenylbenzene (4.12)

In an oven dry 250 mL round bottom flask was charged with a magnetic stirring bar and 4-bromostyrene **(4.11)** (1.8 g, 10 mmol) in 45 mL THF was added to the flask at room temperature under N_2 and allow to cool at -78 °C. After 20 minutes, 6.75 mL (1.63 M, 11 mmol) *n*-BuLi was added to the flask and allow to stir for 2 hours. Then the lithium mixture was added dropwise to another 250 mL round bottom flask which was equipped with the solution of diphenylchlorosilane (2.2 g, 10 mmol) in THF (15 mL) via cannula at -78 °C. Resulting mixture was warmed to room temperature and stirred for 4 hours. After quenching with 20 mL of saturated NH_4Cl, the mixture was extracted with diethyl ether (20 mL, 3 times). The organic layer was washed with 20 mL of water, dried over anhydrous $MgSO_4$, filtered and concentrated using vacuum. Column chromatography was performed using hexane as a solvent. Colorless liquid was obtained as a final product. (2.2 g, 7.8 mmol, Yield = 78%). **^{1}H NMR** (400 MHz, $CDCl_3$) δ ppm 7.57 (m, 6H), 7.39 (m, 8H), 6.75 (m, 1H), 5.79 (d, J = 18 Hz, 1H), 5.47 (s, 1 H), 5.28 (d, J = 9 Hz, 1 H). **^{13}C NMR** (101 MHz, $CDCl_3$) δ ppm 139.0, 136.8, 136.1, 135.8, 133.3, 132.9, 129.9, 128.1, 125.9, 114.8.

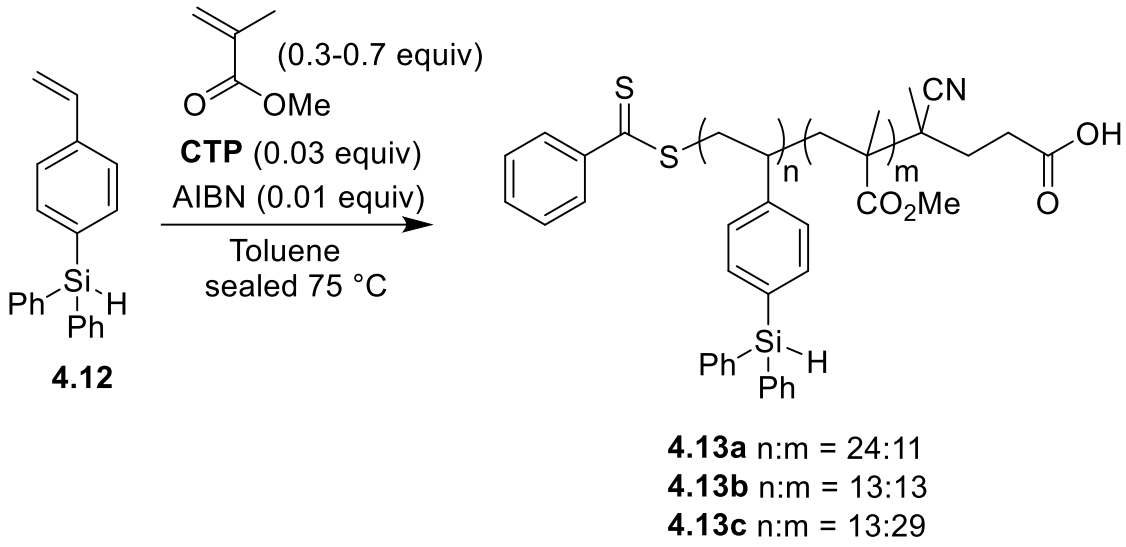

Scheme 4.14 Copolymerization of 4.12 and Methyl Methacrylate

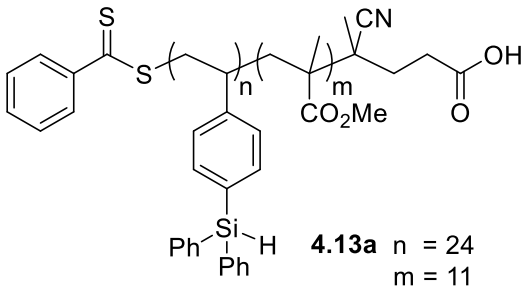

Synthesis of Polymer-Supported Silane and Silyl Chlorides

poly(1-diphenylsilyl-4-ethenylbenzene-co-methyl methacrylate) (**4.13a**)

Monomer 1-diphenylsilyl-4-ethenylbenzene (1.24 g, 4.33 mmol), methyl methacrylate (186.1 mg, 1.86 mmol), 4-Cyano-4-(phenylcarbonothioylthio) pentanoic acid (30.5 mg, 0.11 mmol), and AIBN (5.1 mg, 0.031 mmol) were dissolved in 2.2 mL of toluene in a 10 mL Schlenk flask and then degassed with three cycles of freeze−pump−thaw. The reaction was heated under 75 °C for 24 h. The reaction mixture was precipitated in methanol for three times and vacuum dried. Yield: 1.1 g, 71.6%. The GPC traces of copolymers were showed in below (Figure 4.1) and dispersity (*Đ*) of copolymers were showed in **Table 4.3**.

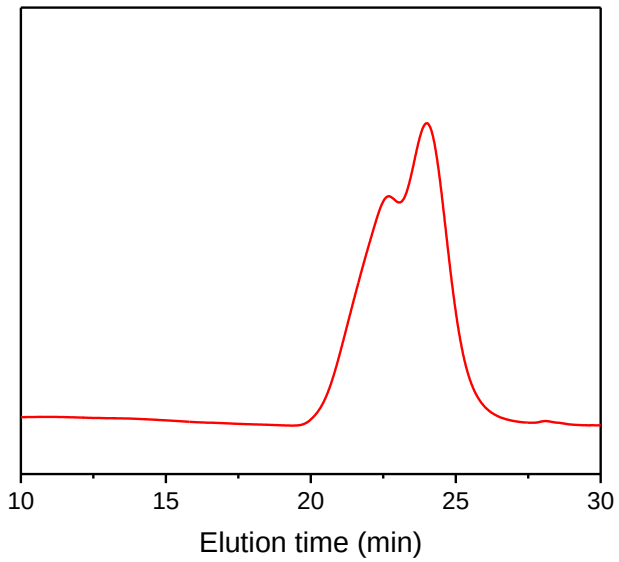

Figure 4.1 GPC Trace of 4.13a

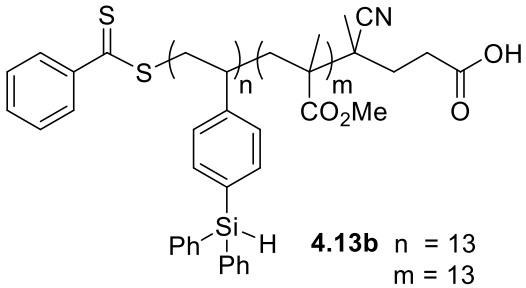

4.13b n = 13
m = 13

poly(1-diphenylsilyl-4-ethenylbenzene-co-methyl methacrylate) (**4.13b**)

Monomer 1-diphenylsilyl-4-ethenylbenzene (1.4 g, 4.89 mmol), methyl methacrylate (489.6 mg, 4.89 mmol), 4-Cyano-4-(phenylcarbonothioylthio) pentanoic acid (44.1 mg, 0.16 mmol), and AIBN (7.8 mg, 0.047 mmol) were dissolved in 3.5 mL of toluene in a 10 mL Schlenk flask and then degassed with three cycles of freeze−pump−thaw. The reaction was heated under 75 °C for 24 h. The reaction mixture was precipitated in methanol for three times and vacuum dried. Yield: 1.5 g, 75.9%. ^{1}H NMR spectrum of the polymer product is given in **Figure 4.6** as an example. The GPC traces of copolymers were showed in below (Figure 4.2) and dispersity (*Đ*) of copolymers were showed in **Table 4.3**.

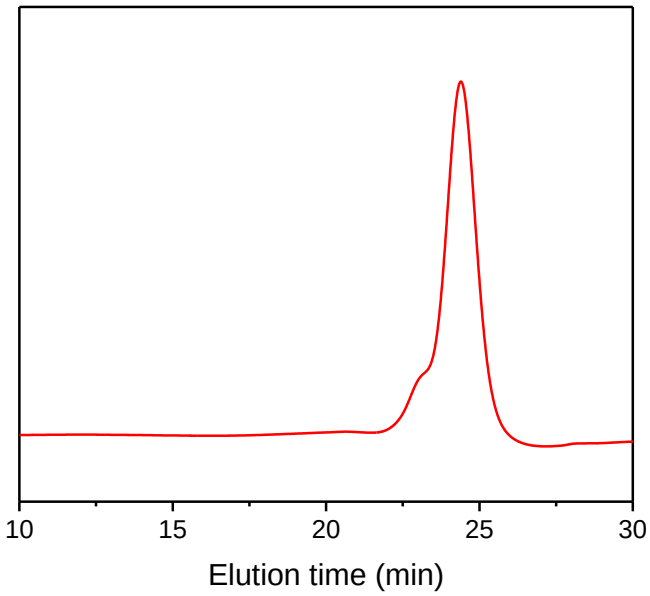

Figure 4.2 GPC Trace of 4.13b

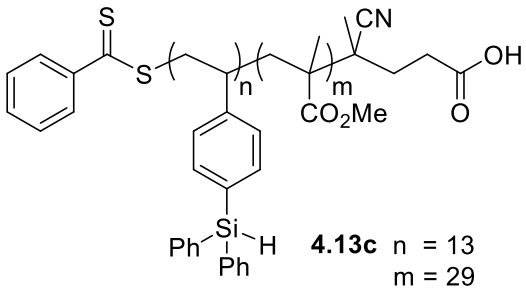

4.13c n = 13
m = 29

poly(1-diphenylsilyl-4-ethenylbenzene-co-methyl methacrylate) (**4.13c**)

Monomer 1-diphenylsilyl-4-ethenylbenzene (1.1 g, 3.84 mmol), methyl methacrylate (898.2 mg, 8.97 mmol), 4-Cyano-4-(phenylcarbonothioylthio) pentanoic acid (42.6 mg, 0.15 mmol), and AIBN (10.5 mg, 0.064 mmol) were dissolved in 4.5 mL of toluene in a 25 mL Schlenk flask and then degassed with three cycles of freeze−pump−thaw. The reaction was heated under 75 °C for 24 h. The reaction mixture was precipitated in methanol for three times and vacuum dried. Yield: 1.7 g, 78.5%. The GPC traces of copolymers were showed in below (Figure 4.3) and dispersity (*Đ*) of copolymers were showed in **Table 4.3**.

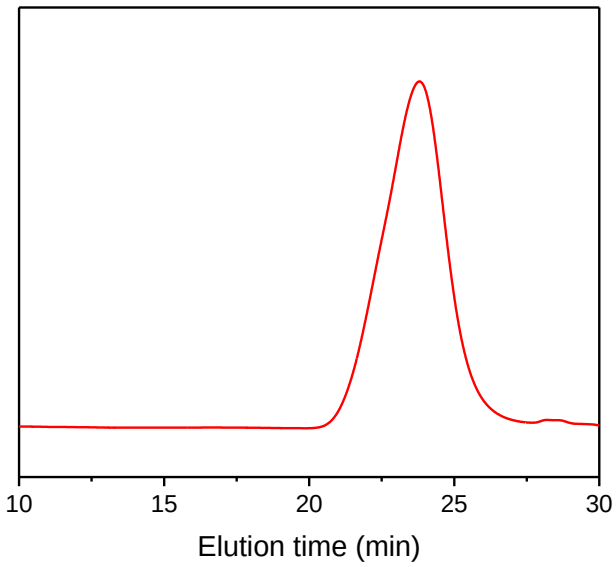

Figure 4.3 GPC Trace of 4.13c

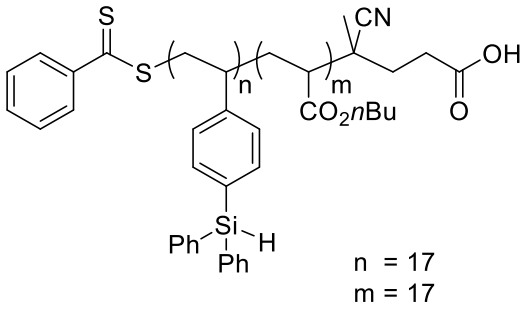

poly(1-diphenylsilyl-4-ethenylbenzene-co-*n*-butyl acrylate) (**4.17**)

Monomer 1-diphenylsilyl-4-ethenylbenzene (1.4 g, 4.79 mmol), n-butyl acrylate (614 mg, 4.79 mmol), 4-Cyano-4-(phenylcarbonothioylthio) pentanoic acid (43.2 mg, 0.16 mmol), and AIBN (7.6 mg, 0.046 mmol) were dissolved in 3.4 mL of toluene in a 25 mL Schlenk flask and then degassed with three cycles of freeze−pump−thaw. The reaction was heated under 75 °C for 24 h. The reaction mixture was precipitated in methanol for three times and vacuum dried. Yield: 1.4 g, 69.5%. ^{1}H NMR spectrum of the polymer product is given in **Figure 4.7** as an example. The GPC traces of copolymers were showed in below (Figure 4.4) and dispersity (*Đ*) of copolymers were showed in **Table 4.3**.

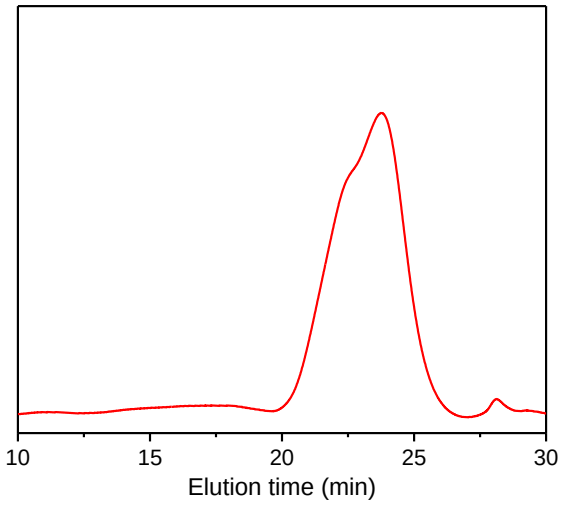

Figure 4.4 GPC Trace of 4.17

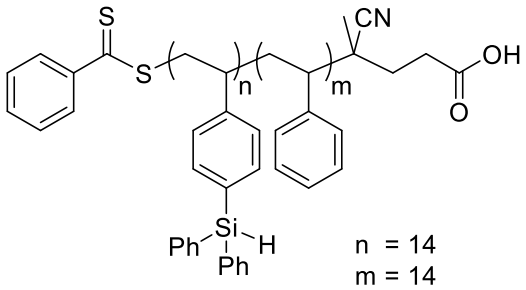

poly(1-diphenylsilyl-4-ethenylbenzene-co-styrene) (**4.18**)

Monomer 1-diphenylsilyl-4-ethenylbenzene (2.2 g, 7.73 mmol), styrene (805 mg, 7.73 mmol), 4-Cyano-4-(phenylcarbonothioylthio) pentanoic acid (69.7 mg, 0.25 mmol), and AIBN (12.3 mg, 0.075 mmol) were dissolved in 5.6 mL of toluene in a 25 mL Schlenk flask and then degassed with three cycles of freeze−pump−thaw. The reaction was heated under 75 °C for 24 h. The reaction mixture was precipitated in methanol for three times and vacuum dried. Yield: 1.9 g, 63.3%. ^{1}H NMR spectrum of the polymer product is given in **Figure 4.8** as an example. The GPC traces of copolymers were showed in below (Figure 4.5) and dispersity (*Đ*) of copolymers were showed in **Table 4.3**.

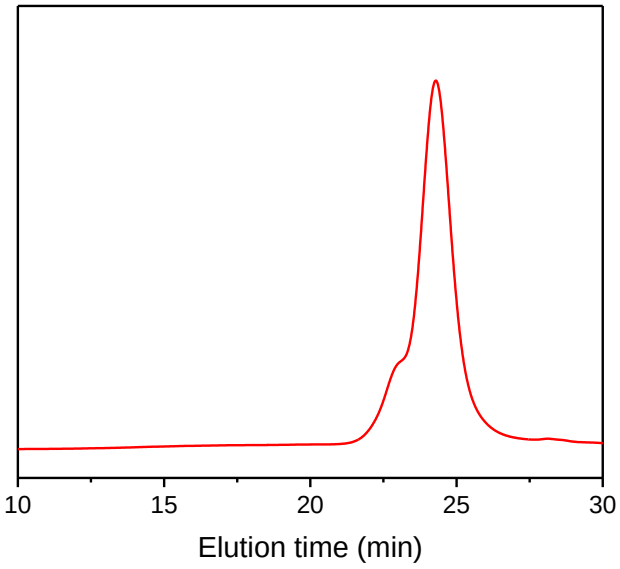

Figure 4.5 GPC Trace of 4.18

Table 4.3 Molecular Weight Parameters of Polymers Characterized from GPC

Polymer	n	m	*Mn* (GPC)	*Đ*
4.13a	24	11	8266	1.5
4.13b	13	13	5628	1.1
4.13c	13	29	6969	1.3
4.17	14	14	5828	1.1
4.18	17	17	7444	1.4

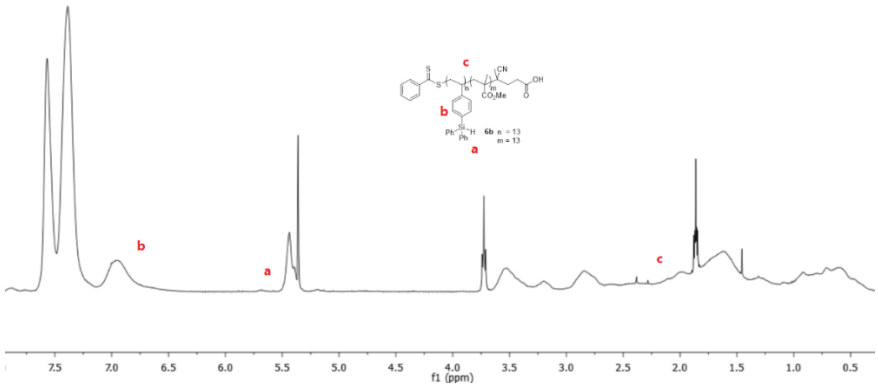

Figure 4.6 ^{1}H NMR (CD_2Cl_2) Spectrum of the Polymer 4.13b

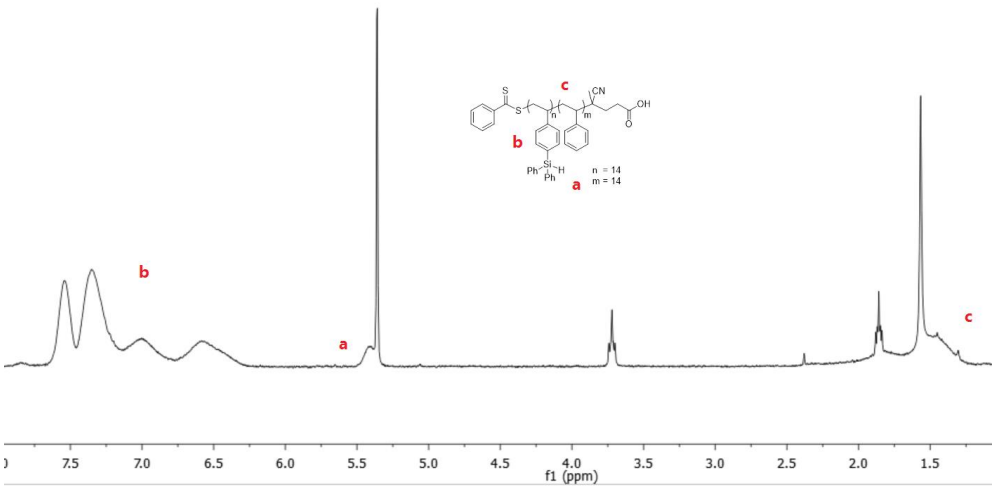

Figure 4.7 ^{1}H NMR (CD_2Cl_2) Spectrum of the Polymer 4.17

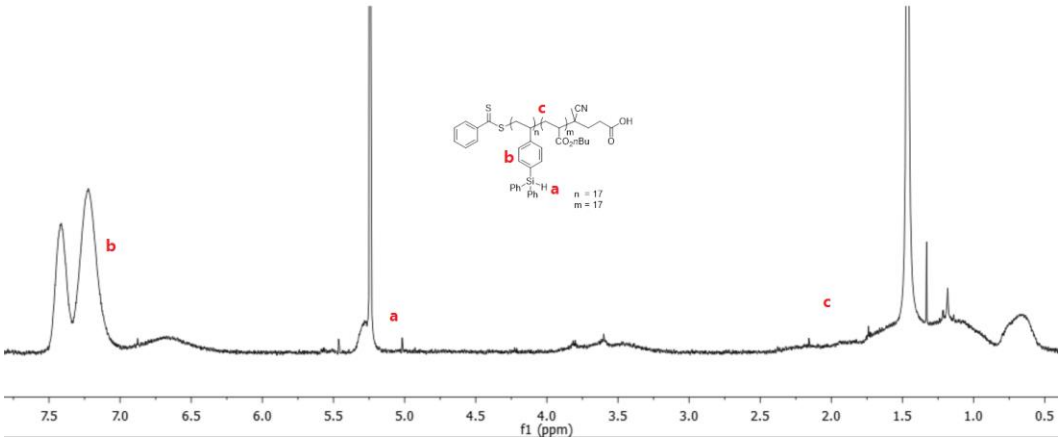

Figure 4.8 ^{1}H NMR (CD_2Cl_2) Spectrum of the Polymer 4.18

Example Procedure for the Chlorination of Polymer-Bound Triphenyl Silane

A 50 mL three neck round bottom flask was equipped with a stir bar. polymer **4.13b** (900 mg, 1.63 mmol, based on silane) in 15 mL of CCl_4 was added into the vessel. The flask was then equipped with a reflux condenser and purged with argon. The solution was warmed to reflux then SO_2Cl_2 (0.39 mL, 4.89 mmol) was added via syringe drop wise. The mixture was allowed to reflux for 3 h at which point complete conversion was achieved as determined by ^{1}H NMR. The solvent was removed under vacuum to yield the chlorinated

polymer **4.14b** ready for use in a kinetic resolution, 1.21 g, pale yellow solid, quantitative yield. For ^{1}H NMR spectra of the chlorinated polymer see the spectroscopic data of select compounds.

General Procedure for the Polymer Supported Silylation-Based Kinetic Resolution of Secondary Alcohols (GP1)

Into a 1-dram vial equipped with a stir bar and activated 4Å molecular sieves, racemic substrate (0.4 mmol) and catalyst (**1.3 or 1.4**) (0.1 mmol) was added. The vial was then purged with argon and sealed with a septum. The starting materials were then dissolved in 1.4 mL of THF. Base, (*i*Pr$_2$NEt, 0.32 mmol), was added via syringe and the vial was cooled to -78 °C in a cryocool for 30 mins. The cooled mixture was then treated with 0.64 mL of a freshly prepared 0.5 M polymer-bound silyl chloride solution in THF. The reaction was left to stir a set amount of time at -78 °C then quenched with 0.3 mL of methanol. The solution was left to warm to room temperature then the contents of the vial were extracted into a 4-dram vial with EtOAc. The solution was concentrated to give an oil, which was diluted with 20 mL of EtOAc. The resulting solution was washed with 5% HCl followed by sat. aq. $NaHCO_3$. The organic layer was then dried over sodium sulfate, filtered and concentrated. The polymer was precipitated from the unreacted starting material by addition of methanol (10 mL). The polymer was filtered away and the supernatant concentrated. The precipitation process was repeated three times. Removal of the methanol afforded the starting material. Further purification on column chromatography was needed (EtOAc /hexanes mixtures) to provide starting material suitable for chiral stationary HPLC.

General Procedure for the Deprotection of Polymer-Bound Products (GP2)

The polymer-bound product obtained by filtration was weighed into a 4-dram vial equipped with a stir bar and septum. The polymer was then dissolved in 1 mL of THF with stirring and treated with 1 mL of TBAF (1 M in THF). The reaction was monitored via TLC (1:3 EtOAc: hexanes). The reactions were generally complete in less than 2 h. The reaction was then quenched with brine, extracted with diethyl ether (2 mL, three times) and dried over anhydrous $MgSO_4$ and filtered. Concentration under vacuum afforded an oil. Subsequent purification on silica gel column chromatography (EtOAc/hexanes mixture) afforded the deprotected products suitable for conversion to the benzoate ester or separation on chiral stationary phase HPLC.

General Procedure for the Benzoylation of Pentolactone (GP3)

A 4-dram vial containing the lactone was fitted with a stir bar and a septum. DMAP (0.1 equiv) was added to the vial. The mixture was then dissolved in 2 mL of dichloromethane with stirring. Triethyl amine (2.0 equiv) was added via syringe and the vessel was cooled to 0 °C in an ice bath. Benzoyl chloride (1.4 equiv) was then added drop wise via syringe and the reaction was left to stir for 30 mins at which point TLC of the crude indicated reaction was complete. The reaction was quenched with sat. sodium bicarbonate and extracted three times with dichloromethane. The combined organic layers were then dried over sodium sulfate. After concentration, the crude was then purified via silica gel column chromatography to obtain the desired benzoylated lactone.

Table 4.4 Kinetic Resolution Data for Table 4.1

Entry	n	m	er SM	er PR	Conv (%)	*s*	Avg *s*
Table 4.1 entry 1	24	11	78.6:21.4	82.6:17.4	46.7	8.4	**9.4**
			80.3:19.7	85.0:15.0	46.4	10.4	
Table 4.1 entry 2	13	13	79.0:21.0	87.7:12.3	43.5	12.7	**11.9**
			82.5:17.5	85.1:14.9	48.1	11.0	
Table 4.1 entry 3	13	29	68.6:31.4	89.8:10.2	31.8	12.8	**12.7**
			67.6:32.4	89.8:10.2	30.5	12.5	

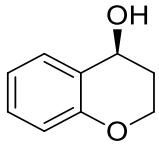

Table 4.1, Entry 1: 30 mg, 49 % recovered. **^{1}H NMR:** (400 MHz, $CDCl_3$) δ 7.32 (dd, *J* = 7.6, 1.6 Hz, 1H), 7.24 – 7.18 (m, 1H), 6.93 (td, 1H), 6.85 (dd, *J* = 8.2, 0.9 Hz, 1H), 4.80 (q, *J* = 4.2 Hz, 1H), 4.35 – 4.19 (m, 2H), 2.21 – 1.96 (m, 2H), 1.82 (d, *J* = 4.9 Hz, 1H). **^{13}C NMR:** (101 MHz, $CDCl_3$) δ ppm 154.6, 129.8, 129.7, 124.3, 120.6, 117.1, 63.3, 61.9, 30.8. HPLC condition: OD-H Column 8% isopropyl alcohol in hexane, flow rate: 1.0 mL/min; t_R 17.9 min for (*S*)-enantiomer and 22.2 min for (*R*)-enantiomer (er = 79:21)

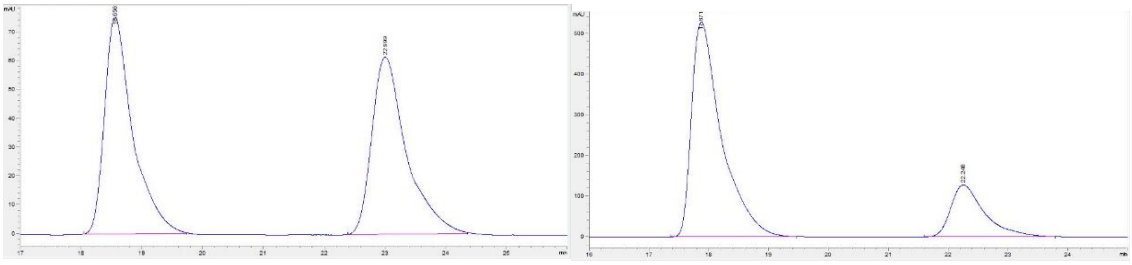

#	Time	Area	Height	Width	Area%	Symmetry
1	18.556	2446.3	75.4	0.4763	50.117	0.551
2	22.999	2434.9	61.5	0.5778	49.883	0.584

#	Time	Area	Height	Width	Area%	Symmetry
1	17.871	18378.6	528.4	0.5088	78.604	0.442
2	22.248	5002.6	127.6	0.5786	21.396	0.551

Figure 4.9 HPLC Data of the SM of Table 4.1 Entry 1

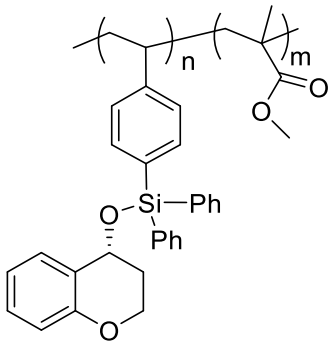

Table 4.1, Entry 1: 52 mg. For **^{1}H NMR** (400 MHz) data see selected spectra. HPLC data is of the desilylated product following GP2, 12 mg, 23 % yield. The same conditions as the recovered starting materials were utilized. (er = 83:17)

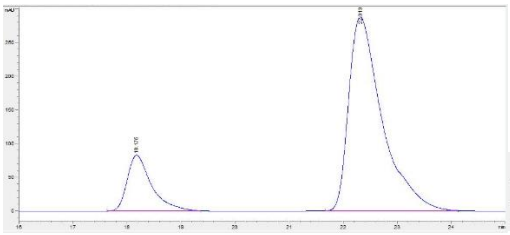

#	Time	Area	Height	Width	Area%	Symmetry
1	18.175	2593.4	82.9	0.472	17.363	0.58
2	22.313	12342.6	287.7	0.6345	82.637	0.493

Figure 4.10 HPLC Data of the PR of Table 4.1 Entry 1

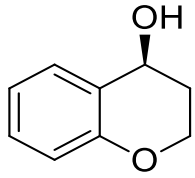

Table 4.1, Entry 2: 31 mg, 51 % recovered. **^{1}H NMR:** (400 MHz, $CDCl_3$) δ 7.32 (dd, *J* = 7.6, 1.6 Hz, 1H), 7.24 – 7.18 (m, 1H), 6.93 (td, *J* = 7.5, 1.1 Hz, 1H), 6.85 (dd, *J* = 8.2, 0.9 Hz, 1H), 4.80 (q, *J* = 4.2 Hz, 1H), 4.35 – 4.19 (m, 2H), 2.21 – 1.96 (m, 2H), 1.82 (d, *J* = 4.9 Hz, 1H). **^{13}C NMR:** (101 MHz, $CDCl_3$) δ ppm 154.6, 129.8, 129.7, 124.3, 120.6, 117.1, 63.3, 61.9, 30.8. HPLC separation was achieved on Chiralpak OD-H Column 8% isopropyl alcohol in hexane, flow rate: 1.0 mL/min, 25 °C; t_R 19.1 min for (*S*)-enantiomer (major) and 23.7 min for (*R*)-enantiomer (minor). (er = 79:21)

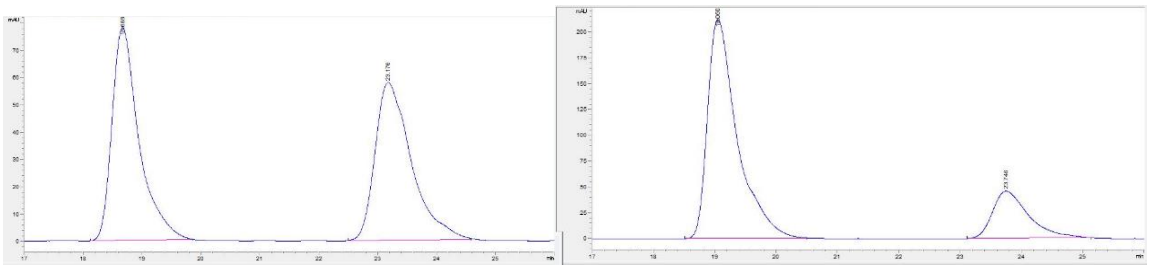

#	Time	Area	Height	Width	Area%	Symmetry
1	18.668	2495.1	78.1	0.4786	50.129	0.593
2	23.176	2482.3	57.9	0.601	49.871	0.545

#	Time	Area	Height	Width	Area%	Symmetry
1	19.05	7129.1	212.5	0.4984	79.042	0.501
2	23.746	1890.3	45.9	0.6246	20.958	0.558

Figure 4.11 HPLC Data of the SM of Table 4.1 Entry 2

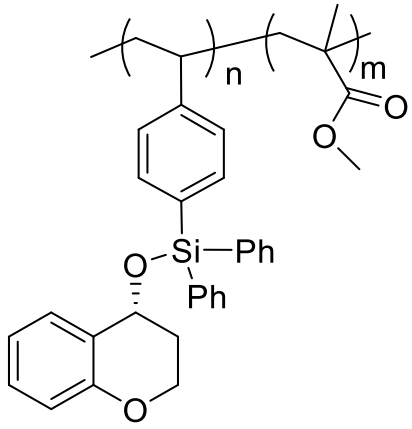

Table 4.1, Entry 2: 53 mg. For **^{1}H NMR** (400 MHz) data see selected spectra. HPLC data is of the desilylated product following GP2, 13 mg, 25 % yield. The same conditions as the recovered starting materials were utilized. (er = 88:12)

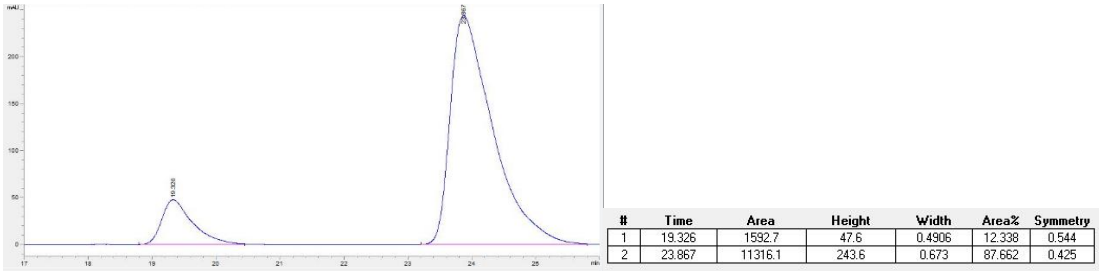

#	Time	Area	Height	Width	Area%	Symmetry
1	19.326	1592.7	47.6	0.4906	12.338	0.544
2	23.867	11316.1	243.6	0.673	87.662	0.425

Figure 4.12 HPLC Data of the PR of Table 4.1 Entry 2

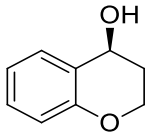

Table 4.1, Entry 3: 33 mg, 54 % recovered. **^{1}H NMR:** (400 MHz, $CDCl_3$) δ 7.32 (dd, *J* = 7.6, 1.6 Hz, 1H), 7.24 – 7.18 (m, 1H), 6.93 (td, *J* = 7.5, 1.1 Hz, 1H), 6.85 (dd, *J* = 8.2, 0.9 Hz, 1H), 4.80 (q, *J* = 4.2 Hz, 1H), 4.35 – 4.19 (m, 2H), 2.21 – 1.96 (m, 2H), 1.82 (d, *J* = 4.9 Hz, 1H). **^{13}C NMR:** (101 MHz, $CDCl_3$) δ ppm 154.6, 129.8, 129.7, 124.3, 120.6, 117.1, 63.3, 61.9, 30.8. HPLC condition OD-H Column 8% IPA in hexane, flow rate: 1.0 mL/min; t_R 18.7 min for (*S*)-enantiomer (major) and 23.2 min for (*R*)-enantiomer (minor). (er = 69:31)

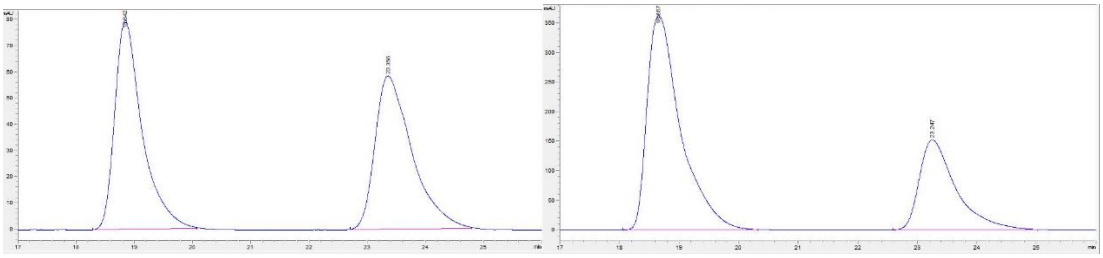

#	Time	Area	Height	Width	Area%	Symmetry
1	18.842	2617.9	79.7	0.4914	50.276	0.579
2	23.356	2589.2	58.6	0.6268	49.724	0.521

#	Time	Area	Height	Width	Area%	Symmetry
1	18.657	14178.2	362	0.582	68.561	0.491
2	23.247	6501.6	152.5	0.6304	31.439	0.513

Figure 4.13 HPLC Data of the SM of Table 4.1 Entry 3

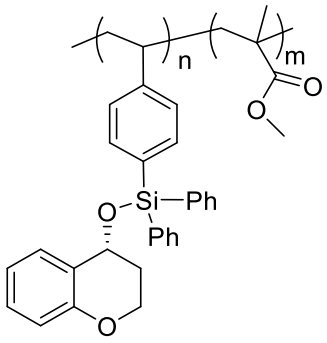

Table 4.1, Entry 3: 43 mg. For **^{1}H NMR** (400 MHz) data see selected spectra. HPLC data is of the desilylated product following GP2, 10 mg, 23 % yield. The same conditions as the recovered starting materials were utilized. (er = 90:10)

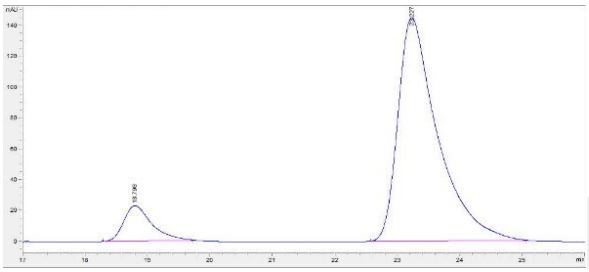

#	Time	Area	Height	Width	Area%	Symmetry
1	18.798	732	23	0.4707	10.236	0.616
2	23.227	6419	144.9	0.6318	89.764	0.495

Figure 4.14 HPLC Data of the PR of Table 4.1 Entry 3

Analytical Data and HPLC Data for Kinetic Resolutions

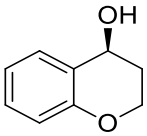

Table 4.2, Entry 1: 31 mg, 51 % recovered. **^{1}H NMR:** (400 MHz, $CDCl_3$) δ 7.32 (dd, *J* = 7.6, 1.6 Hz, 1H), 7.24 – 7.18 (m, 1H), 6.93 (td, *J* = 7.5, 1.1 Hz, 1H), 6.85 (dd, *J* = 8.2, 0.9 Hz, 1H), 4.80 (q, *J* = 4.2 Hz, 1H), 4.35 – 4.19 (m, 2H), 2.21 – 1.96 (m, 2H), 1.82 (d, *J* = 4.9 Hz, 1H). **^{13}C NMR:** (101 MHz, $CDCl_3$) δ ppm 154.6, 129.8, 129.7, 124.3, 120.6, 117.1, 63.3, 61.9, 30.8. HPLC separation was achieved on Chiralpak OD-H Column 8% isopropyl alcohol in hexane, flow rate: 1.0 mL/min, 25 °C; t_R 19.1 min for (*S*)-enantiomer (major) and 23.7 min for (*R*)-enantiomer (minor). (er = 79:21)

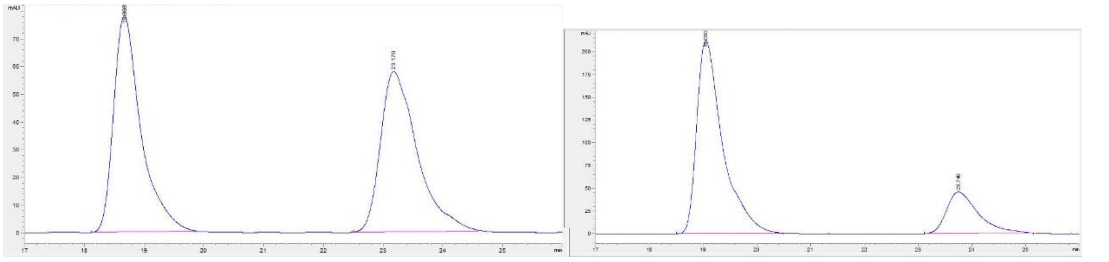

#	Time	Area	Height	Width	Area%	Symmetry
1	18.668	2495.1	78.1	0.4786	50.129	0.593
2	23.176	2482.3	57.9	0.601	49.871	0.545

#	Time	Area	Height	Width	Area%	Symmetry
1	19.05	7129.1	212.5	0.4984	79.042	0.501
2	23.746	1890.3	45.9	0.6246	20.958	0.558

Figure 4.15 HPLC Data of the SM of Table 4.2 Entry 1

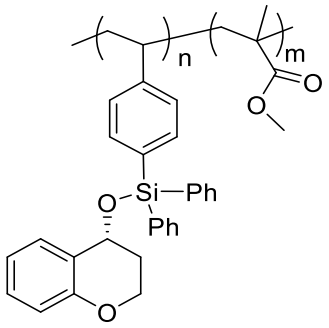

Table 4.2, Entry 1: 53 mg. For **^{1}H NMR** (400 MHz) data see selected spectra. HPLC data is of the desilylated product following GP2, 13 mg, 25 % yield. The same conditions as the recovered starting materials were utilized. (er = 88:12)

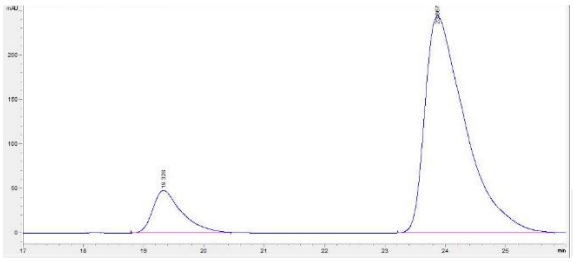

#	Time	Area	Height	Width	Area%	Symmetry
1	19.326	1592.7	47.6	0.4906	12.338	0.544
2	23.867	11316.1	243.6	0.673	87.662	0.425

Figure 4.16 HPLC Data of the PR of Table 4.2 Entry 1

Table 4.5 Kinetic Resolution Data for Table 4.2, Entry 1

Entry	er SM	er PR	Conv (%)	*s*	Avg *s*
1	79.0:21.0	87.7:12.3	43.5	12.7	11.9
2	82.5:17.5	85.1:14.9	48.1	11.0	

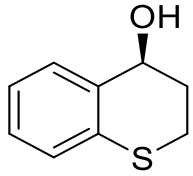

Table 4.2, Entry 2: 33 mg, 50 % recovered. **^{1}H NMR:** (400 MHz, $CDCl_3$) δ ppm 7.33 (d, J = Hz, 1 H), 7.19 – 7.12 (m, 2H), 7.10 – 7.04 (m, 1H), 4.83 (dd, *J* = 4.7, 3.2 Hz, 1 H),

3.33 (td, *J* = 12.3, 3.0 Hz, 1H), 2.93 – 2.78 (m, 1H), 2.36 (dtd, *J* = 13.7, 5.3, 3.0 Hz, 1H), 2.06 (ddt, *J* = 14.0, 11.9, 3.3 Hz, 1H), 1.77 (s, 1H). **^{13}C NMR:** (101 MHz, $CDCl_3$) δ ppm 134.6, 133.3, 130.4, 128.5, 126.8, 124.3, 66.6, 30.0, 21.5. HPLC separation was achieved on Chiralpak OD-H Column 10 % isopropyl alcohol in hexane, flow rate: 1.0 mL/min, 25 °C; t_R 18.4 min for (*S*)-enantiomer (major) and 24.2 min for (*R*)-enantiomer (minor). (er = 84:16) As this material is a known compound, no IR spectrum nor high resolution mass spectrum was required.

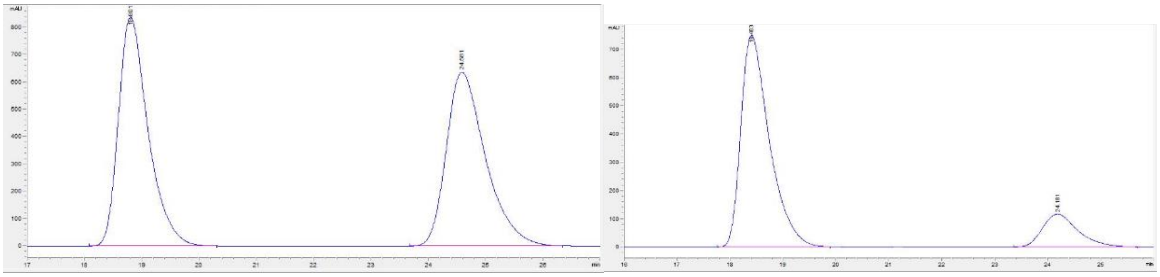

#	Time	Area	Height	Width	Area%	Symmetry
1	18.801	30186.4	838.7	0.5419	49.916	0.643
2	24.581	30287.6	636.9	0.7148	50.084	0.627

#	Time	Area	Height	Width	Area%	Symmetry
1	18.403	28003	749.4	0.564	83.632	0.556
2	24.181	5480.5	116.9	0.7111	16.368	0.693

Figure 4.17 HPLC Data of the SM of Table 4.2 Entry 2

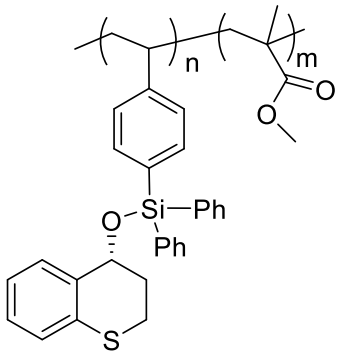

Table 4.2, Entry 2: 63 mg. For **^{1}H NMR** (400 MHz) data see selected spectra. CD_2Cl_2 was applied as the NMR solvent because the reference peak blocks no other peaks. HPLC

data is of the desilylated product following GP2, 18 mg, 29 % yield. The same conditions as the recovered starting materials were utilized. (er = 87:13)

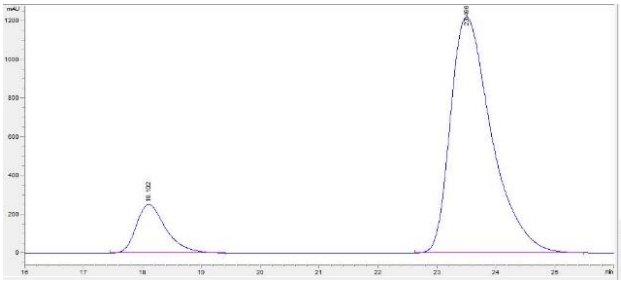

#	Time	Area	Height	Width	Area%	Symmetry
1	18.102	8777.5	250.9	0.5342	12.944	0.675
2	23.496	59036.3	1218.4	0.7413	87.056	0.598

Figure 4.18 HPLC Data of the PR of Table 4.2 Entry 2

Table 4.6 Kinetic Resolution Data for Table 4.2, Entry 2

Entry	er SM	er PR	Conv (%)	*s*	Avg *s*
1	83.6:16.4	87.1:12.9	47.5	13.5	15.1
2	82.8:17.2	89.5:10.5	45.4	16.6	

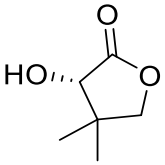

Table 4.2, Entry 3: 27 mg, 51 % recovered. **^{1}H NMR:** (400 MHz, $CDCl_3$) δ ppm 4.11 (s, 1H), 4.00 (d, *J* = 8.9 Hz, 1H), 3.95 (d, *J* = 8.9 Hz, 1H), 1.24 (s, 3H), 1.08 (s, 3H). **^{13}C NMR:** (101 MHz, $CDCl_3$) δ ppm 177.7, 76.4, 75.8, 41.0, 22.9, 18.8.

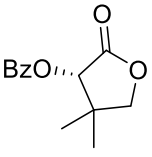

^{1}H NMR: (400 MHz, $CDCl_3$) δ ppm 8.12 (d, *J* = 7.7 Hz, 2H), 7.63 (t, *J* = 7.4 Hz, 1H), 7.49 (t, *J* = 7.7 Hz, 2H), 5.64 (s, 1H), 4.23 – 4.05 (m, 2H), 1.29 (s, 3H), 1.25 (s, 3H). **^{13}C NMR:**

(101 MHz, $CDCl_3$) δ ppm 172.4, 165.4, 133.8, 130.0, 128.8, 128.6, 76.3, 75.5, 40.6, 23.1, 20.1. The recovered starting material was converted to the benzoylated ester according to GP3 for HPLC analysis. HPLC separation was achieved on Chiralpak OD-H Column 6 % isopropyl alcohol in hexane, flow rate: 1 mL/min, 25 °C; t_R 17.4 min for (*R*)-enantiomer (minor) and 20.0 min for (*S*)-enantiomer (major). (er = 80:20)

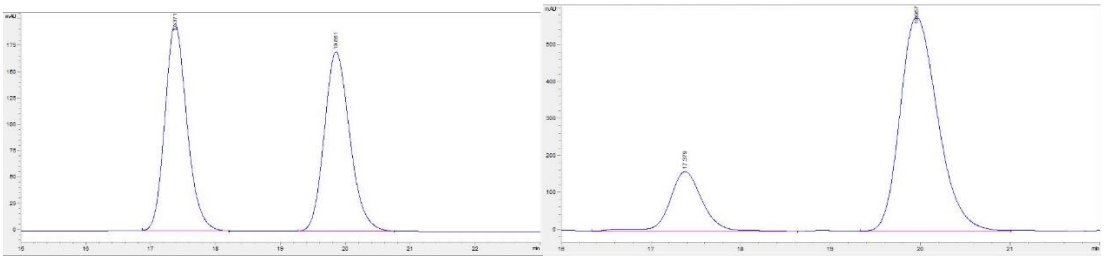

#	Time	Area	Height	Width	Area%	Symmetry
1	17.371	4644.6	196.7	0.3635	49.928	0.818
2	19.851	4657.9	170.3	0.4271	50.072	0.819

#	Time	Area	Height	Width	Area%	Symmetry
1	17.379	4215.4	162.6	0.3904	19.831	0.894
2	19.957	17040.9	582.3	0.4544	80.169	0.738

Figure 4.19 HPLC Data of the SM of Table 4.2 Entry 2

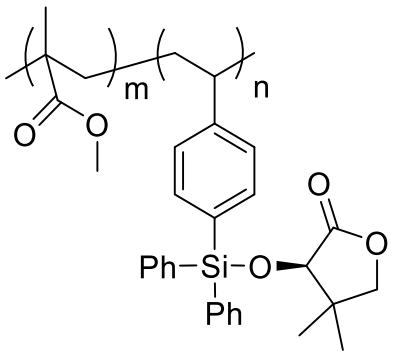

Table 4.2, Entry 3: 58 mg. For **^{1}H NMR** (400 MHz) data see selected spectra. HPLC data is of the desilylated product following GP2, 12 mg, 21 % yield. The desilylated alcohol was then benzoylated according to GP3 for HPLC analysis. The same conditions as the benzoylated starting materials were utilized. (er = 94:6) CD_2Cl_2 was applied as the NMR solvent because the reference peak blocks no other peaks.

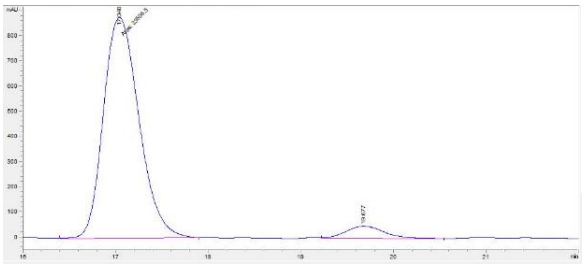

#	Time	Area	Height	Width	Area%	Symmetry
1	17.04	23506.5	878.1	0.4462	93.991	0.788
2	19.677	1502.9	49.8	0.4579	6.009	0.814

Figure 4.20 HPLC Data of the PR of Table 4.2 Entry 3

Table 4.7 Kinetic Resolution Data for Table 4.2, Entry 3

Entry	er SM	er PR	Conv (%)	*s*	Avg *s*
1	80.2:19.8	94.0:6.0	40.7	28.9	28.2
2	82.1:17.9	93.5:6.5	42.5	27.5	

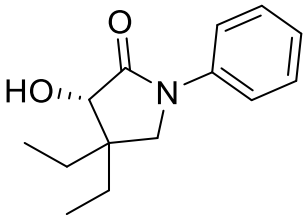

Table 4.2, Entry 4: 66 mg, 71 % recovered. **^{1}H NMR:** (400 MHz, $CDCl_3$) □1H NMR (400 MHz, CDCl3) δ 7.64 (d, J = 7.7 Hz, 2H), 7.37 (t, *J* = 7.7 Hz, 2 H), 7.17 (t, J = 7.4 Hz, 1H), 4.22 (s, 1H), 3.51 (dd, J = 40.3, 9.9 Hz, 2H), 2.84 (s, 1H), 1.76 – 1.62 (m, 3H), 1.51 (dq, J = 14.7, 7.4 Hz, 1H), 1.04 (t, J = 7.5 Hz, 3H), 0.87 (t, J = 7.5 Hz, 3H). **^{13}C NMR:** (101 MHz, $CDCl_3$) ppm 174.1, 139.0, 129.0, 124.9, 119.5, 77.6, 54.0, 44.2, 29.8, 22.6, 8.9, 8.4. HPLC separation was achieved on Chiralpak AD-H column 15 % isopropyl alcohol in hexane, flow rate: 1 mL/min, 25 °C; t_R 30.5 min for (*S*)-enantiomer (major) and 39.8 min for (*R*)-enantiomer (minor). (er = 57:43) Absolute stereochemistry was obtained via optical rotation.

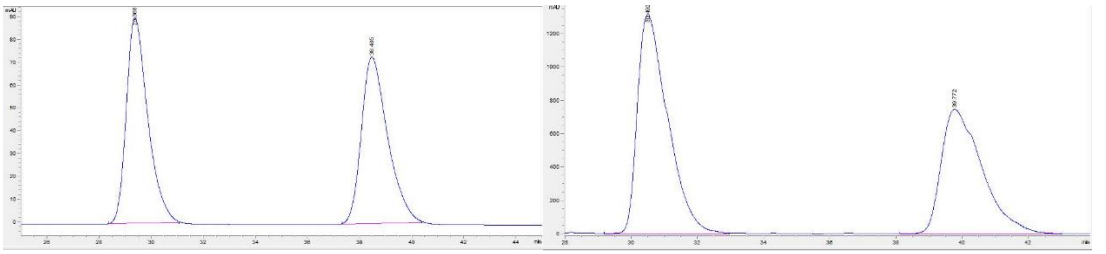

#	Time	Area	Height	Width	Area%	Symmetry
1	29.368	5180.1	90.1	0.8585	50.227	0.639
2	38.465	5133.3	73	1.0428	49.773	0.633

#	Time	Area	Height	Width	Area%	Symmetry
1	30.492	84724.6	1318.7	0.9516	56.484	0.487
2	39.772	65272.6	751	1.23	43.516	0.477

Figure 4.21 HPLC Data of the SM of Table 4.2 Entry 4

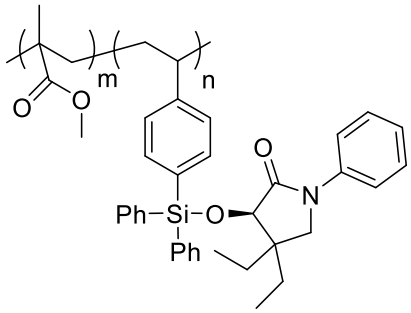

Table 4.2, Entry 4: 101 mg. For **^{1}H NMR** (400 MHz) data see selected spectra. HPLC data is of the desilylated product following GP2, 18 g, 18% yield. (er = 91:9)

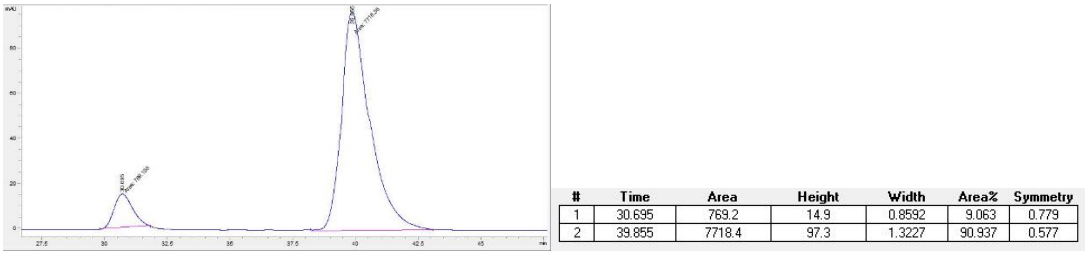

#	Time	Area	Height	Width	Area%	Symmetry
1	30.695	769.2	14.9	0.8592	9.063	0.779
2	39.855	7718.4	97.3	1.3227	90.937	0.577

Figure 4.22 HPLC Data of the PR of Table 4.2 Entry 4

Table 4.8 Kinetic Resolution Data for Table 4.2, Entry 4

Entry	er SM	er PR	Conv (%)	*s*	Avg *s*
1	57.5:42.5	90.9:9.1	15.5	11.5	11.8
2	57.5:42.5	91.3:8.7	15.4	12.0	

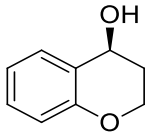

29 mg, 48 % recovered. (Scheme 4.9) **^{1}H NMR:** (400 MHz, $CDCl_3$) δ 7.32 (dd, *J* = 7.6, 1.6 Hz, 1H), 7.24 – 7.18 (m, 1H), 6.93 (td, *J* = 7.5, 1.1 Hz, 1H), 6.85 (dd, *J* = 8.2, 0.9 Hz, 1H), 4.80 (q, *J* = 4.2 Hz, 1H), 4.35 – 4.19 (m, 2H), 2.21 – 1.96 (m, 2H), 1.82 (d, *J* = 4.9 Hz, 1H). **^{13}C NMR:** (101 MHz, $CDCl_3$) δ ppm 154.6, 129.8, 129.7, 124.3, 120.6, 117.1, 63.3, 61.9, 30.8. HPLC separation was achieved on Chiralpak OD-H Column 7% isopropyl alcohol in hexane, flow rate: 1.0 mL/min, 25 °C; t_R 20.0 min for (*S*)-enantiomer (major) and 25.3 min for (*R*)-enantiomer (minor). (er = 71:29)

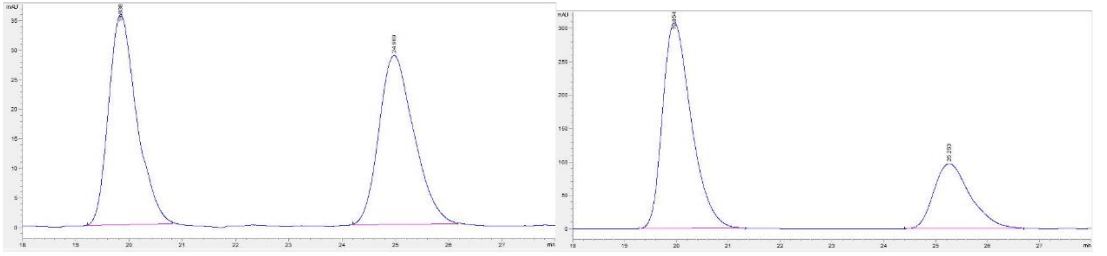

#	Time	Area	Height	Width	Area%	Symmetry
1	19.838	1312.2	35.6	0.5507	50.059	0.705
2	24.969	1309.1	28.6	0.6722	49.941	0.729

#	Time	Area	Height	Width	Area%	Symmetry
1	19.954	11920.5	309.2	0.5848	71.453	0.651
2	25.253	4762.5	97.4	0.7453	28.547	0.691

Figure 4.23 HPLC Data of the SM of 4-Chromanol in Scheme 4.9

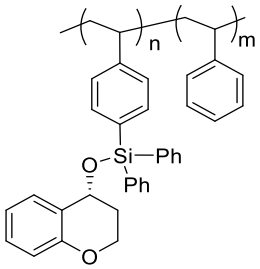

64 mg. For **^{1}H NMR** (400 MHz) data see selected spectra. HPLC data is of the desilylated product following GP2, 17 mg, 27 % yield. The same conditions as the recovered starting materials were utilized. (er = 91:9)

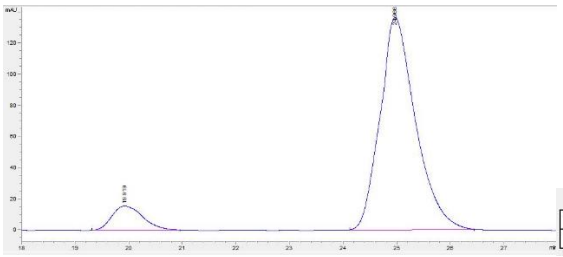

#	Time	Area	Height	Width	Area%	Symmetry
1	19.919	626.4	15.6	0.5723	9.059	0.678
2	24.966	6288.1	136.4	0.665	90.941	0.711

Figure 4.24 HPLC Data of the PR of 4-Chromanol in Scheme 4.9

Table 4.9 Kinetic Resolution Data of 4-Chromanol in Scheme 4.9

Entry	er SM	er PR	Conv (%)	*s*	Avg *s*
1	71.5:28.5	90.9:9.1	34.5	15.1	13.4
2	70.1:29.9	88.6:11.4	34.2	11.6	

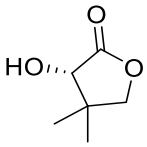

26 mg, 50 % recovered. **^{1}H NMR:** (400 MHz, $CDCl_3$) δ ppm 4.11 (s, 1H), 4.00 (d, *J* = 8.9 Hz, 1H), 3.95 (d, *J* = 8.9 Hz, 1H), 1.24 (s, 3H), 1.08 (s, 3H). **^{13}C NMR:** (101 MHz, $CDCl_3$) δ ppm 177.7, 76.4, 75.8, 41.0, 22.9, 18.8.

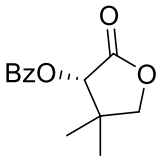

^{1}H NMR: (400 MHz, $CDCl_3$) δ ppm 8.12 (d, *J* = 7.7 Hz, 2H), 7.63 (t, *J* = 7.4 Hz, 1H), 7.49 (t, *J* = 7.7 Hz, 2H), 5.64 (s, 1H), 4.23 – 4.05 (m, 2H), 1.29 (s, 3H), 1.25 (s, 3H). **^{13}C NMR:** (101 MHz, $CDCl_3$) δ ppm 172.4, 165.4, 133.8, 130.0, 128.8, 128.6, 76.3, 75.5, 40.6, 23.1, 20.1. The recovered starting material was converted to the benzoylated ester according to GP3 for HPLC analysis. HPLC separation was achieved on Chiralpak OD-H Column 6 %

isopropyl alcohol in hexane, flow rate: 1 mL/min, 25 °C; t_R 16.2 min for (*R*)-enantiomer (minor) and 19.9 min for (*S*)-enantiomer (major). (er = 70:30)

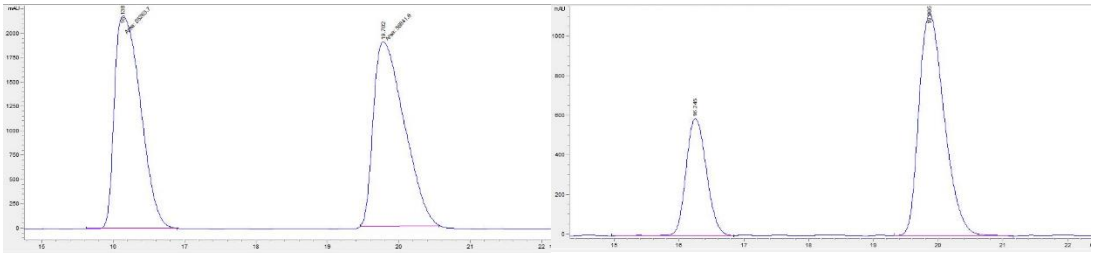

#	Time	Area	Height	Width	Area%	Symmetry
1	16.138	55263.7	2177.6	0.423	49.296	0.485
2	19.782	56841.6	1893.5	0.5003	50.704	0.471

#	Time	Area	Height	Width	Area%	Symmetry
1	16.245	13100.1	592.4	0.348	29.924	0.827
2	19.865	30678.2	1117.8	0.4242	70.076	0.699

Figure 4.25 HPLC Data of the SM of Pentolactone in Scheme 4.9

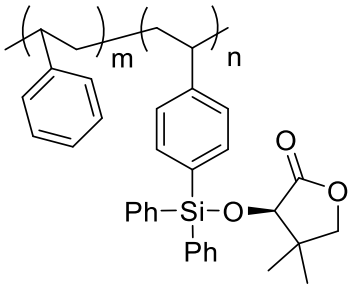

68 mg. HPLC data is of the desilylated product following GP2, 16 mg, 24 % yield. The desilylated alcohol was then benzoylated according to GP3 for HPLC analysis. The same conditions as the benzoylated starting materials were utilized. (er = 91:9)

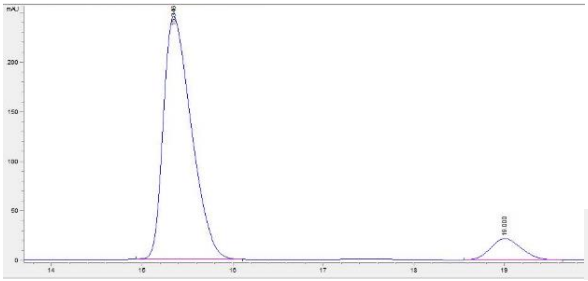

#	Time	Area	Height	Width	Area%	Symmetry
1	15.346	5285.2	245.3	0.3354	91.260	0.56
2	19	506.1	21.5	0.3663	8.740	0.836

Figure 4.26 HPLC Data of the PR of Pentolactone in Scheme 4.9

Table 4.10 Kinetic Resolution Data of Pentolactone in Scheme 4.9

Entry	er SM	er PR	Conv (%)	*s*	Avg *s*
1	70.1:29.9	91.3:8.7	32.7	15.7	15.4
2	70.4:29.6	91.0:9.0	33.2	15.1	

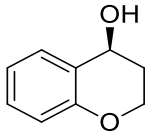

43 mg, 71 % recovered. (Scheme 4.10) **^{1}H NMR:** (400 MHz, $CDCl_3$) δ 7.32 (dd, *J* = 7.6, 1.6 Hz, 1H), 7.24 – 7.18 (m, 1H), 6.93 (td, *J* = 7.5, 1.1 Hz, 1H), 6.85 (dd, *J* = 8.2, 0.9 Hz, 1H), 4.80 (q, *J* = 4.2 Hz, 1H), 4.35 – 4.19 (m, 2H), 2.21 – 1.96 (m, 2H), 1.82 (d, *J* = 4.9 Hz, 1H). **^{13}C NMR:** (101 MHz, $CDCl_3$) δ ppm 154.6, 129.8, 129.7, 124.3, 120.6, 117.1, 63.3, 61.9, 30.8. It is a known compound, so IR and high resolution mass spectrum is not required. HPLC separation[2] was achieved on Chiralpak OD-H Column 8% isopropyl alcohol in hexane, flow rate: 1.0 mL/min, 25 °C; t_R 15.9 min for (*S*)-enantiomer (major) and 19.4 min for (*R*)-enantiomer (minor). (er = 57:43)

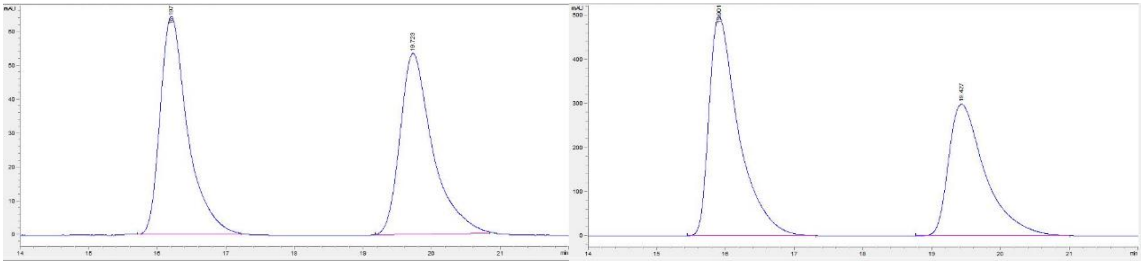

#	Time	Area	Height	Width	Area%	Symmetry
1	16.197	1794.1	64.3	0.4154	50.328	0.619
2	19.723	1770.7	53.5	0.4794	49.672	0.622

#	Time	Area	Height	Width	Area%	Symmetry
1	15.901	14841.4	498.4	0.4364	57.422	0.465
2	19.427	11004.7	298.1	0.5496	42.578	0.504

Figure 4.27 HPLC Data of the SM of 4-Chromanol in Scheme 4.10

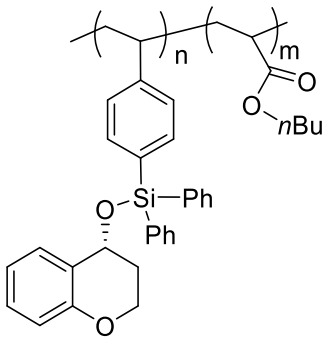

24 mg. For **^{1}H NMR** (400 MHz) data see selected spectra. HPLC data is of the desilylated product following GP2, 6 mg, 25 % yield. The same conditions as the recovered starting materials were utilized. (er = 89:11)

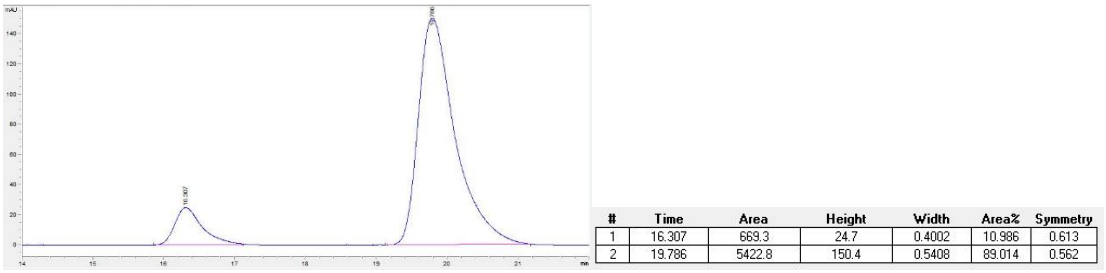

#	Time	Area	Height	Width	Area%	Symmetry
1	16.307	669.3	24.7	0.4002	10.986	0.613
2	19.786	5422.8	150.4	0.5408	89.014	0.562

Figure 4.28 HPLC Data of the PR of 4-Chromanol in Scheme 4.10

Table 4.11 Kinetic Resolution Data of 4-Chromanol in Scheme 4.10

Entry	er SM	er PR	Conv (%)	*s*	Avg *s*
1	57.4:42.6	89.2:10.8	16.2	9.7	9.6
2	57.4:42.6	89.0:11.0	16.3	9.4	

4.7 Reference

1. E. L. Eliel, S. H. Wilen, *Stereochemistry of Organic Compounds, John Wiley & Sons, Inc.*, New York, 1994.

2. Kagan, H.; Fiaud, J., New approaches in asymmetric synthesis. In *Topics in stereochemistry*, Wiley Online Library: 1978; Vol. 10, pp 175-285.

3. Keith, J. M.; Larrow, J. F.; Jacobsen, E. N., Practical considerations in kinetic resolution reactions. *Adv. Synth. Catal.* **2001,** *343* (1), 5-26.

4. Robinson, D. E.; Bull, S. D., Kinetic resolution strategies using non-enzymatic catalysts. *Tetrahedron: Asymmetry* **2003,** *14* (11), 1407-1446.

5. Vedejs, E.; Jure, M., Efficiency in nonenzymatic kinetic resolution. *Angew. Chem. Int. Ed.* **2005,** *44* (26), 3974-4001.

6. Pellissier, H., Catalytic non‐enzymatic kinetic resolution. *Adv. Synth. Catal.* **2011,** *353* (10), 1613-1666.

7. Akhani, R. K.; Clark, R. W.; Yuan, L.; Wang, L.; Tang, C.; Wiskur, S. L., Polystyrene‐Supported Triphenylsilyl Chloride for the Silylation‐Based Kinetic Resolution of Secondary Alcohols. *ChemCatChem* **2015,** *7* (10), 1527-1530.

8. Gladysz, J., Special Issue on Recoverable Catalysts and Reagents. *Chem. Rev* **2002,** *102* (10), 3215-3892.

9. Framery, E.; Andrioletti, B.; Lemaire, M., Recent progress in homogeneous supported asymmetric catalysis: example of the BINAP and the BOX ligands. *Tetrahedron: Asymmetry* **2010,** *21* (9-10), 1110-1124.

10. Clapham, B.; Reger, T. S.; Janda, K. D., Polymer-supported catalysis in synthetic organic chemistry. *Tetrahedron* **2001,** *57* (22), 4637-4662.

11. Bhalay, G.; Dunstan, A.; Glen, A., Supported reagents: opportunities and limitations. *Synlett* **2000,** *2000* (12), 1846-1859.

12. De, B. B.; Lohray, B. B.; Sivaram, S.; Dhal, P. K., Enantioselective epoxidation of olefins catalyzed by polymer-bound optically active Mn (III)-salen complex. *Tetrahedron: Asymmetry* **1995,** *6* (9), 2105-2108.

13. De, B. B.; Lohray, B. B.; Sivaram, S.; Dhal, P. K., Polymeric catalysts for chemo‐ and enantioselective epoxidation of olefins: New crosslinked chiral transition metal complexing polymers. *Journal of Polymer Science Part A: Polymer Chemistry* **1997,** *35* (9), 1809-1818.

14. Minutolo, F.; Pini, D.; Petri, A.; Salvadori, P., Heterogeneous asymmetric epoxidation of unfunctionalized olefins catalyzed by polymer-bound (salen) manganese complexes. *Tetrahedron: Asymmetry* **1996,** *7* (8), 2293-2302.

15. Minutolo, F.; Pini, D.; Salvadori, P., Polymer-bound chiral (salen) Mn (III) complex as heterogeneous catalyst in rapid and clean enantioselective epoxidation of unfunctionalised olefins. *Tetrahedron Lett.* **1996,** *37* (19), 3375-3378.

16. Song, C. E.; Roh, E. J.; Yu, B. M.; Chi, D. Y.; Kim, S. C.; Lee, K.-J., Heterogeneous asymmetric epoxidation of alkenes catalysed by a polymer-bound (pyrrolidine salen) manganese (III) complex. *Chem. Commun.* **2000,** (7), 615-616.

17. Sellner, H.; Seebach, D., Dendritically Cross‐Linking Chiral Ligands: High Stability of a Polystyrene‐Bound Ti‐TADDOLate Catalyst with Diffusion Control. *Angew. Chem. Int. Ed.* **1999,** *38* (13‐14), 1918-1920.

18. Kamahori, K.; Ito, K.; Itsuno, S., Asymmetric Diels− Alder reaction of methacrolein with cyclopentadiene using polymer-supported catalysts: Design of highly enantioselective polymeric catalysts. *J. Org. Chem.* **1996,** *61* (23), 8321-8324.

19. Glos, M.; Reiser, O., Aza-bis (oxazolines): New chiral ligands for asymmetric catalysis. *Org. Lett.* **2000,** *2* (14), 2045-2048.

20. Zheng, X.; Jones, C. W.; Weck, M., Poly (styrene) - Supported Co-Salen Complexes as Efficient Recyclable Catalysts for the Hydrolytic Kinetic Resolution of Epichlorohydrin. *Chem. Eur. J.* **2006,** *12* (2), 576-583.

21. Kumar, M.; Kureshy, R. I.; Shah, A. K.; Das, A.; Khan, N.-u. H.; Abdi, S. H.; Bajaj, H. C., Asymmetric aminolytic kinetic resolution of racemic epoxides using recyclable chiral polymeric Co (III)-salen complexes: A protocol for total utilization of racemic epoxide in the synthesis of (R)-naftopidil and (S)-propranolol. *J. Org. Chem.* **2013,** *78* (18), 9076-9084.

22. Shamoto, K.; Miyazaki, A.; Matsukura, M.; Kobayashi, Y.; Shioiri, T.; Matsugi, M., A Nonenzymatic Kinetic Resolution of (±)-trans-2-Arylcyclohexanols via Esterification Using Polymer-Supported DCC, DMAP, and 3 β-Acetoxyetienic Acid. *Synth. Commun.* **2013,** *43* (10), 1425-1431.

23. Annis, D. A.; Jacobsen, E. N., Polymer-supported chiral Co (salen) complexes: Synthetic applications and mechanistic investigations in the hydrolytic kinetic resolution of terminal epoxides. *J. Am. Chem. Soc.* **1999,** *121* (17), 4147-4154.

24. Matkiewicz, K.; Bukowska, A.; Bukowski, W., Novel highly active polymer supported chiral Co (III)–salen catalysts for hydrolytic kinetic resolution of epichlorohydrin. *J MOL CATAL A-CHEM.* **2013,** *368*, 43-52.

25. Okudomi, M.; Shimojo, M.; Nogawa, M.; Hamanaka, A.; Taketa, N.; Matsumoto, K., Easy separation of optically active products by enzymatic hydrolysis of soluble polymer-supported substrates. *Tetrahedron Lett.* **2007,** *48* (48), 8540-8543.

26. Okudomi, M.; Nogawa, M.; Chihara, N.; Kaneko, M.; Matsumoto, K., Enzyme-mediated enantioselective hydrolysis of soluble polymer-supported dendritic carbonates. *Tetrahedron Lett.* **2008,** *49* (47), 6642-6645.

27. Whalen, L. J.; Morrow, C. J., Resolution of a chiral alcohol through lipase-catalyzed transesterification of its mixed carbonate by poly (ethylene glycol) in organic media. *Tetrahedron: asymmetry* **2000,** *11* (6), 1279-1288.

28. Wallace, J. S.; Reda, K. B.; Williams, M. E.; Morrow, C. J., Resolution of a chiral ester by lipase-catalyzed transesterification with polyethylene glycol in organic media. *J. Org. Chem.* **1990,** *55* (11), 3544-3546.

29. Clark, R. W.; Akhani, R. K.; Wiskur, S. L., Polymers and Kinetic Resolutions: The Insolubility of It All. *ChemCatChem* **2016,** *8* (5), 879-885.

30. Baar, C. R.; Levy, C. J.; Min, E. Y.-J.; Henling, L. M.; Day, M. W.; Bercaw, J. E., Kinetic resolution of chiral α-olefins using optically active ansa-zirconocene polymerization catalysts. *J. Am. Chem. Soc.* **2004,** *126* (26), 8216-8231.

31. Vedejs, E.; Rozners, E., Parallel kinetic resolution under catalytic conditions: a three-phase system allows selective reagent activation using two catalysts. *J. Am. Chem. Soc.* **2001,** *123* (10), 2428-2429.

32. Alexandratos, S. D.; Miller, D. H., *Macromolecules* **1996,** *29*, 8025-8029.

33. Akhani, R. K.; Moore, M. I.; Pribyl, J. G.; Wiskur, S. L., Linear free-energy relationship and rate study on a silylation-based kinetic resolution: mechanistic insights. *J. Org. Chem.* **2014,** *79* (6), 2384-2396.

34. Arai, M., Chlorination by Sulfuryl Chloride. III. The Reactivities of the C–H Bond to Sulfuryl Chloride. *Bull. Chem. Soc. Jpn.* **1964,** *37* (9), 1280-1283.

35. Lee, K., Directive effects in benzylic hydrogen atom abstraction—II: Radical chlorination by sulphuryl chloride. *Tetrahedron* **1969,** *25* (18), 4363-4369.

36. Varaprath, S.; Stutts, D. H., Utility of trichloroisocyanuric acid in the efficient chlorination of silicon hydrides. *J. Organomet. Chem.* **2007,** *692* (10), 1892-1897.

37. Mayo, F. R.; Lewis, F. M., Copolymerization. I. A basis for comparing the behavior of monomers in copolymerization; the copolymerization of styrene and methyl methacrylate. *J. Am. Chem. Soc.* **1944,** *66* (9), 1594-1601.

38. Lindsley, C. W.; Hodges, J. C.; Filzen, G. F.; Watson, B. M.; Geyer, A. G., *J. Comb. Chem.* **2000,** *2*, 550-559.

39. Perrier, S. b., 50th Anniversary Perspective: RAFT Polymerization A User Guide. *Macromolecules* **2017,** *50* (19), 7433-7447.

40. Conversions and selectivity factors are based on the ee of the recovered starting materials and products. Conversion = ees/(ees + eep) and s = ln[(1 − C)(1 – ees)]/ln[(1 −C)(1 + ees)], where ees = ee of recovered starting material and eep = ee of product.

41. Sheppard, C. I.; Taylor, J. L.; Wiskur, S. L., Silylation-based kinetic resolution of monofunctional secondary alcohols. *Org. Lett.* **2011,** *13* (15), 3794-3797.

42. Clark, R. W.; Deaton, T. M.; Zhang, Y.; Moore, M. I.; Wiskur, S. L., Silylation-based kinetic resolution of α-hydroxy lactones and lactams. *Org. Lett.* **2013,** *15* (24), 6132-6135.